

Systematic Review of Geochemical Data from Thermal Springs, Gas Vents and Fumaroles of Southern Italy for Geothermal Favourability Mapping

Minissale A.⁽¹⁾, Donato A.⁽²⁾, Procesi M.⁽³⁾, Pizzino L.⁽³⁾, Giammanco S.⁽⁴⁾

- (1) CNR-Italian Council for Research, Institute of Geosciences and Earth Resources (IGG), Via La Pira 4, 50121 Firenze (Italy). E-mail: angelo.minissale54@gmail.com
- (2) CNR-Italian Council for Research, Institute of Geosciences and Earth Resources (IGG), Via Moruzzi 1, 56124 Pisa (Italy). E-mail: assu.donato@gmail.com
- (3) INGV-Italian National Institute of Geophysics and Volcanology, Via di Vigna Murata 605, 00143 Rome (Italy). E-mail: monia.procesi@ingv.it; luca.pizzino@ingv.it
- (4) INGV-Italian National Institute of Geophysics and Volcanology, P.za Roma 2, 95125 Catania (Italy). E-mail: salvatore.giammanco@ct.ingv.it

Abstract

In recent years, two research projects specifically conceived by Italian Institutions of Research to promote the implementation of the use of geothermal energy in Southern Italy has allowed the review of most data on chemical and isotopic compositions of natural thermal manifestations in the territory of Italy. Two large databases, one for thermal springs and CO₂-rich springs, and a second one for fumarolic condensates and associated gas phase have been produced and are available on line, with data spanning in time from the early 70's to the present.

We have used those data, after careful evaluation of the quality and reliability of them, to produce correlation diagrams and isodistribution maps of some relevant geochemical/geothermal parameters, such as: $p\text{CO}_2$ in thermal springs, %CO₂ and $\delta^{13}\text{C}$ in CO₂ of gas phases, ³He/⁴He ratio and %He. In this way, we have been able to delimit the areal patterns of thermal anomalies potentially related with geothermal reservoirs. The cross correlation among the many parameters (>40) selected has allowed the overview on the circulation of fluids at shallow crust, in one of the most active tectonic boundary of the Earth between the African and the Eurasian continents.

Shallow circulation of hot fluids is particularly active in the Roman Comagmatic Province, the Neapolitan area and Sicily (both at Etna, Aeolian Archipelago and Pantelleria island in the Sicily Channel) where active geothermal systems are already known, whose areal extension is probably much larger than what envisaged at present.

The geothermometric evaluation of data has not allowed to clearly identify new areas apart from those already known but, nevertheless, some areas in the inner Apennines, as well as Sicily and Sardinia have shown anomalous ³He/⁴He values that point to the presence of mantle fluids located inside the crust.

Being most of active volcanic islands likely much smaller than the thermal anomaly they are associated with, a futuristic perspective of utilizing geothermal fluids off shore is suggested. Moreover, the database and the proposed maps can be a useful tool both scientific community and

61
62
63 1 stakeholders to perform geothermal favourability maps and to identify potential new areas
64 2 interesting from a geothermal perspective.

65 3
66 4
67 4 **Key words:** *Geothermal potential; thermal springs; fumaroles; gas vents; geothermal prospection;*
68 5
69 5 *geochemical prospection; southern Italy.*

70 6 71 7 **1. Introduction**

72 8
73 9 In February 2010 the Italian Parliament promulgated a reorganization law, in order to favour
74 10 the exploitation of geothermal energy by private investors. Following this governmental indication,
75 11 the Italian Ministry of Economic Development launched a three-years (2011-2014) project named
76 12 “VIGOR” (<http://www.vigor-geotermia.it>) in order to promote innovative actions for geothermal
77 13 energy exploration in Southern Italy. This was followed by another project, lasted from 2013 to
78 14 2015, funded by the Italian Council for Research entitled “*Geothermal Atlas of Southern Italy*”
79 15 (<http://atlante.igg.cnr.it>). These projects served to gather analytical and technical data to be used to
80 16 locate and categorize all potential geothermal resources in the regions involved (Latium, Abruzzi,
81 17 Molise, Campania, Puglia, Lucania, Calabria, Sicily and Sardinia; Fig. 3). Some of these regions
82 18 host active volcanoes (e.g.: Vesuvius and Phlegraean Fields in Campania; Stromboli Island and
83 19 Etna in Sicily) as well as several others in a quiescent state (e.g.: Ischia Island in Campania; Alban
84 20 Hills in Latium; Vulcano and Pantelleria Islands in Sicily). They also host well-known geothermal
85 21 systems (e.g.: at Vulsini Mts., Ischia, Vulcano and Pantelleria Islands) and a very high number of
86 22 thermal springs, the latter traditionally used for balneotherapy since Roman times.

87 23 One of the outcomes of both of those projects was the production of a Geochemical Atlas
88 24 of geothermal manifestations. This included geochemical databases with the chemical and isotopic
89 25 data available for thermal springs, CO₂-rich waters, fumaroles and gas vents present in the studied
90 26 territory, as well as maps of their precise location and contour maps of the spatial distribution of
91 27 geochemical parameters of geothermal interest.

92 28 The main target of the analysis and use of the chemical parameters acquired with both
93 29 projects was to provide potential stakeholders with an efficient tool for geothermal prospecting
94 30 and/or surveying.

95 31 In the present work we proceeded to: *i*) update all data already gathered in previous similar
96 32 projects, either published (e.g.: [CNR, 1982a](#); [1982b](#); [Cataldi et al., 1995](#)) or unpublished (e.g.:
97 33 [INGV, 2006](#)) and *ii*) review the extensive literature data produced in the past 50 years.

98 34 Careful review of the existing data and production of new ones, where implementation was
99 35 necessary, were carried out jointly by the Italian Council for Research (CNR) and by the Italian
100 36 National Institute of Geophysics and Volcanology (INGV). An extensive report on these activities
101 37 ([Minissale et al., 2016](#)) can be downloaded (in Italian) from:
102 38 <http://atlante.igg.cnr.it/images/stories/volumi/VolumeGeochimicaAtlante-online.pdf>.

103 39 This paper was primarily intended to share with the international community the results of
104
105
106
107
108
109
110
111
112
113
114
115
116
117
118
119
120

121
122
123 1 the long (more than two years) process of elaboration of all geochemical data from the geothermal
124 2 areas of Southern Italy, indicating the criteria used to select the parameters that we considered the
125 3 most relevant for the aims of this study. Secondly, we aimed at providing reliable and robust data
126 4 for the eventual production of geothermal favourability maps of Southern Italy by national and
127 5 international investors.
128
129
130

131 6 132 7 **2. Fluid geochemistry as a tool for geothermal investigation and favourability mapping** 133 8

134 9 At the onset of a geothermal exploration project there is usually a high degree of
135 10 uncertainty on whether the planned activity will be economically viable or not, and/or if it will be
136 11 technically feasible and environmentally compatible. Best practices in the exploration for any
137 12 natural resource should aim at reducing the risk of failure prior to significant capital investment. In
138 13 the case of geothermal resources exploration, the high risk associated with the estimate of the
139 14 resource capacity is one of the key issues that investors have to face. The principal variables
140 15 required to define the resource capacity are: *i*) temperature (enthalpy), volume and depth of the
141 16 resource; *ii*) optimal productivity of extraction wells; *iii*) sustainability of the extraction rate of
142 17 producing wells; and *iv*) the energy market demand. Each phase of a geothermal exploration
143 18 program should be clearly determined before its beginning, in order to address all risks, and each
144 19 type of risk should be accurately evaluated.
145
146
147
148

149 20 Because of the uncertainty involved, in order to minimize the costs and maximize the
150 21 amount of information available for each component of a geothermal project, it has become a
151 22 common practice to divide the preparatory work into several separate phases. In this regard, the
152 23 ESMAP Geothermal Handbook (ESMAP, 2012) provides a guide for developing a geothermal
153 24 project, indicating seven phases, as follows: *i*) preliminary survey; *ii*) exploration; *iii*) drilling tests;
154 25 *iv*) project review and planning; *v*) field development; *vi*) power plant construction and *vii*)
155 26 commissioning and operation. Stage *i*) can be preceded by a *stage zero*, namely a geothermal
156 27 favourability mapping (Fig. 1). It is in fact useful to identify the location of potential geothermal
157 28 areas by combining different types of data through a dedicated software, such as Geographical
158 29 Information Systems (GIS).
159
160
161
162
163

164 30 In stages *i*) and *ii*), geochemical prospecting methods are extensively used and act as a
165 31 valid support for other Earth Sciences disciplines (geological and geophysical, mostly) involved in
166 32 the geothermal project. In particular, fluid geochemistry plays a major role in understanding: *i*)
167 33 distribution of permeable zones; *ii*) areal extension of the potential geothermal reservoir; *iii*)
168 34 typology of geothermal systems (liquid-or vapour-dominated); *iv*) evaluation of the minimum
169 35 temperature at depth; *v*) chemical features of the geothermal fluid; *vi*) existence, location and
170 36 extension of water recharge areas.
171
172
173

174 37 The preliminary phase involves a work program designed to assess any possible evidence
175 38 for geothermal resources in a specific area. This is carried out through an extensive literature
176
177
178
179
180

181
182
183 1 review of hydro-chemical data (from hot/thermal springs, mud pools, etc.), data from natural gas
184 2 manifestations (dry vents, fumaroles, etc.), as well as data from drillings (temperature and
185 3 resistivity logs, etc.). Once geothermal manifestations have been located, and characterized, new
186 4 samples of representative fluids should be taken, especially at sites with high fluid temperature and
187 5 high electrical conductivity. Cold springs or cold wells, with: high electrical conductivity, high gas
188 6 bubbling, unusual odour or strange taste, are further considered for sampling, in places where no
189 7 thermal manifestation is evident.

193 8 Where geothermal fluids reach the surface, their chemical/isotopic composition is used to
194 9 deduce their sub-surface temperature through application of geothermometers that are the most
195 10 used tools in preliminary phases. Geothermometers depend on one or more dissolved component
196 11 in the geothermal fluid, such as: solutes, gases or isotopic ratios. Accordingly, they have been
197 12 classified into three groups: *i*) chemical (or solute); *ii*) gas; and *iii*) isotope geothermometers. They
198 13 are based on the existence at depth of a temperature-dependent mineral-fluid equilibrium that
199 14 constrains the chemical and the isotopic composition of the system. However, when a geothermal
200 15 fluid rises to the surface, it becomes subject to a number of physical and chemical processes that
201 16 change its final composition. Boiling, loss of CO₂, mixing with shallower fluids, conductive cooling,
202 17 etc., can cause additional mineral dissolution or precipitation, because of changing of the
203 18 saturation index with respect to mineral phases. For example, the increase of pH of pristine fluids
204 19 may cause precipitation of hydroxides and carbonates. Furthermore, the top part of a geothermal
205 20 system may be subject to mixing with percolating ground water, with consequent dilution and
206 21 cooling of the geothermal fluid. This process in particular, among other effects, may significantly
207 22 alter the temperature values estimated with geothermometers. It is therefore necessary to use
208 23 geothermometers cautiously, as a suite within their geologic context, in order to properly estimate
209 24 the resource temperature (Armansson, 2012).

218 25 Besides geothermometers, soil gas studies may provide information about the pathways
219 26 used by geothermal fluids to reach the surface. Measurement of gas fluxes and concentrations in
220 27 the soil (Bertrami et al., 1990; Finlayson, 1992; Hernández et al., 2000; Voltattorni et al., 2010;
221 28 Phuong et al., 2012; Fridriksson et al., 2016) sometimes coupled with measurement of soil
222 29 temperature (Lan et al., 2007; Skord, 2013; Maucourant et al., 2014), has been extensively used
223 30 for the exploration of geothermal reservoirs, as well as for the estimate of the location and surface
224 31 extension of heat sources. Noble gases, as well as Hg, are assumed to be released from active
225 32 geothermal systems at depth and their high mobility makes them ideal pathfinders for concealed
226 33 natural resources, as they can escape to the surface along fractures and faults (e.g.: Koga, 1982;
227 34 Fridman, 1990).

233 35 Another largely used application of geochemical data in geothermal prospecting is the
234 36 development of geothermal favourability maps. In general, favourability maps permit to establish a
235 37 hierarchy among geothermal areas, from low to medium and high enthalpy geothermal resources,
236
237
238
239
240

241
242
243 1 based on their geothermal potential (Carranza et al., 2008; Iovenitti et al., 2014; Trumphy et al.,
244 2 2015). Input data are given by spatial analysis of multiple parameters (geological, hydrogeological,
245 3 geophysical and geochemical), performed using a GIS software. Indeed, the use of GIS allows to
246 4 define spatial associations between different thematic information (layers) for a specific area. Each
247 5 layer is converted into a reclassified thematic grid (map); each grid is assigned both a weight and
248 6 an influence (importance) on the basis of statistical criteria or *knowledge-driven* models (based on
249 7 experts' opinion). In this framework, several authors have used geochemical data (from thermal
250 8 springs, gas bubbling pools and fumaroles) in terms of distance from potential geothermal
251 9 reservoirs (Noorollahi et al., 2007; 2008; Yousefi et al., 2010; Aravena and Lahsen, 2013;
252 10 Moghaddam et al., 2014; Procesi et al., 2015). In particular, some authors have defined that
253 11 distance by statistical approaches taking into account already exploited geothermal sites
254 12 (Noorollahi et al., 2007; 2008; Yousefi et al., 2010), whereas others have defined it by *knowledge-*
255 13 *driven* models considering a buffer around the geothermal manifestation (Procesi et al., 2015).

262 14 A different approach was recently proposed by Trumphy et al. (2015) using geochemical
263 15 data in a wide regional context, in terms both of partial pressure of CO₂ (Pco₂) in thermal springs
264 16 and of ³He/⁴He ratio in gas discharges. The ³He/⁴He ratio is a good indicator of degassing from
265 17 mantle-derived magma residing in the crust that, coupled with CO₂, can be also a good indicator of
266 18 degassing from hydrothermal systems fed by deep fluids. Those authors have therefore compiled
267 19 maps as combinations of *geochemical favourability* layers (based on the distribution of ³He/⁴He
270 20 ratios and dissolved Pco₂ values) and other layers, using a dedicated Index Overlay Model.

272 21 273 22 **3. Geochemical database and data selection criteria**

274 23
275 24 Published and unpublished geochemical and isotopic data of the thermal manifestations
276 25 were collected and organized in two files, one for the liquid and one for the gas phase, both
277 26 available as supplementary material at <http://atlante.igg.cnr.it/>.

280 27 The basic reference for this collection was the national geothermal database handled by
281 28 the Italian National Research Council (ENEL, 1988; Barbier et al., 2000; Trumphy and Manzella,
282 29 2017). Useful data were also retrieved from the huge scientific literature of the last 50 years.
283 30 Almost 150 scientific publications were carefully checked, most of which refer to active volcanic
284 31 areas. Only those data including information on the precise location of the emergence were
285 32 considered. In addition, new data were acquired in areas where information was lacking. No
286 33 classification criteria for the waters were applied (e.g.: as a function of salinity or chemical
287 34 composition), and the selection of sites was based on a water temperature threshold set at 20 °C
288 35 for thermal springs, as usual in temperate regions. The database of selected water sites contains
289 36 515 chemical analyses referring to 246 emergence sites; the database of gas sites counts 509
290 37 chemical analyses, including 246 emergences.

296 38 In the first database, some cold waters, such as those rich in CO₂, were also included. The
297
298
299
300

301
302
303 1 presence of relevant CO₂ degassing from secondary superficial aquifers could in fact be an
304 2 indication of the presence, at an undefined depth, of an active parent hydrothermal system,
305 3 possibly just masked by the shallower cold water circulation. In addition, in order to give a
306 4 complete framework of the naturally emitted gaseous fluids in Southern Italy, CH₄-rich emissions,
307 5 generally cold and associated with the presence of thick Neogene sedimentary formations, were
308 6 also included in the gas database.

309 7 A proper screening work was done for water samples: only the analyses showing an
310 8 electronic balance between cations and anions lower than 5% were selected. For the gas samples,
311 9 those clearly affected by air (oxygen) contamination were excluded. Analyses, provided with the
312 10 geographic coordinates of the respective sampling site (in UTM-WGS84 metric units Fuse 33 N)
313 11 were listed, starting from the most recent ones in case of multiple analyses.

314 12 As regards thermal waters, each site in the water file displays: *i*) elevation (in m *a.s.l.*); *ii*)
315 13 flow-rate (in L/sec); *iii*) temperature (in °C); *iv*) pH; *v*) redox potential (as Eh, in mV); *vi*) electrical
316 14 conductivity (in µS/cm) at 25 °C; *vii*) salinity (TDS=total dissolved solids in mg/kg); *viii*) major
317 15 elements (Ca, Mg, Na, K, HCO₃, SO₄ and Cl) and *ix*) minor elements (Sr, F, Br, B, NH₄, NO₃ and
318 16 SiO₂), both expressed in mg/kg; *x*) isotopic ratios of ²H/H (as δ²H) and ¹⁸O/¹⁶O (as δ¹⁸O), both in ‰
319 17 vs. SMOW; *xi*) tritium (in UT unit); *xii*) δ¹³C of carbon in dissolved inorganic carbon (DIC) in ‰ vs
320 18 PDB; *xiii*) pCO₂ (-logPco₂) calculated with the PHREEQC speciation program ([Parkhurst and](#)
321 19 [Appelo, 1999](#)) and *xiv*) reference to the papers where chemical original data were published.

322 20 Taking into account the variability of the gas emissions, the classification proposed was
323 21 made based on the type of emergence. Free gas emissions (*mofette* = mo in the gas table) and
324 22 *mud volcano*es (mv) are not so common; more frequently, gases are associated with water
325 23 emissions or with fumarolic fluids (fu). Bubbling gases can be associated with both cold (and
326 24 hypothermal water (typically from 15 to 20 °C) from shallow aquifers (sg), and from the thermal
327 25 regional aquifers hosted in carbonates (tsg). Sometimes, bubbling gases, both in flowing and/or in
328 26 stagnant (rain-originated) waters, are locally known as “*acque acetose*”, “*acque arzenti*”, “*acque*
329 27 *puzze*”, “*acque bolle*”, etc. ([Minissale, 2004](#)). The values of dissolved gas (stripped) were
330 28 discarded when analyses of free gases were available in the same area. In areas where no other
331 29 information was available, the values of stripped gas were kept.

332 30 Due to its high relevance, the ³He/⁴He ratio (as R/Ra where R is the ratio in the sample and
333 31 Ra is the ratio of air=1.39x10⁻⁶, [Mamyrin and Tolstikhin, 1984](#)) of both bubbling and stripped gas
334 32 samples was reported in the gas file, even in the absence of the analysis of the main gas
335 33 components. The gas table in supplementary material reports both the uncorrected and corrected
336 34 ([Craig et al., 1978](#)) helium isotopic ratio as R/Ra and R/Ra_c, respectively. R/Ra_c was considered
337 35 when the corresponding He/Ne ratio for correction due to air contamination ([Craig et al., 1978](#)) was
338 36 available.

361
362
363 1 After reporting name and locality of each sample, columns in the gas file were organized as
364 2 follows: *i)* type of manifestation, *ii)* year of sampling or year of data publication; *iii)* geographical
365 3 coordinates; *iv)* elevation (or depth with respect to the ground level if the gas comes from a well, or
366 4 the depth respect to the sea level in case of submarine emission); *v)* sampling temperature; *vi)*
367 5 major components (CO₂, N₂, O₂, CH₄, H₂S); *vii)* minor components (H₂, CO, He, Ar, Ne, Rn); *viii)*
368 6 various isotopic ratios, including: ³He/⁴He, ⁴⁰Ar/³⁶Ar, δ¹³C both of CO₂ (gas) and DIC and, finally, *ix)*
369 7 δ¹³C and δ²H in CH₄.

373 8 374 9 **4. Geochemical mapping**

375 10
376 11 To draw isodistribution maps on a regional scale, we decided to follow the same approach
377 12 as [Trumpy et al., \(2015\)](#), who selected the *p*CO₂ in thermal waters and the ³He/⁴He ratio in the gas
378 13 phase, as main chemical parameters in producing geothermal favourability maps. In addition, we
379 14 have also considered: the CO₂ concentration and the ¹³C-co₂ in the gas phase, being these
380 15 parameters strictly related to the *p*CO₂ in waters. Regarding the ³He/⁴He ratio we decided to add
381 16 also the total helium concentration in the gas phase, being a parameter connected with long
382 17 circulation and residence time of underground fluids in areas not affected by huge CO₂
383 18 degassing/dilution.

388 19 389 20 **5. Criteria**

390 21 391 22 *5.1 Carbon parameters*

392 23
393 24 Generally, the gas phase associated with hydrothermal fluids in convergent margins is rich
394 25 in CO₂ and it is related to magma degassing and/or decarbonation reactions ([Barnes et al., 1978](#)).
395 26 CO₂ moves to the surface and is dissolved in shallow aquifers, inducing an increase in their *P*co₂
396 27 (*soda springs*). When aquifers become saturated in CO₂, the gas leaves them and moves upwards
397 28 along fractures. The gas eventually emerges at the surface in the form of focused or diffuse soil
398 29 degassing, or it is further dissolved into shallow cold and thermal waters. Therefore, high *P*co₂
399 30 values in groundwater are normally associated with geothermal fluids, although at undefined
400 31 depth, and together with the isotopic signature of carbon they can be effective indicators of
401 32 geothermal reservoirs at depth ([Panichi and Tongiorgi, 1976](#)). Both parameters can be used to
402 33 map the areal extension of geothermal systems, as already done in central Italy along the peri-
403 34 Tyrrhenian margin ([Minissale, 1991b](#); [Chiodini et al., 1995](#); [Doveri et al., 2010](#); [Giordano et al.,](#)
404 35 [2014](#)), where active geothermal systems discharge huge amounts of CO₂ ([Chiodini et al., 2004](#)).
405 36 The reason why CO₂ works well in central Italy, is that the local geothermal systems are hosted in
406 37 permeable Mesozoic carbonate rocks often covered by impermeable Quaternary volcanoclastic
407 38 material and/or Neogene clay-rich post-orogenic sedimentary deposits that act as a good cap-rock
408 39 for the rising CO₂.

421
422
423 1 In order to define the different classes of P_{CO_2} in waters for the drawing of isodistribution
424 2 maps we choose a statistical approach through the analysis of data using the Normal Probability
425 3 Plot (NPP; [Sinclair, 1964](#)). Three main classes were recognised: *i*) highly anomalous, with $pCO_2 >$
426 4 0.75 ($P_{CO_2} > 0.18$ bar); *ii*) weakly anomalous, with $-1.75 < pCO_2 < -0.75$ (0.078 bar $< P_{CO_2} < 0.18$
427 5 bar; and *iii*) non-anomalous, with $pCO_2 < -1.75$ ($P_{CO_2} < 0.078$ bar) (Fig. 2). It is worth of note that
428 6 these classes, obtained on a regional scale, roughly correspond to those proposed by [Doveri et al](#)
429 7 ([2010](#)) for Latium region (north and south of Rome) to define and delimit the areal extension of
430 8 potential geothermal system.

431 9 Referring to the CO_2 concentration and the $\delta^{13}C-CO_2$ in the gas phase, classes defined by
432 10 the NPP analysis have resulted: *i*) < 8.0 , *ii*) from 8.0 to 50.0 , *iii*) from 50.0 to 85.0 , *iv*) ≥ 85.0 percent;
433 11 and *i*) from $+3.0$ to -3.0 , *ii*) from -3.0 to -7.0 , *iii*) from -7.0 to -20.0 and *iv*) ≤ -20.0 delta permil,
434 12 respectively.

441 13 5.2 Helium parameters

442 14 As well known, the $^3He/^4He$ ratio is a strong indicator of mantle-magma residing in the crust
443 15 ([Mamyurin and Tolstikhin, 1984](#)) that, coupled with CO_2 anomalies, can be a good indicator of
444 16 degassing from hydrothermal systems and, eventually, converging towards the presence of
445 17 potential geothermal reservoirs at depth. Helium ratios can also trace crustal and atmospheric
446 18 sources (or contamination) in different geodynamics contexts ([O'Nions and Oxburg, 1988](#)).

447 19 Typical crustal values of R/Ra are in the range $0.001-0.2$, while mantle values range
448 20 between 0.2 ([Marty and Jambon, 1987](#)) and 8.0 , according to the degree of crustal contamination
449 21 of the primary gas rising from the mantle ([Poreda and Craig, 1989](#); [Hilton et al., 1993](#); [Hulston and](#)
450 22 [Lupton, 1996](#)). R/Ra value of ~ 8.0 is entirely derived from mid-ocean ridge basalts (MORB) or
451 23 upper mantle components. The large difference between crustal and mantle makes the $^3He/^4He$
452 24 ratio an effective tracer of subducting slabs in areas of arc magmatism ([Craig et al., 1978](#)).

453 25 Relatively high R/Ra values in Southern Italy were measured in gases discharged from the
454 26 active volcanic areas of: Mt Etna (6.9 ; [Allard et al., 1997](#)), Vulcano island (6.2 ; [Tedesco and](#)
455 27 [Scarsi, 1999](#)), Pantelleria island (7.32 ; [Parello et al., 2000](#)) and from the quiescent Vulture volcano
456 28 (6.35 ; [Caracausi et al., 2015](#)). Lower R/Ra values were measured in hydrothermal systems in the
457 29 Neapolitan area: at Campi Flegrei ($2.0-3.2$; [Tedesco et al., 1990](#)), Vesuvius ($2.2-2.7$; [Federico et](#)
458 30 [al., 2002](#)), Ischia island ($1.6-3.7$; [Inguaggiato et al., 2000](#)) and spotty in the inner Apennine chain
459 31 (e.g.: Mefite d'Ansanto, 2.84 (#108); [Caracausi et al., 2013](#)).

460 32 In peri-Tyrrhenian area of Tuscany and Latium gases have lower R/Ra values from 0.4 to
461 33 0.8 ([Hooker et al. 1985](#); [Minissale et al, 1997a](#); [Cinti et al., 2011](#); [2014](#)), although a significant 3He
462 34 enrichment was measured in geothermal fluids from Larderello (up to 3.2 ; [Minissale et al., 1997a](#)),
463 35 Cesano ($1.2-2.0$; [Minissale et al., 1997a](#); [Cinti et al., 2017](#)) and in the gas discharges from the
464 36 Alban Hills ($0.9-1.9$; [Barberi et al., 2007](#)) and Roccamonfina volcano (1.89 ; [Cuoco et al., 2017](#)).

481
482
483 1 The variability of the helium isotopic ratio from south to north Italy reflects the complex
484 2 geodynamic setting of the country. Sano et al. (1989) related the $^3\text{He}/^4\text{He}$ ratios measured in Italy
485 3 to the upwelling mantle in the Tyrrhenian Bathyal Plain, which is characterized by a very thin
486 4 oceanic crust (8-10 km; Panza and Calcagnile, 1979) and by heat flow values even higher than
487 5 200 mW/m² (Della Vedova et al., 1991). Other studies suggested that the low $^3\text{He}/^4\text{He}$ ratios
488 6 measured in the northern Tyrrhenian sector reflect the composition of the subducted crust enriched
489 7 in ^4He because of northward contamination by metasomatic fluids derived from the partly
490 8 subducted Apennines (Polyak et al., 1979; Frezzotti et al., 2009).

495 9 What reported above highlights that R/Ra ratios lower than those from volcanic areas (e.g.:
496 10 Mt. Etna), can derive from geothermal systems typically affected by meteoric recharge and hence
497 11 by ^4He atmospheric contamination, and in this framework the Larderello geothermal system in
498 12 Tuscany represents an excellent example. This consideration suggests that the use of the R/Ra
499 13 ratio for geothermal prospecting purposes must take into account the local geological and
500 14 geodynamic setting to avoid deceptive evaluations.

504 15 In light of the above discussion, we decided to consider five classes of R/Ra (or
505 16 R/Ra_c): *i*) <0.2; *ii*) from 0.2 to 1.0; *iii*) from 1.0 to 3.0; *iv*) from 3.0 to 5.0 and *v*) >5.0, respectively.

507 17 **6. Mapping methods**

509 18 The areal data distribution of the selected geochemical parameters *i.e.*: *i*) the partial
510 19 pressure of CO₂ in thermal springs, shallow wells and cold CO₂-rich waters; *ii*) CO₂ gas content; *iii*)
511 20 $\delta^{13}\text{C}$ of CO₂ along with *iv*) the $^3\text{He}/^4\text{He}$ ratio and *v*) total helium in the gas discharges, were
512 21 interpolated using the Inverse Distance Weight (IDW) method. This deterministic algorithm,
513 22 available into GIS environment, is a spatial interpolation method for multivariate analysis of points
514 23 in a defined area. The usefulness of this method arises from the need to extrapolate reliable values
515 24 where they are missing. Compared to other methods, IDW has the advantage of being easy to
516 25 use. It requires: *i*) the definition of few contour parameters; *ii*) allows the estimation of the
517 26 phenomenon at a given point; *iii*) shows anomalous cases attributable to specific situations which
518 27 should be deepened, from time to time, to produce realistic output isodistribution maps.

524 28 Main disadvantages of IDW method are: absence of estimation of the error associated to
525 29 the interpolation process and the strong dependence of the samples distribution on interpolation
526 30 reliability. The output cartography, being deterministic, provides for the measured points a value
527 31 equal to the one actually observed. The result of the interpolation is a surface in raster format,
528 32 function of the spatial coordinates *x* and *y* which represents the value assumed by each single
529 33 parameter considered in the interpolation space. Considering the dimensions of the investigated
530 34 area and the distribution of samples, the size of the output grid cell we have adopted was one km
531 35 per side.
532 36
533 37
534 38
535 39

537 39 **7. Geological and hydrogeological setting of southern Italy**

538
539
540

541
542
543
544
545
546
547
548
549
550
551
552
553
554
555
556
557
558
559
560
561
562
563
564
565
566
567
568
569
570
571
572
573
574
575
576
577
578
579
580
581
582
583
584
585
586
587
588
589
590
591
592
593
594
595
596
597
598
599
600

1
2
3
4
5
6
7
8
9
10
11
12
13
14
15
16
17
18
19
20
21
22
23
24
25
26
27
28
29
30
31
32
33
34
35
36
37
38

Southern Italy is located in between the African and Eurasian tectonic plates, whose collisional boundary is located somewhere in the southern Tyrrhenian Sea and the north-east sector of Sicily (*Taormina line*; Fig. 3). Its territory includes all possible geodynamic environments: *i*) trusting chains (*i.e.*, *Apennines* and *Magrebids*), *ii*) stable trusted crystalline Paleozoic block (*i.e.*, *Sardinia-Corsica Massif*), *iii*) trusted-long drifted and still trusting Alpine crystalline blocks (*i.e.*, *Calabrids*), *iv*) back-arc micro oceans still under formation (*i.e.*, the *Tyrrhenian Sea*), *v*) rifting areas (*i.e.*, *Sicily Channel*) and related volcanism (Pantelleria Island), *vi*) active subduction of oceanic crust (*i.e.*, northwestward subducting Mesozoic Ionian basin underneath the Calabrian Arc) *vii*) transpressive faults (among the many, the *Ancona line*, the *Sanginetto line*, etc), *viii*) active andesitic arc volcanism (*i.e.*, *Aeolian Arc*) and, finally, *ix*) stable foreland areas (*Iblean*, *Pelagian* foreland in Sicily and *Apulian* foreland along the southern Adriatic Sea). All these tectonic units and geodynamic environments are shown in figure 3.

Apart from stable flat foreland areas, the territory is characterized by a rugged morphology, strong seismicity (*e.g.*: [Chiarabba et al., 2005](#)) and active or recent volcanism. The latter produced and still produces rocks of extremely different composition: from calc-alkaline in the Aeolian Arc ([Barberi et al., 1974](#)), to strongly silica undersaturated, the latter being K-rich (*leucitites*) in the Roman and Neapolitan volcanic province ([Washington, 1906](#)) and Na-rich (*pantellerites*) on Pantelleria Island in the Sicily Channel. New oceanic basaltic crust is actively forming (*e.g.*: *Marsili* and *Palinuro* seamounts; Fig. 3) in the Tyrrhenian Sea ([Boccaletti and Manetti, 1978](#)), and recent Quaternary intraplate basalts are present both in Sardinia (*Logudoro*; [Peccerillo, 2005](#)) and Sicily (Etna volcano and Iblei Mts; [Peccerillo, 2003](#)) islands (Fig. 3).

The continental Apennines, Calabria and Sicily regions are characterized by a general strong tectonic compression, whereas the Tyrrhenian Sea and the Sicily channel are affected by extensional tectonic stresses. Such extension, due to the formation of the Tyrrhenian Sea as a back-arc basin after the south-west-directed subduction of the Adria Plate ([Boccaletti and Manetti, 1978](#)), is the ultimate reason for the presence of abundant Pliocene-Quaternary volcanism along the NW-SE trending peri-Tyrrhenian margin of Italy. Geochronological data for the main magmatic centres show that there is a general decrease in age from north to south, where volcanism is presently very active.

The main lithostratigraphic feature of Southern Italy is the presence of potential permeable geothermal regional reservoirs hosted inside widespread and thick Mesozoic platform and pelagic carbonate sequence ([Pescatore and Ortolani, 1979](#)). They are in places overlain by allochthonous pelitic low-permeability flysch series and Neogene sediments in the many NW-SW basins present and tectonic troughs, such as the *Bradanic* (Lucania) and *Caltanissetta* (Sicily), respectively (Fig. 3). The carbonate sequences are similar, in lithology, to the coeval unfolded *Apulian* and *Pelagian* (African) foreland sequences. Locally, when buried, the limestone may even host huge magmatic chambers, such as the supervolcano of the Phlegraean (*burning* in Greek) Fields ([Armenti et al.,](#)

601
602
603 1 1984) and Vesuvius areas (Barberi et al., 1981) in the Campania region.

604 2 This active volcanism is clearly associated with a strong geothermal potential and, this led
605 3 in the past to carry out successful (at least in terms of discovery of anomalous geothermal
606 4 gradients) geothermal drillings : i) in the Roman Co-magmatic Province (Fig. 3), at *Laterra* volcano
607 5 (Bertrami et al., 1984), *Torre Alfina* (Cataldi and Rendina, 1973) and *Sabatini Mts* (Cesano in
608 6 figure 4: Calamai et al., 1976; Funicello et al., 1979), ii) at *Ischia Island* (Penta and Conforto,
609 7 1951) and in the Neapolitan area (Carlino et al., 2012), iii) at *Vulcano Island* in the Aeolian volcanic
610 8 arc (Sommaruga, 1984) and iv) at *Pantelleria Island* in the Sicily Channel (Gianelli and Grassi
611 9 2001). On the contrary, unproductive (“cold”) wells have been drilled in the area between the
612 10 Roman and the Neapolitan volcanic areas, around the *Alban Hills* (Giordano et al., 2014) and
613 11 *Roccamonfina* (Watts, 1987) volcanoes, as well as in Sardinia east of the Quaternary basaltic
614 12 *Logudoro* volcanic area (Regione Autonoma Sarda, 2013).

615 13 The contemporary presence of buried thick carbonate sequences and shallow magma
616 14 chambers in many places triggers the formation of huge quantities of hydrothermal CO₂ (Kerrick,
617 15 2001), whose origin and discharge to the surface have been largely studied in the past (Panichi
618 16 and Tongiorgi, 1976; Minissale 1991; Chiodini et al., 1995; 2000; 2004;). At the same time, the
619 17 carbonate sequences form the highest mountains, that act as the main collector of rain (due to
620 18 their high permeability) in the Apennines, and the regional ground water flow that heads towards
621 19 the Tyrrhenian Sea apparently lowers the local heat flow. As a matter of fact, many springs that
622 20 emerge at the foot of the Apennines along the Tyrrhenian coast have huge discharges (up to
623 21 several m³/sec) of water of meteoric origin, with temperature of 8-10 °C (Minissale, 2004).
624 22 However, there are also several meso-thermal springs, with outlet temperature of about 20 °C, and
625 23 even more springs with higher temperature, whose thermalism is caused by horizontal advective
626 24 heat flushed along the circuit from the mountains to the sea (e.g.: Minissale and Vaselli, 2011;
627 25 Chiodini et al., 2013). Any eventual presence of active hydrothermal systems affected by such
628 26 regional circulation can be therefore easily hidden, as it happens, for example, along the southern
629 27 boundary of the famous Larderello geothermal field in Tuscany. In that case, suspended and
630 28 relatively cold unconfined aquifers (T° = 90-95 °C) hosted inside the outcropping limestones are
631 29 very close to the high temperature vapor-dominated (200-250 °C) area isolated from the steam-
632 30 dominated zone, by an effective sealed barrier (Ceccarelli et al., 1987; Minissale 1991a).

647 31 648 32 **8. Geographical distribution of thermal waters and gases**

649 33
650 34 In the European context, Central-Southern Italy is certainly the region with the highest
651 35 concentration of natural thermal springs, CO₂ emissions and active or fossil travertine deposits
652 36 (Minissale, 2004 and references therein). Such abundance is paralleled by the presence of several
653 37 active and dormant volcanic areas, evenly distributed from the Roman Volcanic Province in the
654 38 north, to the volcanic island of Pantelleria to the south. The position of thermal and gas emissions
655
656
657
658
659
660

661
662
663 1 considered in the present survey is shown in figure 3. Precise location and relative number in the
664 2 data bases (in italic for the gas data), region by region, are reported in figures 4 through 6.

666 3 In Latium and Campania regions, most springs and gases are located along the Tyrrhenian
667 4 coast, whereas in the Neapolitan area and in Sicily they are clearly associated with the several
668 5 volcanic islands at: Ischia, Stromboli, Vulcano, Lipari, Panarea and Salina and Pantelleria. Isolated
670 6 quiescent volcanoes, either located in the Tyrrhenian coastal sector (such as Roccamonfina, 70
672 7 km NW of Naples), or inside the Apennines (Vulture, 90 km ENE of Naples), as well as Iblei Mts in
673 8 Sicily, and Logudoro basalts in the northern sector of Sardinia have, at their surroundings, some
675 9 thermal and/or CO₂-rich gas emissions.

676 10 Among the thermal springs and the CO₂-rich gas vents not clearly related to volcanic or
677 11 geothermal areas, two different types need specific attention. The first one refers to isolated
678 12 manifestations located deep inside the Apennine chain, sometimes at high elevation, clearly
679 13 related to the several relevant E-W- or SW-NE-directed transpressive faults that cross Italy from
682 14 the Tyrrhenian coast to the Adriatic and Ionian coasts. Examples are along the Ancona-Anzio (#
683 15 22,33 in Fig. 4; [Pizzi and Galadini, 2009](#)), the Roccamonfina-Ortona (e.g.: # 55,97 in Fig. 5; [Milano
685 16 et al., 2008](#)) and the Sangineto (e.g.: # 124,152 in Fig. 6; [Totaro et al., 2014](#)) tectonic lines (Fig. 3).

687 17 The second group of thermal emissions refers to coastal thermal springs emerging a few
688 18 meters above the sea level, but sometimes even at sea level along the shoreline. Examples of this
689 19 group, on moving from north to south are: the Osa spring (# 6,9) located 90 km NW of Rome (Fig.
691 20 4), the Sineussiane springs (# 58-59,91) about 50 km NW of Naples (Fig. 5), the Terme Luigiane
692 21 (# 125,163) in the NW sector of Calabria (Fig. 6) and Ali and Termini Imerese (# 155,177) in Sicily
694 22 (Fig. 6). Sometimes this type of emergence occurs even in a foreland setting, such as the Santa
695 23 Cesarea spring (# 111-117,137 in Fig. 5; [Santaloia et al., 2016](#)) located at the extreme east heel of
696 24 Italy.

698 25 Both types of emissions, quite common worldwide, have a tectonic origin (e.g.: [Minissale et
699 26 al., 2000b](#)) and they are generally not connected with active geothermal areas. In fact, they have
701 27 generally a N₂-rich associated gas phase reflecting their strictly meteoric origin, or sometimes a
702 28 CH₄-rich phase when associated with hydrocarbon deposits. In Italy, they represent a minority
704 29 among the thermal emissions, but, locally, they may be present not far from active volcanoes.
705 30 Typical is the case of the Etna volcano that host CH₄ rich gas emission at the NW (# 191) and E (#
707 31 201) margins of the edifice (Fig. 6). Although these types of emissions, sometimes cold, are not
708 32 related to active hydrothermalism, they have been included for completeness in the databases and
710 33 in the following general discussion and diagrams.

711 34 712 35 **9. Geochemistry of waters** 713 36

715 37 As a general principle, the chemical composition of groundwater is largely controlled by the
716 38 reaction of water with rocks and minerals. Water is a solvent and, as such, is capable of dissolving
717
718
719
720

721
722
723 1 and interacting with organic and inorganic components of soils, minerals that make up
724 2 unconsolidated deposits (e.g.: sand and gravel), and with various types of bedrock (e.g.:
725 3 limestone, evaporite, crystalline rocks, volcanics). Dissolution of soil minerals from groundwater is
726 4 a process that can take days, years or centuries, depending on: *i)* the solubility of materials and
727 5 the kinetic of dissolution processes, *ii)* water/rock ratio; *iii)* groundwater residence time, *iv)* specific
728 6 surface of material (granulometry) *v)* physical-chemical characteristics, such as temperature, pH
729 7 and redox potential (Eh), *vi)* presence of acidic (*i.e.* CO₂) and/or reducing (*i.e.* H₂S) gases, *vii)*
730 8 presence of bacteria, etc.. All these factors control cations and anions contents in solution, as well
731 9 as their ionic ratios and contribute to the amount of the saline content (*i.e.* the total dissolved
732 10 solids, onward TDS) characterizing the different groundwater.

733 11 As reported in previous paragraphs, the hydro-geological setting of southern Italy is very
734 12 complex; aquifers are hosted by and interact with rocks having very different origin and
735 13 mineralogy. From sedimentary to volcanic and metamorphic environments, groundwater circulates
736 14 in sectors characterised by anomalous geothermal gradients, corresponding to fractured and/or
737 15 faulted areas and dissolve huge quantity of deep-originated CO₂ produced both in geothermal and
738 16 volcanic systems. Accordingly, springs, irrespective of their outlet temperature, display a
739 17 remarkable variety of chemical compositions as a function of the different geochemical processes
740 18 occurring along the hydrological paths. Considering these processes, the chemical composition of
741 19 water samples is described in terms of major ion contents, in: *i)* the [Langelier-Ludwig \(1942\)](#)
742 20 diagram of figure 7; *ii)* the Ca, Mg and Na+K ternary diagram (Fig. 8, right) and *iii)* the main anions
743 21 Cl, SO₄ and HCO₃ contents (Fig. 8, left). By comparison, the composition of seawater is also
744 22 reported. Due to the wide range in their outlet temperature (11-133 °C), the analysed waters were
745 23 arbitrarily divided into three groups: cold (<25°C), warm (25-50 °C) and hot (>50°C). The
746 24 classification diagrams indicate the occurrence of the following waters types:

747 25 Ca-HCO₃ - It is the chemical composition showed by the majority of cold waters, several
748 26 warm waters and few hot waters. Cold waters migrated through shallow hydrological circuits and
749 27 represent the early stage of the interaction between rain and local soil and bedrock. Ca-HCO₃ is
750 28 the likely original composition of the groundwater forming the thermal waters in Italy, as results
751 29 from isotopic data ([Minissale, 1991b](#)). Some cold waters (# 39-44, 55) of the Tyrrhenian side of
752 30 Latium and Campania regions spreading southwards from the Roman Comagmatic Province (RCP
753 31 onward) receive a huge CO₂ input from depth; they have acidic pH and are enriched in Na and K
754 32 leached from volcanic rocks they interact with. Warm waters # 61, 108, 146, 150, 152, 222, located
755 33 in Campania, Sardinia and Sicily, dissolve a deep CO₂ gas phase in carbonate environments and
756 34 circulate in faulted areas. The different (*i.e.* deeper) depths reached by these hydraulic circuits,
757 35 with respect to the cold ones, are strongly emphasized by their outlet water temperatures (up to
758 36 37°C).

781
782
783 1 Ca-SO₄ - It is prevalently due to the dissolution of Triassic anhydrite beds at the base of the
784 2 Mesozoic carbonate sequence, which is particularly thick in the northern sector of the study area
786 3 ([Patacca et al., 2008](#)). Waters are quite exclusively warm-to-hot, and emerge mainly in: *i*) central
787 4 Italy (RCP, e.g.: # 4-5, 11, 15-21, 32, 35-37), showing high $p\text{CO}_2$, *ii*) main Apennines (# 1) as well
789 5 as in *iii*) northern and central Calabria (# 123, 126; [Duchi et al., 1991](#)). In sample # 126, gypsum-
790 6 rich formations are contained in the Mesozoic carbonates outcropping in a tectonic window
792 7 ([Italiano et al., 2010](#)).

793 8 Acidic (pH<2.9)-SO₄-dominated. They are represented by the near-boiling acidic pool of the
795 9 *Solfatara* area (# 65, 68; Phlegraean Fields) and # 175 located in the Vulcano island in Sicily. This
796 10 particular composition originated through rising magmatic gases (mainly H₂S) interacting with (and
797 11 heating) shallow meteoric waters. The oxidation of H₂S to H₂SO₄ (H₂S+2O₂ → 2H⁺+SO₄²⁻), driven
799 12 by atmospheric O₂, determines the sulphate signature and the very low pH conditions, which is the
800 13 cause of the absence of HCO₃ converted into volatile H₂CO₃.

802 14 Na-Cl - This composition contains the largest number of waters, irrespective of their
803 15 temperature, although hot samples are dominant. They have different salinity but mostly classified,
804 16 following [Freeze and Cherry \(1979\)](#), as brackish (1,000< TDS ≤10,000 mg/L) or saline (TDS
805 17 >10,000 mg/L) waters. Several processes, acting sometimes together, can be invoked to explain
808 18 the salinity. In particular:

- 809 19 *i*) mixing between freshwater and seawater for cold samples discharging along the shore line
810 20 (e.g.: # 47, 82, 109, 110, 112, 113, 117, 158);
812 21 *ii*) mixing between seawater, the latter sometimes modified through water-rock interaction at
813 22 high temperature, and hot deep saline waters [e.g.: # 58-59, 89, 97, 100, 141, 169-172, 181,
815 23 182, 203, 233; these waters discharge in the main hydrothermal basins of southern Italy: in
817 24 Campania (Ischia Is., Phlegraean Fields), Sardinia (Campidano graben) and Sicilian
818 25 volcanoes (Pantelleria Is., Panarea Is., Vulcano Is., Stromboli Is. ad Sciacca)];
820 26 *iii*) rising magmatic H₂S, SO₂, CO₂ and HCl interacting with shallow meteoric waters.
821 27 Representative of this group is thermal sample # 64 (Phlegraean Fields) where the chemical
822 28 features suggest a direct ascent of both gases and water from the “major upflow zone”
824 29 ([Giggenbach, 1988](#));
825 30 *iv*) high saline content (TDS>13,000 mg/L) waters stemming from brines associated with
827 31 hydrocarbons, as supported by high CH₄ concentrations in the gas phase associated with the
828 32 springs ([Madonia et al., 2011](#)). These weakly thermal samples are emitted by mud volcanoes
830 33 scattered in the territory, (# 56, 168, etc.);
831 34 *v*) interaction with marine sediments and/or mixing with formation/connate waters (<25 °C
833 35 samples: # 124, 129), as well as extensive and prolonged interaction with both metamorphic
834 36 and crystalline rocks (warm samples # 122, 125, 127, 128, 130, 131-136). These warm
836 37 waters discharge diffusely in Calabria ([Italiano et al., 2010](#)) mostly along regional fault
837
838
839
840

841
842
843 1 systems, and hot waters also issuing from the crystalline basement in the central part of
844 2 Sardinia (# 213 and 215; [Angelone et al., 2005](#)).

846 3 Na-HCO₃ - The origin of these waters (top right sector of Fig. 7) in the study area is due to
847 4 the interaction of CO₂-rich fluids with volcanic rocks, in which feldspars are converted to clays,
848 5 generating aqueous solutions typically rich in Na⁺(K⁺) and HCO₃⁻ (e.g.: [Drever, 1982](#)). These CO₂-
850 6 rich samples are representative of the waters discharging at the periphery of the main
852 7 hydrothermal systems ([Giggenbach, 1988](#)). Waters of this group are found in the most known CO₂
853 8 degassing areas of southern Italy: Campania (Phlegaeen Fields, Ischia Isl., Vesuvius volcano),
854 9 Sardinia (Campidano graben, Logudoro), Basilicata (# 119 and # 120), Sicily (Iblei Mts: # 161) and
856 10 Latium (e.g.: # 45 in the Alban Hills).

858 11 The Ca, Mg and Na+K triangular plot of figure 8 (right) and the Cl, SO₄ and HCO₃ triangular
859 12 plot in figure 8 (left) give an insight into the origin of the constituents of groundwater, highlighting
860 13 the various processes governing their chemistry. These plots achieve their goals by overcoming
862 14 the ambiguities presented by the Langelier-Ludwig diagram in where, for example, Cl and SO₄, as
863 15 well as Ca and Mg, are shown in pair. In addition to the information provided by figure 7, the
865 16 cations triangular plot allows: *i*) to recognize the progressive enrichment in both Na and K of the
866 17 CO₂-rich calcium-bicarbonate waters of Latium and Campania regions interacting with alkali-rich
868 18 volcanics; *ii*) to evidence the Mg peculiar enrichment of samples # 76, # 163, # 166 ad # 167,
869 19 relatively warm waters circulating in the Vesuvius and Etna volcanic areas where Mg is likely
870 20 brought into solutions through the leaching, in acidic environment, of ferromagnesian minerals
872 21 contained in the volcanic rocks; *iii*) to point out the noticeable differentiation between Ca-rich and
873 22 (Na+K)-rich hot waters; the former interacting with evaporites, while the latter mix with seawater
874 23 (samples close to the blue star) and/or undergo alkali enrichment via water-rock interaction
875 24 (samples towards the Na+K corner). Similar indications derive from warm waters, which result
878 25 more scattered in the plot due to possible mixing at various degree with freshwater or with the two
879 26 reported Ca-rich or Na(K)-rich hot end members.

881 27 According to [Giggenbach \(1988\)](#), the Cl, SO₄ and HCO₃ triangular plot in figure 8 highlights
882 28 the presence of characteristic fields, in which waters can be grouped and different chemical
883 29 processes assessed. Accordingly, we find: *i*) HCO₃ waters, typical of both volcanic (RCP,
884 30 Plegraeen Fields, Ischia Is., Vesuvius, Aeolian Archipelago, Pantelleria Is., Etna) and geothermal
887 31 (Campidano and Logudoro in Sardinia; Campania region; NE Sicily sector) areas, where
888 32 dissolution of large amounts of deep-derived CO₂ promotes intense leaching of the permeable
890 33 volcanic rocks (peripheral waters); *ii*) SO₄-dominated samples located in Lipari Is. and Plegraeen
891 34 Fields: waters are interpreted as being heated by H₂S-rich vapour exolved from deep geothermal
892 35 systems; *iii*) Cl-and-SO₄-rich waters characterized by high discharge temperatures, issuing from
894 36 the main geothermal systems located in southern Italy (Ischia Is., Plegraeen Fields, Aeolian

901
902
903 1 Islands, Pantelleria Is.); mass and heat exchange with hot water-bearing fluids are maximal in
904 2 these areas.

906 3 Summing up, water chemistry, in terms of anion, can be due to hot brines rising from
907 4 deeper hydrothermal reservoirs or evolving through a complex interplay of several processes, best
908 5 described as a mixing between a shallow meteoric component, hydrothermal fluids (both steam
909 6 and brines) and seawater. Na-Cl waters plotting close to the field of mature geothermal waters can
910 7 be considered the most representative of the deep thermal liquid reservoir (Giggenbach, 1988).

913 8 In term of isotopic composition of thermal emergences in southern Italy, the classic $\delta^{18}\text{O}$ - δD
915 9 diagram of figure 9 (left) reports, according to the number of available data, the average values for
916 10 each single site. The figure shows, apart from the Global Meteoric Water Line (GMWL; Craig,
918 11 1961), the Mediterranean and east Mediterranean meteoric water lines (Gat and Carmi, 1970) and
919 12 the recently assessed Sicilian meteoric line (Liotta et al., 2013). The figure also shows, for
920 13 comparison with samples, the position of the average composition of rainfall in Central Italy
922 14 (Minissale, 2004) and the average values of the entire set of considered spring data in Southern
924 15 Italy.

925 16 It is evident that the large majority of the samples, both: cold, warm or hot, are constrained
926 17 in the area delimited by the Global and the eastern Mediterranean water lines. A few samples,
928 18 especially if with associated vigorous CO_2 emissions (e.g.: #102) are quite shifted to the left of the
929 19 GMWL due to strong and prolonged ^{18}O exchange between water and CO_2 (Karolyte et al., 2017);
930 20 others lie to the right of the GWML if located in active volcanic areas [e.g.: # 68 in the Phlegraean
932 21 Fields (Cortecci et al., 1978); or # 184 in the Isle of Vulcano (Federico et al., 2010)] because of
934 22 typical high temperature ^{18}O shifts.

935 23 As already reported on a regional scale (Minissale, 1991b), several evaporation lines can
937 24 be drawn in those places where volcanic or geothermal systems are located near the Sea (e.g.:
938 25 Sciacca in Sicily; Capaccioni et al., 2011). To go a little deeper into this mixing process near the
940 26 Mediterranean Sea, the δD -Cl diagram is shown in figure 9 (right). The figure shows several
941 27 possible mixing lines, in particular the mixing lines with low elevation rainfalls and high elevation
943 28 rainfalls, in the area between which, most samples are located. A few samples are in quite
944 29 anomalous position, such as the S.ta Cesarea (# 112, 115, 116; location in Fig. 5) and the mud
946 30 pond inside the Solfatara crater (# 65); the first with excess chlorine with respect to the
947 31 Mediterranean Sea possibly related to hydrocarbon deposits (Santaloia et al., 2016), the latter for
949 32 strong local evaporation of steam condensate of the near Solfatara fumarole. It is worth noting that
950 33 all active volcanic islands [Ischia (e.g # 83), Vulcano (e.g.: # 184) and Pantelleria (e.g.: # 203)
951 34 islands], where there are sufficient samples to derive local evaporation lines, have relevant
953 35 portions of seawater inflows into their hydrothermal circuits (systems).

955 36 956 37 **10. Geochemistry of gases** 957 38

961
962
963 1 In the regions of Italy under investigation, free CO₂ gas is normally found associated with
964 2 the ground water (Minissale, 2004 and literature therein cited), as described in the previous
965 3 section, even at sites located far away from active volcanic areas or from hydrothermal systems
966 4 associated with volcanism.

969 5 Apart from CO₂, atmospheric gases (chiefly N₂ and Ar) can also be found in Southern Italy
970 6 thermal waters, being at times the only gas species dissolved (e.g.: Minissale et al., 2000a). This is
971 7 due to their abundance in rainwater recharging the carbonate aquifers, as well as to the
972 8 remarkable thickness and the high permeability of the carbonate rocks making up the Apennines.
973 9 Another common gas continuously forming inside the sometimes very thick Neogene sediments, is
974 10 CH₄ (Mattavelli and Novelli, 1987). Generally it accumulates and diffuses by escaping from over-
975 11 pressurized buried hydrocarbon reservoirs, or from bacterial reduction of organic matter in a
976 12 shallow subaerial environment (Schoell, 1988).

981 13 Three major components alone of the gas phase above described (i.e., CO₂, N₂ and CH₄)
982 14 usually represent >98% in concentration of all natural gas manifestations, being either associated
983 15 with thermal waters or bubbling through cold superficial water or through focused gas vents or
984 16 diffusely from the soil. The CO₂ vs. N₂ diagram of figure 10 shows that the large majority of the gas
985 17 samples from hydrothermal areas displays two opposite compositions, one with CO₂ >90% and the
986 18 other with N₂ > 80%, with a clear mixing line between these two gases. Only a few samples plot
987 19 along another mixing line between N₂ > 80% and N₂ < 25%, being CO₂ always lower than 10%.
988 20 These samples show a prevailing CH₄ composition and are mostly from mud volcanoes located
989 21 into sedimentary basins. The main compositional dualism of hydrothermal gases is a consequence
990 22 both of the upward convective motion of high-enthalpy fluids rich in CO₂, which is readily released,
991 23 and of the concurrent downward gravitational motion of cold recharge waters, rich in N₂, mostly
992 24 coming from the superficial carbonate formations. As the recharge water from the carbonate
993 25 mountains in the Apennines gets deeper and hotter along the flowing towards the Tyrrhenian
994 26 coast, it releases N₂ due to its decreased solubility (Minissale et al., 1997a). This explains why
995 27 most of the N₂-rich samples in figure 10 are from dissolved gases from water springs or wells,
996 28 whereas most of the CO₂-rich samples are from free gas emissions like mofettes and hot
997 29 fumaroles.

1000 30 Regarding CO₂, the isotopic ¹³C/¹²C ratio of carbon helps in discriminating among the
1001 31 different sources (Deines et al., 1974) that may contribute to the total CO₂ released with
1002 32 hydrothermal fluids in Southern Italy. The CO₂ vs. δ¹³C_{CO2} diagram of figure 11 (top) shows that, as
1003 33 the CO₂ content increases in concentration, its isotope composition shows a clear trend towards
1004 34 more positive values, up to about +3.0 ‰ (PDB). The most positive δ¹³C_{CO2} values are in samples
1005 35 from fumaroles and mofettes, again underlining the more direct connection between free gases
1006 36 and deep hydrothermal sources of CO₂. This trend also suggests an increasing contribution of ¹³C-
1007 37 rich CO₂ from mantle fluids in samples of -7.0 < ¹³C < -4.0 range (Rollison, 1993), as well as a
1008
1009
1010
1011
1012
1013
1014
1015
1016
1017
1018
1019
1020

1021
1022
1023 1 contribution of isotopically much heavier CO₂ either from dissolution of limestones or from their
1024 2 metamorphism under hydrothermal conditions (Craig, 1963).

1026 3 Where available, we plotted the C-isotope values of free-gas CO₂ versus those of Dissolved
1027 4 Inorganic Carbon (D.I.C.) in the associated water or condensed steam phase (Fig. 11, bottom).
1028 5 Despite its largely empirical nature (the fractionation between the different species of carbon in
1029 6 solution depends on many parameters, such as pH and temperature), this correlation shows that a
1030 7 large number of samples, including all those from fumaroles and almost all from mofettes and mud
1031 8 volcanoes, have a C-isotope composition in the free-gas CO₂ abnormally enriched in the “heavy”
1032 9 isotope. According to Mook et al. (1974), at temperature above 120 °C the fractionation factor in
1033 10 water between gaseous CO₂ and dissolved HCO₃⁻ favours ¹³C enrichment in the residual gas
1034 11 phase, thus shifting the isotopic composition of carbon towards more positive values of δ¹³C_{CO2}.
1035 12 This points to an excess of free CO₂ in those samples, with the gas phase separated at
1036 13 temperature of up to about 300 °C (considering a maximum isotopic shift of 7-8‰; Mook et al.,
1037 14 1974). The free CO₂ gas would be in isotopic disequilibrium with that dissolved in water and the
1038 15 disequilibrium would be kept in the rising gas, particularly in that eventually issued from mofettes
1039 16 and fumaroles, because of its high velocity of motion towards the surface.

1041 17 If we consider the δ¹³C_{CO2} versus δ¹³C_{CH4} (Giggenbach, 1982) plot (Fig. 12), the theoretical
1042 18 lines of isotope fractionation at increasing temperatures (Bottinga, 1969), suggest that, as
1043 19 observed for Larderello and in general for central-northern Apennines (Minissale et al., 2000a),
1044 20 the origin of CH₄ for most of the samples in Southern Italy is abiogenic, and in some cases
1045 21 thermogenic. Figure 12 shows also that, as already suggested from literature (Tassi et al., 2012),
1046 22 methane from most of the mud volcanoes of Sicily and, more generally, from CH₄-dominant gas
1047 23 emissions, is biogenic. In fact, both δ¹³C_{CO2} and δ¹³C_{CH4} values from those samples are highly
1048 24 negative.

1049 25 Another gas species that gives valuable information on the origin of the fluids is helium. In
1050 26 general, high content of He in a gas phase at the surface indicates long residence time of the
1051 27 parent fluid within the crust, due to the α-decay of U-Th radiogenic chains. The relative abundance
1052 28 of ³He and ⁴He in gas samples provides clues to the possible contribution of magmatic/mantle gas.
1053 29 Figure 13 (left) shows the correlation between the two He isotopes. Despite the general good
1054 30 correlation between them, ³He is clearly enriched in samples of fumarole gases in volcanic areas,
1055 31 as expected. The R/Ra values plotted versus the respective ³He contents (Figure 13, right),
1056 32 however, show no strong correlation between the two parameters, especially for dissolved gas
1057 33 samples. This is explained by massive input of ⁴He constantly produced by radioactive decay in
1058 34 the crust. This isotope, therefore, accumulates in “old” gases, typically associated with long-lasting
1059 35 water circulation into the Mesozoic limestone and emerging as thermal springs prevalently at low
1060 36 topography at the edges of the coastal outcropping areas. In any case, R/Ra values higher than
1061 37 2.0 were found in samples from volcanic fumaroles and the highest values measured were slightly
1062 38

1081
1082
1083 1 higher than 7.0 (maximum R/Ra = 7.32 at Pantelleria Island; [Parello et al., 2000](#)). These values are
1084 2 very close to those typical of a MORB-type source (8.0 ± 1.0 Ra, according to [Gautheron and](#)
1086 3 [Moreira, 2002](#)), which once more testifies the marked influence of magmatic/mantle fluids in the
1087 4 development of geothermal conditions in southern Italy.

1089 5 **11. Geothermometry**

1090 6 Brief notes on the geothermometric significance of data are presented in this paragraph
1093 7 with the aim of helping and reinforcing the geothermal assessment of individual areas in Southern
1094 8 Italy.

1095 9
1096 10 By following the approach of [Giggenbach \(1986; 1988\)](#) we show in Fig. 14 its popular K-Na-
1097 11 Mg ternary diagram applied to the springs and fumaroles data with temperature > 25 °C only,
1098 12 divided in two groups: <50 °C and >50 °C, respectively. The diagram is based on the assumption
1099 13 that, in a hydrothermal system of average crustal composition, the K/Na ratio increases according
1100 14 to the equilibrium between K-feldspar and plagioclase, and Mg is removed during the precipitation
1102 15 of chlorite and muscovite at high temperature, increasing therefore the K/Mg ratio, as a second
1103 16 geothermometer ([Giggenbach, 1991](#)). A full equilibrium line is defined with Na, K and Mg
1105 17 concentrations fixed by temperature, whereas the line of rock dissolution represents the natural
1106 18 evolution, over time, of cold groundwater composition at fixed Na/K ratio, typically at very low
1108 19 temperature. The main drawback of this diagram is that: the addition of even small quantities of
1109 20 cold, Mg-rich, shallow, cold waters (mixing) to deep hydrothermal rising fluids, easily shifts the
1111 21 original compositions from the full equilibrium line towards the Mg corner. This shifting actually
1112 22 strongly reduces the possibility of interpretation of springs data in terms of geothermometry, even
1114 23 in places where the composition of fluids produced by geothermal wells is well known (e.g. Mt.
1115 24 Amiata geothermal field in Tuscany; [Minissale et al., 1997b](#)).

1117 25
1118 26 The diagram applied to all considered samples, including fumarolic condensates, shows
1119 27 that there is only one sample from Pantelleria Island (# 205; data from [Gianelli and Grassi, 2001](#))
1121 28 that lies along the left side of the full equilibrium curve at high temperature (260 °C), and the
1122 29 reason is that this is the only sample reported in the data base coming from a deep geothermal
1124 30 well, and therefore likely “free” from shallow cold contamination or mineral precipitation. On the
1125 31 cold right side of the equilibrium curve there are several samples, mostly emerging from the
1127 32 crystalline rocks of Calabria (#127, 130, 136) and Sardinia (# 217, 226, 215, 216), in areas of
1128 33 normal thermal gradients. They are all characterized by having nitrogen as associated gas phase,
1130 34 and they really represent fully equilibrating, deep circulating solutions. All of them are associated to
1131 35 relevant fault systems both in Sardinia ([Angelone et al., 2005](#)) and Calabria regions ([Italiano et al.,](#)
1133 36 [2010](#)).

1134 37 As often happens when applying this diagram to potential geothermal areas, there are a lot
1135 38 of samples lying near the Mg corner, and not much can be derived from them in terms of
1137
1138
1139
1140

1141
1142
1143 1 geothermometric interpretation. In these samples, the mixing with Mg-rich shallow components
1144 2 prevails over the deep Mg-depleted hot component. Then, there are also quite a lot of samples
1145 3 located in the partial equilibrium and/or dilution area, and at least one possible regional mixing line
1146 4 can be drawn, suggesting a common deep component at 180°C in many places, including
1147 5 Pantelleria (p), Ischia (i) and Vulcano (Vu) islands, as well as Phlegraean Fields (s). Two more
1148 6 mixing lines are possible, one pointing to 260 °C, including Pantelleria (# 205), Ischia (# 91) and
1149 7 Phlegraean Fields (# 71), and the other to 320 °C for Vulcano (# 185) and Phlegraean Fields (# 64,
1150 8 69), respectively. Finally, the diagram shows several samples (mostly from shallow hot wells) in
1151 9 the Vesuvius aquifer (Ve) and Vulcano Island aquifer (Vu) lying directly on the rock dissolution line.
1152 10 This is, in general, the best indirect indication of a very high, local conductive heat flux. In fact, a
1153 11 shallow, hot, low salinity, HCO₃ in composition aquifer is likely related to very high secondary
1154 12 conductive heat flow, especially in volcanic areas (Minissale, 2018).

1155 13 As a general comment on this diagram, it seems that all active volcanic areas of Southern
1156 14 Italy have water samples in anomalous positions that suggest high deep temperatures, and that in
1157 15 many places, excluding Calabria and Sardinia regions, there are, possibly in the Mesozoic
1158 16 carbonate reservoir, temperatures around 180°C.

1159 17 A parallel geothermal evaluation to water samples is made using gas compositions in figure
1160 18 15. Again the chosen diagram is one of the several proposed by Giggenbach (1991; 1992; 1993)
1161 19 where the ratio of log(CH₄/CO₂) is plotted versus the log(H₂/Ar). The advantage of representing
1162 20 data with ratios of components is in the fact that ratios are relatively independent by the
1163 21 steam/water ratio, a parameter well known only for samples taken from wells. The diagram is
1164 22 constrained, at temperatures of geothermal interest, by the rock buffer given by the couple
1165 23 Fe²⁺/Fe³⁺ where the H₂/H₂O ratio ($R_H = \log(f_{H_2}/f_{H_2O})$ where f stands for fugacity) is assumed to be
1166 24 independent by temperature and fixed at a value of -2.8 (Giggenbach, 1987). The equilibrium
1167 25 curve, at boiling condition, limits a “two phase” area where liquid and vapour phases are
1168 26 coexisting. The large area between the boiling line and the gas compositions constrained by the
1169 27 lower temperature buffer *calcite-anhydrite*, gives an idea of: *i*) how samples are far from the
1170 28 equilibrium line in oxidizing conditions (H₂ converted to H₂O) and/or *ii*) how much is the addition of
1171 29 “shallow” biogenic CH₄ not deriving from the equilibrium CO₂+H₂=CH₄+H₂O. Actually, the iso-
1172 30 temperature lines shown in the diagram represent the relative proportions of H₂, CO₂, CH₄ and Ar
1173 31 of the latter reaction at different R_H values.

1174 32 As seen from the figure, there are only few samples taken from fumaroles (# 122, 215, 217,
1175 33 228 and 232) along the equilibrium line and the two phases area. All the remaining samples, either
1176 34 taken from springs, wells, mofettes and fumaroles, including all the fumaroles from the Etna
1177 35 volcano, plot far from the equilibrium line. It is noteworthy to note, that, although out of equilibrium,
1178 36 most fumaroles are located to the right of the 250 °C isoline, somehow corroborating what shown
1179 37 in Fig. 14 for waters, that the geothermal potential of all volcanic areas (excluding the Alban Hills,
1180
1181
1182
1183
1184
1185
1186
1187
1188
1189
1190
1191
1192
1193
1194
1195
1196
1197
1198
1199
1200

Roccamonfina and the Vulture volcanoes) is very high. There are gas samples from springs and mofettes, including those from the geothermal areas of Latium (e.g.: # 12, 20, 26, 32, etc) that, although far from the equilibrium line, cluster around the 200 °C isocontour line, and that this is, again, somehow paralleled with the 180 °C line of figure 20 for water samples.

12. Isodistribution maps of: P_{CO_2} (pCO_2) in liquid phase, CO_2 concentration and $\delta^{13}C$ of CO_2 in gas phase, total He and R/Ra in gas phase

As mentioned, CO_2 is a gas of relevant presence in Central and Southern Italy, whose origin and occurrence has been studied by several authors (Chiodini et al., 1995; 2004; Minissale, 1991b; 2004 and references therein). At the top of figure 16 is shown the isodistribution map of this component (in % by vol.) in the gas emissions and/or in the gas phase associated with springs (both hot and cold), from which is evident that the Roman and the Neapolitan volcanic areas and the volcanic areas of Sicily (Etna and Iblean Mts.) have strong and wide CO_2 anomalies. Such CO_2 anomalies encompass the volcanic areas and certainly derive from the dissolution of the buried Mesozoic limestone (Panichi and Tongiorgi, 1976), being the isotopic composition of carbon often $>-3.0 \delta^{13}C$ PDB (Fig. 16, centre) clearly overlapping the anomalous areas of CO_2 concentration. The calculated P_{CO_2} in springs (Fig. 16, bottom), no matter if cold, warm or hot, again overlaps the same areas, a further evidence of the anomalous emission of CO_2 Italy as already reported in the literature (e.g. Rogie et al., 2001). Certainly, the presence of active hydrothermal systems makes a primary role in the degassing and lateral diffusion inside and expulsion outside the regional carbonate reservoir, with strong and focused emissions along faults. For example, the Mefite d'Ansanto mofette (# 108) emits about 2,000 t/day of CO_2 to the atmosphere (Chiodini et al., 2010). Conversely, Fig. 16 (centre) shows also areas where the $\delta^{13}C$ of CO_2 is much lower (up to $<-20.0 \delta^{13}C$ PDB) than typical hydrothermal values (e.g.: in Calabria) as suggested also by the CO_2 - $\delta^{13}C$ in CO_2 diagram of figure 11. The reason is that, in southern (and central) Italy, CO_2 may also form by the alteration of organic material embedded in Neogene sediments above the Mesozoic limestone (Marini and Chiodini, 1994; Minissale et al., 1997a) and/or because of depletion of carbon-13 in multiple step phases of precipitation and re-dissolution of calcite in veins or fracture during the motion from the hydrothermal systems to the surface (Minissale et al., 2002b). Figure 11 also suggests that there are several samples in the $\delta^{13}C$ range of CO_2 rising from the mantle ($-8.0 < \delta^{13}C < -4.0$; Rollison, 1993) whose values do not differ much from the ratio of atmospheric CO_2 , as a result of equilibrium after long term Earth degassing. In this range there are several fumaroles from the quiescent volcanoes of Pantelleria Island (e.g.: # 228, 232) in the Sicily channel, and Ischia Island (e.g.: # 131) in the Neapolitan area, but most of all in the inactive Vulture volcano (e.g.: # 139) or the Logudoro basaltic area in northern Sardinia (# 236).

As regards the isodistribution map of the $^3He/^4He$ ratio, figure 17 (bottom) shows the very anomalous cases of Etna, Iblei Mts and Vulture volcanoes, characterized by strong "intra-

1261
1262
1263 1 *continent*” mantle degassing. Indeed, the lavas produced by these volcanoes are quite primitive
1264
1265 2 intraplate basalts. This list must include also the Pantelleria *rifting* volcano and the Aeolian Arc,
1266 3 both with abundant mantle degassing. On moving northwards in the Neapolitan and Roman
1267
1268 4 volcanic areas, there is an increase in crustal contamination in the mantle-derived magma, as
1269 5 revealed by the increase of the $^{87}\text{Sr}/^{86}\text{Sr}$ ratio (Polyak et al., 1979), with a contemporary decrease
1270
1271 6 of the $^3\text{He}/^4\text{He}$ ratio. The same correlation was later proposed by Tedesco (1997), Martelli et al.
1272 7 (2004) and Frezzotti et al. (2009) who suggested, generically, a northward increased assimilation
1273
1274 8 and melting of crust into the Tyrrhenian mantle. The crustal material comes from subducted slabs
1275 9 rich in carbonate rocks from the Adriatic (Adria)-Ionian (African) plates .

1276
1277 10 By comparing the isodistribution map of total He in the gas phase (Fig. 17, top) with the
1278 11 respective $^3\text{He}/^4\text{He}$ ratios (Fig. 17, bottom), the results shown in the diagram of figure 13 are more
1279 12 clear from a territorial point of view. There is apparently more crustal radiogenic helium-4 on
1280
1281 13 moving towards Calabria, but this is not supported neither by a similar decrease in the total CO_2
1282 14 emission nor by a positive isotopic shift of $\delta^{13}\text{C}$ of carbon in CO_2 . (Fig. 16). Being helium-4
1283
1284 15 decoupled (or diluted) by hydrothermal CO_2 , it is difficult to ascertain if the decarbonation of
1285 16 limestone occurs in a subducted slab, as suggested by Minissale (1991b) and Frezzotti et al.,
1286
1287 17 (2009), or at a much shallower crustal depth, as originally proposed by Panichi and Tongiorgi
1288 18 (1976). What is relevant, from a geothermal point of view, is that the northern geothermal fields of
1289
1290 19 Latium are located in areas where the $^3\text{He}/^4\text{He}$ ratio is always $<1.5 \text{ Ra}$, but where also crustal
1291 20 helium-4 is apparently low, because of the dilution by hydrothermal CO_2 . By putting these
1292
1293 21 observation together it is possible to affirm that in the Latium area there is no transpressive fault
1294 22 that is deep enough to reach the mantle, or, if any, it is sealed. Furthermore, it is reasonable that
1295 23 the local crust is likely characterized by granitization at depth, like in northern Tuscany (Boccaletti
1296
1297 24 et al., 1997), and that the anomalies of CO_2 are produced at shallow depth, inside the Mesozoic
1298 25 limestones.

1300 26 **13. Conclusive remarks**

1301 27
1302 28 The strong dynamics of the mantle at the boundary between the African and the Eurasian
1303 29 continental plates, especially at the eastern and southern edges of the Tyrrhenian Sea, is
1304 30 characterized by: subduction, extension, active volcanism, strong heat flux and shallow Moho
1305
1306 31 (Panza and Calcagnile, 1980). The concurrence of all these features make Southern Italy a perfect
1307 32 place for the presence of volcanoes, hydrothermal and geothermal systems. In fact, with the
1308
1309 33 exclusion of the stable cratonic granitic area of Sardinia and the foreland territories of Puglia and
1310 34 southeast Sicily (Iblean platform, Fig. 3), several high enthalpy areas are known to be present.
1311
1312 35 These areas coincide with the Latial volcanic districts (Roman Magmatic Province), active
1313 36 volcanoes around Naples (including Ischia Island and Phlegraean Fields) and with most of Sicilian
1314 37 volcanic islands (including those in the Channel of Sicily).
1315
1316 38
1317
1318
1319
1320

1321
1322
1323 1 The contemporary presence of shallow magma chambers and of a regional high permeable
1324 2 carbonate reservoir surrounding them, the latter being in many places several km thick ([Pescatore](#)
1326 3 [and Ortolani, 1973](#)), is the ultimate reason for the presence of a large number of thermal springs
1327 4 (additional material, table 1) and of hydrothermal discharges including active and fossil travertine
1328 4 deposits. These occur both on-shore and off-shore, the latter especially in the southern border of
1329 5 the Tyrrhenian Sea ([Lupton et al., 2011](#)).
1330 6

1332 7 Boiling fumaroles, with gas emissions at atmospheric pressure, are present at Stromboli,
1333 8 Ischia, Vesuvius, Lipari and Pantelleria Islands; superheated fumaroles are present at Vulcano
1334 8 Island and occasionally also at Etna summit crater(s). A steam-saturated ($T^{\circ} = 160^{\circ}\text{C}$) fumarole is
1335 9 permanently present at the Solfatara volcano in the Phlegraean Fields, 15 km north of Naples,
1336 10 which likely represents the surface expression of a shallow vapor-dominated system at the
1337 11 maximum enthalpic point ([Cioni et al., 1984](#)). These volcanic areas are evidently places of strong
1339 12 geothermal potential but, although deep hot wells have been drilled there at several places, a
1340 13 serious geothermal development plan has been achieved yet.
1342 14

1344 15 Some inactive and quiescent volcanoes, such as the Sabatini Mts (Cesano in Fig. 4) and
1345 16 Vulsini Mts volcanic districts, and Alban Hills volcanoes (last eruption 35 ka ago; [Fornaseri,](#)
1346 17 [1985](#)), located north and south of Rome, respectively, Roccamonfina (last eruption 50 ka; [Radicati](#)
1348 18 [di Brozolo et al., 1988](#)) or Vulture (140 ka; [Capaldi et al., 1985](#)) in the Apennines (Fig. 3), all have
1349 19 several CO_2 emission sites and cold natural sparkling mineral waters outpouring in their
1350 20 surroundings. In these places, geothermal exploration is still in its infancy, and it needs more
1351 21 investigations in the future, although deep temperature values from geothermometers in those
1352 22 areas are not promising. In fact, the two geothermometric diagrams shown in figure 14 and figure
1353 23 15 for waters and gases, respectively, do not suggest any anomalous temperature for samples
1354 24 from these areas, nor of the occurrence of high enthalpy fluids at shallow depth.

1358 25 If lower enthalpy fluids are considered, then the entire southern Italy including Sardinia
1359 26 (Logudoro volcanic area), with the only possible exclusion of Calabria, have high geothermal
1360 27 potential, as recently demonstrated for western Sicily ([Montanari et al., 2017](#)). In fact, although
1361 28 Mesozoic limestones are a preferential way for the infiltration of cold rain water through their
1362 29 outcrops, once in buried condition they allow a fast rise of fluids from convective systems residing
1363 30 deep into the often thick (several kilometres) Mesozoic platforms.

1367 31 Conversely, limestones also act as reservoirs for CO_2 formed inside the hydrothermal
1368 32 systems. This gas can exsolve and expand laterally in those places where the carbonate reservoir
1369 33 is covered by impermeable material, even moving far away from the hydrothermal systems
1370 34 themselves. In these cases, CO_2 is favoured by the strong regional continuity of the Mesozoic
1371 35 limestone series and it may naturally dilute the crustal ^4He formed. Therefore, low values of the
1372 36 total He/CO_2 ratio in the gas phase, especially when associated to occurrence of “*regional*” thermal
1373 37 springs emerging at the feet of the regional limestone reservoir, can be a good indication of
1374 38

1381
1382
1383 1 hydrothermal systems nearby. This is certainly true for the Latium and Campania geothermal
1384 2 areas where low He/CO₂ ratios are quite common in gas emissions, but it is less valid for the
1385 3 Sicilian volcanic islands, including Pantelleria, as well as for Etna volcano if their magma chambers
1386 4 are not connected with the Mesozoic limestone where CO₂ may accumulate in huge quantities.

1389 5 All Sicilian islands certainly have a high geothermal potential, partly already discovered,
1390 6 and most of them could produce geothermal power using small binary power plants, at least for the
1392 7 local consumption. Being the geothermal anomaly associated with those islands likely much larger
1393 8 than the islands themselves, exploration and exploitation of off-shore geothermal resources in the
1394 9 Tyrrhenian Sea and Sicily Channel, although not convenient at present, could be the target of
1396 10 future geothermal projects.

1398 11 **14. Acknowledgements**

1400 12 This work was financed by the Italian project "VIGOR" (<http://www.vigor-geotermia.it>)
1401 13 funded by the Italian Ministry of Economic Development and the Italian project "Atlante Geotermico
1402 14 del Mezzogiorno" (<http://atlante.igg.cnr.it>) funded by the Italian Council for Research.

1405
1406
1407
1408
1409
1410
1411
1412
1413
1414
1415
1416
1417
1418
1419
1420
1421
1422
1423
1424
1425
1426
1427
1428
1429
1430
1431
1432
1433
1434
1435
1436
1437
1438
1439
1440

1441
1442
1443 **15. References**
1444
1445

- 1446 4 Aiuppa A., Dongarrà G., Capasso G. and Allard P. (2000) Trace elements in the thermal
1447 5 groundwater of Vulcano Is. (Sicily). *J. Volcanol. Geothermal Res.* **98**, 189-207
1448 6 Aiuppa A., D'Alessandro W., Federico C., Palumbo B. and Valenza M. (2003) The aquatic
1449 7 geochemistry of arsenic in volcanic groundwaters from southern Italy. *Appl. Geochem.* **18**,
1450 8 1283-1296
1451 9 Aiuppa A., Allard P., D'Alessandro W., Giammanco S., Parello F. and Valenza M. (2004) Magmatic
1452 10 gas leakage at Mt. Etna (Sicily, Italy): relationships with the volcano-tectonic structures, the
1453 11 hydrological pattern and the eruptive activity. In: "Mt. Etna: Volcano Laboratory", A.G.U.
1454 12 *Geophys. Monograph Series* **143**, 129-145
1455 13 Alaimo R. (1984) Il bacino idrotermale di Sciacca. Nota III: Geotermia delle acque termali e
1456 14 modello di miscuglio per le acque emergenti. In: "Risorse Termali della Sicilia", Univ. of Palermo
1457 15 *Publish.*, 211-225
1458 16 Alaimo R. and Censi P. (1983) Determinazioni di $\delta^{18}\text{O}$ e di δD su campioni di acque sotterranee
1459 17 siciliane: implicazioni idrogeologiche e geotermiche. *Mineral. Petrog. Acta* **27**, 183-200
1460 18 Alaimo R., Carapezza M., Dongarrà G. and Hauser S. (1978) Geochimica delle sorgenti termali
1461 19 siciliane. *Rend. Soc. Ital. Mineral. Petrol.* **34**, 577-590
1462 20 Allard P., Maiorani A., Tedesco D., Cortecchi G. and Turi B. (1991) Isotopic study of the origin of
1463 21 sulfur and carbon in Solfatara fumaroles, Campi Flegrei caldera. *J. Volcanol. Geothermal Res.*
1464 22 **48**, 139-159
1465 23 Allard P., Jean-Baptiste P., D'Alessandro W., Parello F., Parisi B. and Flehoc C. (1997) Mantle
1466 24 derived helium and carbon in groundwater and gases of Mt. Etna, Italy. *Earth Planet. Sci. Lett.*
1467 25 **148**(3-4), 501-516
1468 26 Angelone M., Gasparini C., Guerra M., Lombardi S., Pizzino L., Quattrocchi F., Sacchi E. and
1469 27 Zuppi G.M. (2005) Fluid geochemistry of the Sardinian Rift-Campidano graben (Sardinia, Italy):
1470 28 faults segmentation, seismic quiescence of geochemically "active" faults, and new constraints
1471 29 for selection of CO₂ storage sites. *Appl. Geochem.* **20**, 317-340
1472 30 Aravena D. and Lahsen A. (2013) A geothermal favourability map of Chile: preliminary results.
1473 31 *Geothermal Resources Council, Transactions* **37**, 923-926
1474 32 Ármannsson H. (2012) Geochemical Aspects of Geothermal Utilization. In: "Comprehensive
1475 33 Renewable Energy", Sayigh A. (ed.), vol. 7., Oxford: Elsevier, 95-168
1476 34 Armienti P., Barberi F. and Innocenti F. (1984) A model of the Phlegraean Fields magma chamber
1477 35 in the last 10,500 years. *Bull. Volcanol.* **47**, 349-358
1478 36 Arnone G. (1979) Studio delle sorgenti termali del Lazio settentrionale. *Rend. Soc. Ital. Mineral.*
1479 37 *Petrol.* **35**, 647-666
1480 38 Balderer W., Martinelli G., Weise S. and Wolf M. (2000) ³He/⁴He anomalies in the Irpinia-Basilicata
1481 39 area (south Italy): geochemical signature of a seismically active region. *Bull. Idrogeol.* **18**, 147-
1482 40 160
1483 41 Baldi P. and Ferrara G.C. (1974) Hydrogeochemical features of the northern Latium (central Italy)
1484 42 with particular reference to the Stigliano thermal springs. *Proc. 1st Water-Rock Interaction Conf.,*
1485 43 *Prague, Czechoslovakia*, Sept. 1974, 3-11
1486 44 Baldi P., Ferrara G.C. and Panichi C. (1975) Geothermal research in western Campania (southern
1487 45 Italy): chemical and isotopic studies of thermal fluids in the Campi Flegrei. *Proc. 2nd UN Symp.*
1488 46 *on Geothermal Energy*, San Francisco USA, 20-29 May, 687-697
1489 47 Barbier E., Bellani S. and Musumeci F. (2000) The Italian geothermal database. *Proc. 2000 World*
1490 48 *Geothermal Congress*, May 28-June 10, Kyushu-Tohoku, Japan, 3,991-3,995
1491 49 Barberi F., Innocenti F., Ferrara G., Keller J. and Villari L. (1974) Evolution of Aeolian arc
1492 50 volcanism. *Earth Planet. Sci. Lett.* **21**(3), 269-276
1493 51 Barberi F., Bizouard H., Clocchiatti R., Metrich N., Santacroce R. and Sbrana A. (1981) The
1494 52 Somma-Vesuvius magma chamber: a petrological and volcanological approach. *Bull. Volcanol.*
1495 53 **44**(3), 295-315
1496 54 Barberi F., Carapezza M.L., Ranaldi M. and Tarchini L. (2007) Gas blowout from shallow
1497 55 boreholes at Fiumicino (Rome): induced hazard and evidence of deep CO₂ degassing on the
1498 Tyrrhenian margin of Central Italy. *J. Volcanol. Geothermal Res.* **165**(1-2) 17-31
1499
1500

- 1501
1502
1503 1 Barnes I., Irwin W. and White D. (1978) Global distribution of CO₂ and major zones of seismicity.
1504 2 *U.S. Geol. Surv., Open-File Report 78-39c*
- 1505 3 Battaglia A., Ceccarelli A., Ridolfi A., Frohlich K. and Panichi C. (1992) Radium isotopes in
1506 4 geothermal fluids in central Italy. *Proc. Intern. Symp. on Isotope Techn. in Water Resources*
1507 5 *Development, I.A.E.A., Wien, Austria, 363-383*
- 1508 6 Bencini A. and Duchi V. (1988) Boron content of thermal waters of Tuscany and Latium, central
1509 7 Italy. *Proc. 5th Water-Rock Interaction Conf., Reykjavik, Island, 8-17 Aug., 45-47*
- 1510 8 Bertrami R., Cameli M., Lovari F. and Rossi U. (1984) Discovery of Latera geothermal field:
1511 9 problems of the exploration and research. *Proc. Semin. on Utiliz. of Geothermal Energy for*
1512 10 *Electric Power Production, May 1984, Florence, Italy, 18pp*
- 1513 11 Bertrami R., Buonasorte G., Ceccarelli A., Lombardi S., Pieri S. and Scandiffio G. (1990) Soil
1514 12 gases in geothermal prospecting: two case histories (Sabatini Mts. and Alban Hills, Latium,
1515 13 Central Italy). *J. Geophys. Res.* **95**(B13), 21,475-21,481
- 1516 14 Billy J.R. (2009) Geothermal Resource of the United States. National Renewable Energy
1517 15 Laboratory for the US Department of Energy (<http://www.nrel.gov/gis/geothermal.html>)
- 1518 16 Boccaletti M. and Manetti P. (1978) The Tyrrhenian Sea and adjoining regions. In: "*The ocean*
1519 17 *basins and margins*", A.E.M. Nairn et al. (eds.), Plenum Press, New York, 149-200
- 1520 18 Boccaletti M., Gianelli G. and Sani F. (1997) Tectonic regime, granite emplacement and crustal
1521 19 structure in the inner zone of the Northern Apennines Tuscany, Italy: A new hypothesis.
1522 20 *Tectonophysics.* **270**, 127-143
- 1523 21 Bolognesi L. and D'Amore F. (1993) Isotopic variation of the hydrothermal system on Vulcano
1524 22 Island, Italy. *Geochim. Cosmochim. Acta* **57**, 2,069-2,082
- 1525 23 Bolognesi L., Noto P. and Nuti S. (1986) Studio chimico e isotopico della solfatara di Pozzuoli:
1526 24 ipotesi sull'origine e sulle temperature profonde dei fluidi. *Rend. Soc. Ital. Mineral. Petrol.* **41**,
1527 25 281-295
- 1528 26 Bottinga Y. (1969) Calculated fractionation factors for carbon and hydrogen isotope exchange in
1529 27 the system calcite - carbon dioxide - graphite - methane - hydrogen - water vapor. *Geochim.*
1530 28 *Cosmochim. Acta* **33**, 49-64
- 1531 29 Bove M.A., Ayuso R.A., De Vivo B., Lima A. and Albanese S. (2011) Geochemical and isotopic
1532 30 study of soils and waters from an Italian contaminated site: Agro Aversano (Campania). *J.*
1533 31 *Geochem. Explor.* **109**, 38-50
- 1534 32 Brusca L., Aiuppa A., D'Alessandro W., Parello F., Allard P. and Michel A. (2001) Geochemical
1535 33 mapping of magmatic gas-water-rock interactions in the aquifer of Mt. Etna volcano. *J. Volcanol.*
1536 34 *Geothermal Res.* **108**, 199-218
- 1537 35 Caboi R. and Noto P. (1982) Dati isotopici sulle acque termali e fredde dell'area del Campidano.
1538 36 In: "*Ricerche Geotermiche in Sardegna*", CNR-PFE, RF-10, PEG Publish., Rome, Italy, 124-132
- 1539 37 Caboi R., Cidu R., Fanfani L., Sitzia R. and Zuddas P. (1985) Considerazioni su alcuni elementi
1540 38 minori disciolti nelle acque termali della Sardegna. CNR-PFE, SI-4, PEG Publish., Rome, Italy,
1541 39 215-229
- 1542 40 Caboi R., Cidu R., Cristini A., Fanfani L. and Zuddas P. (1987) Studio geochimico delle acque
1543 41 termali di Casteldoria. CNR-PFE, SI-5, PEG Publish., Rome, Italy, 597-613
- 1544 42 Caboi R., Cidu R., Fanfani L. and Zuddas P. (1993) Geochemistry of the high pCO₂ waters in
1545 43 Logudoro, Sardinia, Italy. *Appl. Geochem.* **8**, 153-160
- 1546 44 Calamai A., Cataldi R., Dall'Aglio M. and Ferrara G.C. (1976) Preliminary report on the Cesano hot
1547 45 brine deposit (northern Latium, Italy). *Proc. 2nd U.N. Symp. on the Develop. and Use of*
1548 46 *Geothermal Energy*, 20-29 May 1975, San Francisco, USA, 305-313
- 1549 47 Calamai A., Cataldi R., Locardi E. and Praturlon A. (1977) Distribuzione delle anomalie
1550 48 geotermiche nella fascia preappenninica Tosco-Laziale (Italia). *Proc. Intern. Symp. Sobre*
1551 49 *Energia Geotermica en America Latina*, 16-23 Oct. 1976, Guatemala City, 189-229
- 1552 50 Calcagnile C. and Panza C.F. (1980) The main characteristics of the lithosphere-asthenosphere
1553 51 system in Italy and surrounding regions. *Pure Appl. Geophys.* **119**, 865-879
- 1554 52 Caliro S., Chiodini G., Avino R., Cardellini C. and Frondini F. (2005) Volcanic degassing at
1555 53 Somma-Vesuvio (Italy) inferred by chemical and isotopic signatures of groundwater. *Appl.*
1556 54 *Geochem.* **20**, 1,060-1,076
- 1556
1557
1558
1559
1560

1561
1562
1563
1564
1565
1566
1567
1568
1569
1570
1571
1572
1573
1574
1575
1576
1577
1578
1579
1580
1581
1582
1583
1584
1585
1586
1587
1588
1589
1590
1591
1592
1593
1594
1595
1596
1597
1598
1599
1600
1601
1602
1603
1604
1605
1606
1607
1608
1609
1610
1611
1612
1613
1614
1615
1616
1617
1618
1619
1620

Caliro S., Chiodini G., Moretti R., Avino R., Granieri D., Russo M. and Fiebig J. (2007) The origin of the fumaroles of La Solfatara (Campi Flegrei, south Italy). *Geochim. Cosmochim. Acta* **71**, 3,040-3,055

Calvi E., Del Chicca F., Fancelli R., Giorgi R., Nuti S. and Taffi L. (1990) Studio geochimico di acque termali della Sicilia occidentale: rapporto sulla campagna dell'Aprile 1990. *CNR(Italian Research Council)-IIRG (IGG) Internal Report 7009*, Pisa (Italy), 7pp

Camarda M. (2004) Soil CO₂ Flux measurements in volcanic and seismic areas: laboratory experiments and field applications. *PhD Thesis, University of Palermo (Italy)*

Capaccioni B., Vaselli O., Tassi F., Santo A. and Delgado-Huertas A. (2011) Hydrogeochemistry of the thermal waters from Sciacca geothermal field (Sicily, Southern Italy). *J. Hydrol.* **396**, 292-311

Capaldi G., Civetta L. and Gillot P.Y. (1985) Geochronology of Plio-Pleistocene volcanic rocks from Southern Italy. *Ital. Soc. Mineral. Petrol. Rend.* **40**(1), 25-44

Capasso G., Favara R., Grassa F., Inguaggiato S. and Longo M. (2005) On-line technique for preparing and measuring stable carbon isotope of total dissolved inorganic carbon in water samples ($\delta^{13}\text{C-TDIC}$). *Annals of Geophysics* **48**, 159-166

Caracausi A., Favara R., Italiano F., Nuccio P.M. Paonita A. and Rizzo A. (2005a) Active geodynamics of the central Mediterranean sea: heat and helium evidences for a trans-tensional zone connecting the Sicily Channel to the southern Tyrrhenian Sea. *Geophys. Res. Lett.* **32**, doi:10.1029/2004GL021608

Caracausi A., Ditta M., Italiano F., Longo M., Nuccio M., Paonita A. and Rizzo A. (2005b) Changes in fluid geochemistry and physical-chemical conditions of geothermal systems caused by magmatic input: the recent abrupt outgassing of the Island of Panarea (Aeolian Islands, Italy). *Geochim. Cosmochim. Acta* **69**, 3,045-3,059

Caracausi A., Nicolosi M. and Nuccio M. (2013) Active degassing of mantle-derived fluid: a geochemical study along the Vulture line (Italy). *GeoGeoGeo* **14**(5), 1,605-1,625

Caracausi A., Paternoster M. and Nuccio M. (2015) Mantle CO₂ degassing at Mt. Vulture volcano (Italy): Relationship between CO₂ outgassing of volcanoes and the time of their last eruption. *Earth Planet. Sci. Lett.* **411**, 268-280

Carapezza M., Cusimano G., Liguori V., Alaimo R., Dongarrà G. and Hauser S. (1977) Nota introduttiva allo studio delle sorgenti termali dell'isola di Sicilia. *Boll. Soc. Geol. Ital.* **96**, 813-836

Carapezza M.L. and Federico C. (2000) The contribution of fluid geochemistry to the volcano monitoring of Stromboli. *J. Volcanol. Geotherm. Res.* **95**, 227-245

Carapezza M.L. and Tarchini L. (2007) Accidental gas emission from shallow pressurized aquifers at Alban Hills volcano (Rome, Italy): geochemical evidence of magmatic degassing ? *J. Volcanol. Geotherm. Res.* **165**, 5-16

Carapezza M.L., Badalamenti B., Cavarra L. and Scalzo A. (2003) Gas hazard assessment in a densely inhabited area of Colli Albani volcano (Cava dei Selci). *J. Volcanol. Geotherm. Res.* **123**, 81-94

Carapezza M.L., Barberi F., Tarchini L., Cavarra L. and Granieri D. (2005) Le emissioni gassose dell'area vulcanica dei Colli Albani. In: "Nuovi dati sull'attività recente del cratere del Lago Albano e sul degassamento dei Colli Albani". *Rend. Fis. Acc. Lincei.* **218**, 229-242

Carapezza M.L., Barberi F., Ranaldi M., Ricci T., Tarchini L., Barrancos J., Fischer C., Granieri D., Lucchetti C., Melian G., Perez N., Tuccimei P., Vogel A. and Weber K. (2012) Hazardous gas emissions from the flanks of the quiescent Colli Albani volcano (Rome, Italy). *Appl. Geochem.* **27**, 1,767-1,782

Carlino S., Somma R., Troise C. and De Natale G. (2012) The geothermal exploration of Campania volcanoes: historical review and future development. *Renew. & Sustain. Energy Rev.* **16**, 1,004-1,030

Carranza E.J.M., Wibowo H., Barritt S.D. and Sumintadireja P. (2008) Spatial data analysis and integration for regional-scale geothermal potential mapping West Java, Indonesia. *Geothermics* **37**, 267-299

Cataldi R. and Rendina M. (1973) Recent discovery of a new geothermal field: Alfina. *Geothermics* **2**, 106-116

Cataldi R., Mongelli F., Squarci P., Taffi L., Zito G. and Calore C. (1995) Geothermal ranking of Italian territory. *Geothermics* **24**, 115-129

- 1621
1622
1623 1 Ceccarelli A., Celati R., Grassi S., Minissale A. and Ridolfi A. (1987) The southern boundary of
1624 2 Larderello geothermal field. *Geothermics* **16**, 505-515
1625 3 Celico P., De Gennaro M., Ghiara M.R. and Stanzione D. (1979) Le sorgenti termominerali della
1626 4 valle del Sele (SA): indagini strutturali, idrogeologiche e geochemiche. *Rend. Soc. Ital. Mineral.
1627 5 Petrol.* **31**, 389-409
1628 6 Celico P., De Gennaro M., Ferreri M., Ghiara M.R. and Stanzione D. (1982) Geochemica delle
1629 7 sorgenti mineralizzate della Piana di Paestum (Campania, Italy). *Per. Mineral.* **51**, 249-274
1630 8 Chiarabba C., Jovane L. and Di Stefano R. (2005) A new view of Italian seismicity using 20 years
1631 9 of instrumental recordings. *Tectonophys.* **395**, 251-268
163210 Chiocchini U., Madonna S., Manna F., Puoti F. and Chimenti P. (2001) Risultati delle indagini
163311 sull'area delle manifestazioni termominerali di Viterbo. *Geol. Tecnica & Appl.* **1**, (1/4), 17-34
163412 Chiodini G. (1994) Temperature, pressure and redox conditions governing the composition of the
163513 cold CO₂ gases discharged in North Latium (Italy). *Appl. Geochem.* **9**, 287-295
163614 Chiodini G., Frondini F. and Ponziani F. (1995) Deep structures and carbon CO₂ degassing in
163715 central Italy. *Geothermics* **24**, 81-94
163816 Chiodini G., D'Alessandro W. and Parello F. (1996) Geochemistry of gases and waters discharged
163917 by the mud volcanoes at Paternò, Mt. Etna (Italy). *Bull. Volcanol.* **58**, 51-58
164018 Chiodini G., Frondini G., Cardellini C., Parello F. and Peruzzi L. (2000) Rate of diffuse carbon
164119 dioxide earth degassing estimated from carbon balance of regional aquifers: the case of central
164220 Apennine, Italy. *J. Geophys. Res.* **105**, 8,423-8,434
164321 Chiodini G., Marini L. and Russo M. (2001) Geochemical evidence for the existence of high-
164422 temperature hydrothermal brines at Vesuvio volcano, Italy. *Geochim. Cosmochim. Acta* **65**,
164523 2,129-2,147
164624 Chiodini G., Cardellini C., Amato A., Boschi E., Caliro S., Frondini F. and Ventura G. (2004) CO₂
164725 Earth degassing and seismogenesis in Central and Southern Italy. *Geophys. Res. Lett.* **31**, pp.
164826 L07615 1-4
164927 Chiodini G., Granieri D., Avino R., Caliro S., Costa A., Minopoli C. and Vilardo G. (2010a) Non-
165028 volcanic CO₂ Earth degassing: case of Mefite d'Ansanto (southern Apennines), Italy. *Geophys.
165129 Res. Lett.* **37**, doi.org/10.1029/2010GL04285
165230 Chiodini G., Caliro S., Cardellini C., Granieri D., Avino R., Baldini A., Donnini M. and Minopoli C.
165331 (2010b) Long-term variations of the Campi Flegrei (Italy) volcanic system as revealed by the
165432 monitoring of hydrothermal activity. *J. Geophys. Res.* **115**, doi:10.1029/2008JB006258
165533 Chiodini G., Caliro S., Cardellini C., Frondini F., Inguaggiato S. and Matteucci F. (2011)
165634 Geochemical evidence for and characterization of CO₂-rich gas sources in the epicentral area of
165735 the Abruzzo 2009 earthquake. *Earth Planet. Sci. Lett.* **304**, 389-398
165836 Chiodini G., Cardellini C., Caliro S., Chiarabba C. and Frondini F. (2013) Advective heat transport
165937 associated with regional Earth degassing in central Apennine (Italy). *Earth Planet. Sci. Lett.*
166038 **373**, 65-74
166139 Cinti D., Procesi M., Tassi F., Montegrossi G., Sciarra A., Vaselli O. and Quattrocchi F. (2011)
166240 Fluid geochemistry and geothermometry in the western sector of the Sabatini Volcanic District
166341 and the Tolfa Mts (Central Italy). *Chem. Geol.* **284**, 160-181
166442 Cinti C., Poncia P.P., Procesi M., Galli G. and Quattrocchi F. (2013) Geostatistical techniques
166543 application to dissolved radon hazard mapping: an example from the western sector of the
166644 Sabatini volcanic district and the Tolfa Mts (Central Italy). *Appl. Geochem.* **35**, 312-324
166745 Cinti D., Tassi F., Procesi M., Bonini M., Capecchiacci F., Voltattorni N., Vaselli O. and Quattrocchi
166846 F. (2014) Fluid geochemistry and geothermometry in the unexploited geothermal field of the
166947 Vicano-Cimino Volcanic District (Central Italy). *Chem. Geol.* **371**, 96-114
167048 Cinti D., Tassi F., Procesi M. et al. (2017) Geochemistry of hydrothermal fluids from the eastern
167049 sector of the Sabatini Volcanic District (central Italy). *Appl. Geochem.* **84**, 187-201
167150 Cioni R., Corazza E. and Marini L. (1984) The gas/steam ratio as indicator of heat transfer at the
167251 Solfatara fumaroles, Phlegraean Fields (Italy). *Bull. Volcanol.* **47**(2), 295-302
167352 Cioni R., Corazza E., Magro G., Guidi M. and Marini L. (1988) Reactive and inert gases in low
167453 temperature fumaroles (Aeolian Islands, Italy). *Rend. Soc. Ital. Mineral. Petrol.* **43**, 1,003-1,011
167554 Ciotoli G., Etiope G., Florindo F., Marra F., Ruggiero L. and Sauer P.E. (2013) Sudden deep gas
167655 eruption nearby Rome's airport of Fiumicino. *Geophys. Res. Lett.* **40**, 5,632-5,636
1677
1678
1679
1680

- 1681
1682
1683 1 CNR (1982a) Contributo alla conoscenza delle risorse geotermiche del territorio Italiano.
1684 2 *CNR(Italian Council for Research)-PFE, RF-13*, PEG Publish., Rome, Italy, (2 vol. and maps)
1685 3 CNR (1982b) Contributo alla conoscenza delle potenzialità geotermiche della Toscana e del Lazio.
1686 4 *CNR (Italian Council for Research)-PFE, RF-15*, PEG Publish., Rome, Italy, (1 vol. and maps),
1687 5 47pp
1688 6 Corazza A. and Lombardi L. (1995) Idrogeologia dell'area del centro storico di Roma. *Mem.*
1689 7 *Descrittive Carta Geol. d'Italia* **1**, 179-211
1690 8 Corniello A. (1988) Considerazioni su alcune acque minerali della provincia di Caserta. *Mem. Soc.*
1691 9 *Geol. Ital.* **41**, 1,053-1,063
169210 Cortecci G., Noto P. and Panichi C. (1978) Environmental isotopic study of the Campi Flegrei
169311 (Naples, Italy) geothermal field. *J. Hydrol.* **36**, 143-159
169412 Craig H. (1961) Isotopic variations in meteoric waters. *Science* **33**, 1,702-1,703
169513 Craig H. (1963) The isotopic geochemistry of water and carbon in geothermal areas. In: "*Nuclear*
169614 *Geology on Geothermal Areas*", E. Tongiorgi (ed.), Spoleto, Italy, 17-54
169715 Craig H., Lupton J.E. and Horibe Y. (1978) A mantle helium component in circum-Pacific volcanic
169816 gases: Hakone, the Marianas and Mt. Lassen. In: "*Terrestrial rare gases*", Alexander E.G. and
169917 Ozima M. (eds.), Central Academic Publish., Tokio, Japan, 3-16
170018 Cuoco E. (2004) Geochimica e geochimica isotopica delle acque sotterranee nell'area di
170119 Mondragone. *Unpubl. Thesis, 2nd Univ. of Naples*, Caserta, Italy
170220 Cuoco E., Minissale A., Di Leo M., Tamburrino S., Iorio M. and Tedesco D. (2017) Fluid
170321 geochemistry of the Mondragone hydrothermal systems (southern Italy): water and gas
170422 compositions vs. geostructural setting. *Intern. J. Earth Sci.* **106**, 2,429-2,444
170523 Dadomo A., Lemmi M., Martinelli G., Menichetti M. and Telesca L. (2013) Springwater continuous
170624 monitoring in the L'Aquila area in concomitance with the April 2009 seismic swarm in central
170725 Italy: constraining factors to possible deep-seated fluid emissions. *Chem. Geol.* **339**, 169-176
170826 D'Alessandro W., Parello F. and Valenza M. (1996) Gas manifestations of Mt. Etna area: historical
170927 notices and new geochemical data (1990-1993). *Acta Vulcanol.* **8**, 23-29
171028 D'Alessandro W., De Gregorio S., Dongarrà G., Gurrieri S., Parello F. and Parisi B. (1997)
171129 Chemical and isotopic characterization of the gases of Mt Etna (Italy). *J. Volcanol. Geothermal*
171230 *Res.* **78**, 65-76
171331 D'Alessandro W., Bellomo S., Brusca L., Fiebig J., Longo M., Martelli M., Pecoraino G. and
171432 Salerno F. (2009) Hydrothermal methane fluxes from the soil at Pantelleria island (Italy). *J.*
171533 *Volcanol. Geothermal Res.* **187**, 147-157
171634 Dall'Aglio M. (1966) Rilievo geochimico della Sicilia occidentale. *Rivista Mineraria Siciliana* **17**,
171735 n.100/102, 175-191
171836 Dall'Aglio M. (1970) Geochemistry of stream and groundwaters from western Sicily: the changes in
171937 spring water chemism after the 1968 earthquake. *Proc. Conf. Intern. on Acque Sotterranee*,
172038 E.S.A., Palermo, Italy, 226-239
172139 Dall'Aglio M., Duchi V., Minissale A., Guerrini A. and Tremori M. (1994a) Hydrogeochemistry of the
172240 volcanic district in the Tolfa and Sabatini Mts in central Italy. *J. Hydrol.* **154**, 195-217
172341 Dall'Aglio M., Pagani F. and Quattrocchi F. (1994b) Geochemistry of groundwaters in the Etna
172442 region before and after the paroxysmal phase of the eruption of Dec. 1991: implications for the
172543 geochemical surveillance of Mt Etna. *Acta Vulcanol.* **4**, 149-156
172644 D'Amore F., Panichi C., Squarci P., Bertrami R. and Ceccarelli A. (1979) Studio idrogeochimico dei
172745 sistemi termali della zona di Latera-Canino (Lazio settentrionale). *Proc. 1st Semin. Energia*
172846 *Geotermica*, CNR-PFE, SI-1, PEG Publish., Rome, Italy, 470-481
172947 D'Amore F., Fancelli R. and Caboi R. (1987) Observations on the application of geothermometers
173048 to some hydrothermal systems in Sardinia. *Geothermics* **16**, 271-282
173149 D'Amore F., Mussi M., Grassi S. and Alaimo R. (1995a) Pantelleria Island (Sicily, Italy): a gas
173250 geochemical survey. *Proc. 1995 World Geothermal Congress*, Florence, Italy, 1,007-1,012
173351 D'Amore F., Antonio A.D. and Lombardi S. (1995b) Considerazioni geochimiche e
173452 geotermometriche sul sistema idrotermale di Suio. *Geol. Romana* **31**, 319-328
173553 De Gennaro M., Ferreri M. Ghiara M.R. and Stanzione D. (1984) Geochemistry of thermal waters
173654 on the island of Ischia (Campania, Italy). *Geothermics* **13**, 361-374
173755 De Gregorio S., Diliberto I.S., Giammanco S., Gurrieri S. and Valenza M. (2002) Tectonic control
173856 over large-scale diffuse degassing in eastern Sicily (Italy). *Geofluids* **2**, 273- 284
1738
1739
1740

- 1741
1742
1743 1 Deines P., Langmuir D. and Harmon R.S. (1974) Stable carbon isotope ratios and the existence of
1744 2 a gas phase in the evolution of carbonate ground waters. *Geochim. Cosmochim. Acta* **38**,
1745 3 1,147-1,164
1746 4 Della Vedova B., Mongelli F., Pellis G., Squarci P., Taffi L. and Zito G. (1991) Heat-flow map of
1747 5 Italy. *C.N.R.-Italian Council for Research map*, Rome, Italy
1748 6 Dettori B., Fancelli R., Noto P. and Nuti S. (1979) Caratteristiche geochemiche delle acque
1749 7 profonde della Sardegna settentrionale. *Proc. 1st Semin. Energia Geotermica, CNR-PFE, SI-1*,
1750 8 *PEG publish*, Rome, Italy, 556-570
1751 9 Dettori B., Zanzari R. and Zuddas P. (1982) Le acque termali della Sardegna. In: "*Ricerche*
175210 *Geotermiche in Sardegna*", *CNR-PFE, RF-10, PEG publish*, Rome, Italy, 56-86
175311 Di Napoli R., Aiuppa A., Bellomo S., Brusca L., D'Alessandro W., Gagliano-Candela E., Longo M.,
175412 Pecoraino G. and Valenza M. (2009) A model for Ischia hydrothermal system: evidence from
175513 the chemistry of thermal groundwaters. *J. Volcanol. Geothermal Res.* **186**, 133-159
175614 Dongarrà G. and Hauser S. (1982) Isotopic composition of dissolved sulphate and hydrogen
175715 sulphide from some thermal springs of Sicily. *Geothermics* **11**, 193-200
175816 Dongarrà G., Hauser S., Alaimo R., Carapezza R. and Tonani F. (1983) Hot waters on Pantelleria
175917 Is.: geochemical features and preliminary geothermal investigations. *Geothermics* **12**, 49-63
176018 Doveri M., Lelli M., Marini L. and Raco B. (2010) Revision, calibration and application of the
176119 volume method to evaluate the geothermal potential of some recent volcanic areas of Latium,
176220 Italy. *Geothermics* **39**, 260-269
176321 Drever J.I. (1982) *The Geochemistry of Natural Waters. Prentice-Hall Publish.*, Englewood Cliffs,
176422 NJ, USA, 888pp
176523 Duchi V. and Minissale A. (1995) Distribuzione delle manifestazioni gassose nel settore
176624 peritirrenico tosco-laziale e loro interazione con gli acquiferi. *Ital. Soc. Geol. Bull.* **114**, 337-351
176725 Duchi V., Minissale A. and Romani L. (1985) Studio geochemico su acque e gas dell'area
176826 geotermica di Vico-M.ti Cimini. *Atti Soc. Tosc. Sci. Nat.* **92**, 237-254
176927 Duchi V., Minissale A. and Prati (1987a) Chemical composition of thermal springs, cold springs,
177028 streams and gas vents in the Mt. Amiata geothermal region (Tuscany, Italy). *J. Volcanol.*
177129 *Geothermal Res.* **31**, 321-332
177230 Duchi V., Minissale A., Ortino S. and Romani L. (1987b) Geothermal prospecting by geochemical
177331 methods on natural gas and water discharges in the Vulsini Mts. volcanic district, central Italy.
177432 *Geothermics* **16**, 147-157
177533 Duchi V., Paolieri M. and Pizzetti A. (1991a) Geochemical study on natural gas and water
177634 discharges in the southern Latium (Italy): circulation, evolution of fluids and geothermal potential
177735 in the region. *J. Volcanol. Geothermal Res.* **47**, 221-235
177836 Duchi V., Bencini A., Cortese G. and Minissale A. (1991b) Caratteristiche geochemiche dei fluidi
177937 della Calabria centro-settentrionale e loro potenzialità geotermiche. *Ital. Geol. Soc. Bull.* **110**,
178038 273-280
178139 Duchi V., Minissale A., Thompson M. and Campana M.E. (1994) Geochemistry of thermal fluids on
178240 the volcanic island of Pantelleria, southern Italy. *Appl. Geochem.* **9**, 147-160
178341 Duchi V., Minissale A., Vaselli O. and Ancillotti M. (1995) Hydrogeochemistry of the Campania
178442 region in southern Italy. *J. Volcanol. Geotherm. Res.* **67**, 313-328
178543 ENEL-Italian Electricity Agency (1988) *Inventario delle risorse geotermiche nazionali: indagine*
178644 *d'insieme sul territorio nazionale. Italian Ministry of Economic Development Report*, Rome, Italy,
178745 75pp
178846 ESMAP-Energy Sector Management Assistance Program (2012) *Geothermal handbook: planning*
178947 *and financing power generation. The World Bank Group Publish., Technical report 002/12*,
179048 Washington D.C., USA, 164pp
179149 Etiope G., Caracausi A., Favara R., Italiano F. and Baciù C. (2002) Methane emission from the
179250 mud volcanoes of Sicily (Italy). *Geophys. Res. Lett.* **29**, doi 10.1029/2001GL014340
179351 Fancelli R., Nuti S., Taffi L., Monteleone S. and Pipitone G. (1994) Studio idrogeochemico e termico
179452 per la valutazione della Sicilia occidentale. In: "*Inventario delle risorser geotermiche nazionali*",
179553 Italian Ministry for Industry and Commerce Report, Rome, Italy, 38pp
179654 Favara R., Grassa F., Inguaggiato S. and D'Amore F. (1998) Geochemical and hydrogeological
179755 characterization of thermal springs in western Sicily. *J. Volcanol. Geothermal Res.* **84**, 125-141
1797
1798
1799
1800

1801
1802
1803
1804
1805
1806
1807
1808
1809
1810
1811
1812
1813
1814
1815
1816
1817
1818
1819
1820
1821
1822
1823
1824
1825
1826
1827
1828
1829
1830
1831
1832
1833
1834
1835
1836
1837
1838
1839
1840
1841
1842
1843
1844
1845
1846
1847
1848
1849
1850
1851
1852
1853
1854
1855
1856
1857
1858
1859
1860

Favara R., Grassa F., Inguaggiato S. and Valenza M. (2001) Hydrogeochemistry and stable isotopes of thermal springs: earthquake related chemical changes along the Belice Fault (western Sicily). *Appl. Geochem.* **16**, 1-17

Federico C., Aiuppa A., Allard P., Bellomo S., Jean-Baptiste P., Parello F. and Valenza M. (2002) Magma-derived gas influx and water-rock interactions in the volcanic aquifer of Mt. Vesuvius, Italy. *Geochim. Cosmochim. Acta* **66**, 963-981

Fiebig J., Chiodini G., Caliro S., Rizzo A., Spangenberg J. and Hunziker J.C. (2004) Chemical and isotopic equilibrium between CO₂ and CH₄ in fumarolic gas discharges: generation of CH₄ in arc magmatic-hydrothermal systems. *Geochim. Cosmochim. Acta* **68**, 2,321-2,334

Finlayson J.B. (1992) A soil gas survey over Rotorua geothermal field, Rotorua, New Zealand. *Geothermics* **21**, 181-195

Fornaseri M. (1985) Geochronology of volcanic rocks from Latium (Italy). *Ital. Mineral. Petrol. Soc. Rend.* **40**, 73-105

Freeze R.A. and Cherry J.A. (1979) Groundwater. *Prentice-Hall Publish.*, Englewood Cliffs, N.J., USA, 604pp

Frezzotti M.L., Peccerillo A. and Panza G. (2009) Carbonate metasomatism and CO₂-lithosphere-asthenosphere degassing beneath the Western Mediterranean: an integrated model arising from petrological and geophysical data. *Chem. Geol.* **262**, 108-120

Fridman A.I. (1990) Application of naturally occurring gases as geochemical pathfinders in prospecting for endogenetic deposits. *J. Geochem. Explor.* **38**, 1-11

Fridriksson T., Padron E., Oskarsson F. and Perez N.M. (2016) Application of diffuse gas flux measurements and soil gas analysis to geothermal exploration and environmental monitoring: Example from the Reykjanes geothermal field, SW Iceland. *Renew. Energy* **86**, 1295-1307

Froncini F., Caliro S., Cardellini C., Chiodini G., Morgantini N. and Parello F. (2008) Carbon dioxide degassing from Tuscany and Northern Latium (Italy). *Global Planet. Change* **61**, 89-102

Funiciello R., Mariotti G., Parotto M., Preite-Martinez M., Tecce F., Toneatti B. and Turi B. (1979) Geology, mineralogy and stable isotope geochemistry of the Cesano geothermal field, Sabatini Mts. volcanic system (northern Latium, Italy). *Geothermics* **8**, 55-73

Gat J.R. and Carmi I. (1970) Evolution of the isotopic composition of atmospheric waters in the Mediterranean Sea area. *J. Geophys. Res.* **75**, 3,032-3,048

Gautheron C. and Moreira M. (2002) Helium signature of the subcontinental lithospheric mantle. *Earth Planet. Sci. Lett.* **199**, 39-47

Ghiara M.R. and Stanzione D. (1988) Studio geochimico sul sistema idrotermale dei Campi Flegrei (Campania, Italia). *Rend. Accad. Sci. Fis. Matem.* **55**, 61-83

Giammanco S., Palano M., Scaltrito A., Scarfi L. and Sortino F. (2008) Possible role of fluid overpressure in the generation of earthquake swarms in active tectonic areas: the case of the Peloritani Mts. (Sicily, Italy). *J. Volcanol. Geothermal Res.* **178**, 795-806

Gianelli G. and Grassi S. (2001) Water-rock interaction in the active geothermal system of Pantelleria, Italy. *Chem. Geol.* **191**, 113-130

Giggenbach W.F. (1982) Carbon-13 exchange between CO₂ and CH₄ under geothermal conditions. *Geochim. Cosmochim. Acta* **46**, 159-165

Giggenbach W.F. (1986) Graphical techniques for the evaluation of water/rock equilibration conditions by use of Na, K, Mg and Ca-contents of discharge waters. *Proc. 8th New Zealand Geothermal Work.*, 37-44

Giggenbach W.F. (1987) Redox processes governing the chemistry of fumarolic gas discharges from White Island, New Zealand. *Appl. Geochem.* **2**, 143-161

Giggenbach W.F. (1988) Geothermal solute equilibria: Derivation of Na-K-Mg-Ca geothermometers. *Geochim. Cosmochim. Acta* **52**, 2,749-2,765

Giggenbach W.F. (1991) Chemical techniques in geothermal exploration. In: "Application of Geochemistry in Geothermal Reservoir Development", F. D'Amore (ed.), UNITAR Publish., Rome, Italy, 119-144

Giggenbach W. F. (1992) The composition of gases in geothermal and volcanic systems as a function of tectonic setting. *Proc. 7th Int. Symp. Water-Rock Interaction*, Park City, USA, 873-878

Giggenbach W.F. (1993) Redox control of gas compositions in Philippine volcanic-hydrothermal systems. *Geothermics* **22**, 575-587

1861
1862
1863
1864
1865
1866
1867
1868
1869
1870
1871
1872
1873
1874
1875
1876
1877
1878
1879
1880
1881
1882
1883
1884
1885
1886
1887
1888
1889
1890
1891
1892
1893
1894
1895
1896
1897
1898
1899
1900
1901
1902
1903
1904
1905
1906
1907
1908
1909
1910
1911
1912
1913
1914
1915
1916
1917
1918
1919
1920

Giggenbach W.F., Minissale A. and Scandiffio G. (1988) Isotopic and chemical assessment of geothermal potential of the Colli Albani area, Latium region, Italy. *Appl. Geochem.* **3**, 475-486

Gino G.F. and Sommaruga C. (1953) Le manifestazioni idrotermali della Sicilia. *Rivista Mineraria Siciliana* **22/23**, 3-14

Giordano G., De Benedetti A., Bonamico A., Ramazzotti P. and Mattei M. (2014) Incorporating surface indicators of reservoir permeability into reservoir volume calculations: application to the Colli Albani caldera and the Central Italy geothermal province. *Earth Sci. Rev.* **128**, 75-92

Giustini F., Blessing M., Brilli M., Lombardi S., Voltattorni N. and Wildory D. (2013) Determining the origin of CO₂ and CH₄ in the gaseous emissions of the San Vittorino plain (central Italy) by means of stable isotopes and noble gas analysis. *Appl. Geochem.* **34**, 90-101

Grassa F. (2001) Geochemical processes governing the chemistry of groundwater hosted within the Hyblean aquifers (south-eastern Sicily, Italy). *Ph.D. Thesis, University of Palermo*, Palermo, Italy

Grassa F., Capasso G., Favara R. and Inguaggiato S. (2004) Molecular and isotopic composition of free hydrocarbon gases from Sicily, Italy. *Geophys. Res. Lett.* **31**, doi: 10.1029/2003GL019362

Grassa F., Capasso G., Favara R. and Inguaggiato S. (2006) Chemical and isotopic composition of waters and dissolved gases in some thermal springs of Sicily and adjacent volcanic islands, Italy. *Pure Appl. Geophys.* **163**, 781-807

Gurrieri S., Hauser S. and Valenza M. (1984) Indagine preliminare su alcune sorgenti termali della Calabria per una futura sorveglianza geochimica dell'attività sismica. *Miner. Petrogr. Acta* **28**, 101-122

Hernández P.A., Pérez N.M., Salazar J.M.L., Sato M., Notsu K. and Wakita H. (2000) Soil gas CO₂, CH₄, and H₂ distribution in and around Las Cañadas caldera, Tenerife, Canary Islands, Spain. *J. Volcanol. Geothermal Res.* **103**, 425-438

Hilton D.R., Hammerschmidt K., Look G. and Friedrichsen H. (1993) Helium and argon isotope systematics of the central Lau Basin and Vula Fa Ridge: Evidence of crust/mantle interactions in back-arc basin. *Geochim. Cosmochim. Acta* **57**, 2,819-2,841

Hooker P.J., Bertrami R., Lombardi S., O'Nions R.K. and Oxburgh E.R. (1985) Helium-3 anomalies and crust-mantle interaction in Italy. *Geochim. Cosmochim. Acta* **49**, 2,505-2,513

Hulston J.R. and Lupton J.E. (1996) Helium isotope studies of the geothermal fields in the Taupo volcanic zone, New Zealand. *J. Volcanol. Geothermal Res.* **74**, 297-321

Inguaggiato S., Pecoraino G. and D'Amore F. (2000) Chemical and isotopic characteristics of fluid manifestations of Ischia Is. (Italy). *J. Volcanol. Geothermal Res.* **99**, 151-178

INGV-Italian Institute for Geophysics and Volcanology (2006) GooGas Project: the catalogue of Italian gas emissions. Visible at: <http://googas.ov.ingv.it/>

Iovenitti J., Ibser F.H., Clyne M., Sainsbury J. and Callahan O. (2014) Spatial analysis and multi-criteria decision making for regional-scale geothermal favourability map. *Geothermics* **50**, 189-201

Italiano F., Martelli M., Martinelli G. and Nuccio M. (2000) Geochemical evidence of melt intrusions along lithospheric faults of the Southern Apennines, Italy: geodynamic and seismogenic implications. *J. Geophys. Res.* **105**, 13,569-13,578

Italiano F., Martelli M., Martinelli G. and Nuccio M. (2001) Significance of earthquake-related anomalies in fluids of Val D'Agri (Southern Italy). *Terra Nova* **13**, 249-257

Italiano F., Bonfanti L., Pizzino L. and Quattrocchi F. (2010) Geochemistry of fluids discharged over the seismic area of the southern Apennines (Calabria region, southern Italy): implications for fluid-fault relationships. *Appl. Geochem.* **25**, 540-554

Karolyte R., Serno S., Johnson G. and Gilfillan S.M.V. (2017) The influence of oxygen isotope exchange between CO₂ and H₂O in natural CO₂-rich spring waters: Implications for geothermometry. *Appl. Geochem.* **84**, 173-186

Kerrick D.M. (2001) Present and past nonanthropogenic CO₂ degassing from the solid Earth. *Rev. of Geophys.* **39**, 565-585

Koga A. (1982) The use of volatile constituents in geothermal fluids for assessing the type, potential and near surface permeability of a geothermal system: the Broadlands geothermal area, New Zealand. *Proc. 4th New Zealand Geothermal Work.*, 135-138

- 1921
1922
1923 1 Lan T., Yang T., Lee H., Chen Y., Chen C.H., Song S.R. and Tsao S. (2007) Compositions and
1924 2 flux of soil gas in Liu-Huang-Ku hydrothermal area, northern Taiwan. *J. Volcanol. Geothermal*
1925 3 *Res.* **165**, 32-45
1926 4 Langelier W. and Ludwig H. (1942) Graphical methods for indicating the mineral character of
1927 5 natural waters. *J. Amer. Water Assoc.* **34**, 335-352
1928 6 Liotta M., Grassa F., D'Alessandro W., Favara R., Gagliano-Candela E., Pisciotta A. and Scaletta
1929 7 C. (2013) Isotopic composition of precipitation and groundwater in Sicily, Italy. *Appl. Geochem.*
1930 8 **34**, 199-206
1931 9 Lupton J., de Ronde C., Sprovieri M., Baker E., Bruno P., Italiano F., Walker S., Faure K.,
193210 Leybourne M., Britten K. and Greene R. (2011) Active hydrothermal discharge on the
193311 submarine Aeolian Arc. *J. Geophys. Res.* **116**, B02102, doi:10.1029/2010JB007738
193412 Madonna P., Grassa F., Cangemi M. and Musumeci C. (2011) Geomorphological and geochemical
193513 characterization of the 11 Aug. 2008 mud volcano eruption at S. Barbara village (Sicily, Italy)
193614 and its possible relationship with seismic activity. *Nat. Hazards & Earth System Sci.* **11**, 1,545-
193715 1,557
193816 Magro G. and Pennisi M. (1991) Noble gases and nitrogen: mixing and temporal evolution in the
193917 fumarolic fluids of Vulcano, Italy. *J. Volcanol. Geothermal Res.* **47**, 237-247
194018 Magro G., Ruggieri G., Gianelli G. and Bellani S. (2003) Helium isotopes in paleofluids and
194119 present-day fluids of the Larderello geothermal field: Constraints on the heat source. *J.*
194220 *Geophys. Res.* **108**, DOI: 10.1029/2001JB001590
194321 Mamyrin B.A. and Tolstikhin I. (1984) Helium isotopes in nature. *Elsevier Publish.*, Amsterdam,
194422 The Netherland, 264pp
194523 Marini L. and Chiodini G. (1994) The role of carbon dioxide in the carbonate-evaporite geothermal
194624 systems of Tuscany and Latium (Italy). *Acta Vulcanol.* **5**, 95-104
194725 Mariucci M.T., Pierdominici S., Pizzino L., Marra F. and Montone P. (2008) Looking into a volcanic
194826 area: an overview on the 350 m scientific drilling at Colli Albani (Rome, Italy). *J. Volcanol.*
194927 *Geoterm. Res.* **176**, 225-240
195028 Martelli M., Nuccio M., Stuart F.M. Burgess R., Ellam R.M. and Italiano F. (2004) Helium-strontium
195129 isotope constraints on mantle evolution beneath the Roman Comagmatic Province, Italy. *Earth*
195230 *Planet. Sci. Lett.* **22**, 295-308
195331 Martinelli G., Cremonini S. and Samonati E. (2012) Geological and geochemical setting of natural
195432 hydrocarbon emissions in Italy. In: "Advances in Natural Gas Technology", Hamid Al-Magren
195533 (ed.), DOI: 10.5772/37446, 79-120
195634 Martini M., Giannini L., Buccianti A., Prati F., Legittimo P., Iozzelli P. and Capaccioni B. (1991)
195735 1980-1990: ten years of geochemical investigation at Phlegraean Fields (Italy). *J. Volcanol.*
195836 *Geoterm. Res.* **48**, 161-171
195937 Marty B. and Jambon A. (1987) C³He fluxes from the solid Earth: Implications for carbon
196038 geodynamics. *Earth Planet. Sci. Lett.* **83**, 16- 26
196139 Marty B., Trull T., Lussiez P., Basile I. and Tanguy J.C. (1994) He, Ar, O, Sr and Nd isotope
196240 constraints on the origin and evolution of Mt. Etna magmatism. *Earth Planet. Sci. Lett.* **126**, 23-
196341 39
196442 Mattavelli L. and Novelli L. (1987) Geochemistry and habitat of natural gases in Italy. *Proc. 13th*
196543 *Intern. Meeting on Organic Geochem. in Petroleum Explor.*, 21-25 Sept., Venice, Italy, 1-13
196644 Maucourant S., Giammanco S., Greco F., Dorizon S. and Del Negro C. (2014) Geophysical and
196745 geochemical methods applied to investigate fissure-related hydrothermal systems on the
196846 summit area of Mt. Etna volcano (Italy). *J. Volcanol. Geotherm. Res.* **280**, 111-125
196947 Milano G., Di Giovambattista R. and Ventura G. (2008) Seismic activity in the transition zone
197048 between Southern and Central Apennines (Italy): evidences of longitudinal extension inside the
197149 Ortona-Roccamonfina tectonic line. *Tectonophysics.* **457**, 102-110
197250 Minissale A. (1991a) The Larderello geothermal field: a review. *Earth Sci. Rev.* **31**, 133-151
197351 Minissale A. (1991b) Thermal springs in Italy: their relation to recent tectonics. *Appl. Geochem.* **6**,
197452 201-212
197553 Minissale A. (1992) Isotopic composition of natural thermal discharges on Vulcano Isl., southern
197654 Italy. *J. Hydrol.* **139**, 15-25
197755 Minissale A. (2004) Origin, transport and discharge of CO₂ in central Italy. *Earth Sci. Rev.* **66**, 89-
197856 141
1978
1979
1980

- 1981
1982
1983 1 Minissale A. (2018) A simple geochemical prospecting method in flat areas. *Geothermics* **72**, 258-
1984 2 267
1985 3 Minissale A. and Duchi V. (1988) Geothermometry on fluids circulating in a carbonate reservoir in
1986 4 north-central Italy. *J. Volcanol. Geothermal Res.* **35**, 237-252
1987 5 Minissale A. and Vaselli O. (2011) Karst springs as “natural” pluviometers: constraints on the
1988 6 isotopic composition of rainfall in the Apennines of central Italy. *Appl. Geochem.* **26**, 838-852
1989 7 Minissale A., Evans W.C., Magro G. and Vaselli O. (1997a) Multiple source components in gas
1990 8 manifestations from north-central Italy. *Chem. Geol.* **142**, 175-192
1991 9 Minissale A., Magro G., Vaselli O., Verrucchi C. and Perticone I. (1997b) Geochemistry of water
199210 and gas discharges from the Mt. Amiata silicic complex and surrounding areas (central Italy). *J.*
199311 *Volcanol. Geothermal Res.* **79**, 223-251
199412 Minissale A., Magro G., Tassi F., Vaselli O. and Frau F. (1999) The origin of gas emissions from
199513 Sardinia island, Italy. *Geochem. J.* **33**, 1-12
199614 Minissale A., Magro G., Martinelli G., Vaselli O. and Tassi F. (2000a) Fluid geochemical transect in
199715 the Northern Apennines (central-northern Italy): fluid genesis and migration and tectonic
199816 implications. *Tectonophysics.* **319**, 199-222
199917 Minissale A., Vaselli O., Chandrasekharam D., Magro G., Tassi F. and Casiglia A. (2000b) Origin
200018 and evolution of “intracratonic” thermal fluids from central-western peninsular India. *Earth*
200119 *Planet. Sci. Lett.* **181**, 377-394
200220 Minissale A., Kerrick D., Magro G., Murrell M.T., Paladini M., Rihs S., Sturchio N.C., Tassi F. and
200321 Vaselli O. (2002a) Geochemistry of Quaternary travertine in the region north of Rome (Italy):
200422 structural, hydrologic and paleoclimatic implications. *Earth Planet. Sci. Lett.* **203**, 709-728
200523 Minissale A., Vaselli O., Tassi F., Magro G. and Grechi G.P. (2002b) Fluid mixing in carbonate
200624 aquifers near Rapolano (central Italy: chemical and isotopic constraints. *Appl. Geochem.* **17**,
200725 1,329-1,342
200826 Minissale A., Donato A., Procesi M., Giammanco S. and Pizzino L. (2016) Dati e carte
200927 geochimiche del Mezzogiorno d’Italia. In: “*Atlante Geotermico per il Mezzogiorno d’Italia*”. CNR-
201028 Italian Council for Research Publish., Pisa, Italy, 120pp
201129 Moghaddam M.K., Samadzadegan F., Noorollahi Y., Sharifi M.A. and Itoi R. (2014) Spatial
201230 analysis and multi-criteria decision making for regional-scale geothermal favourability map.
201331 *Geothermics* **50**, 189-201
201432 Mook W.G., Bommerson J.C. and Staverman W.H. (1974) Carbon isotope fractionation between
201533 dissolved bicarbonate and gaseous carbon dioxide. *Earth Planet. Sci. Lett.* **22**, 169-176
201634 Montanari D., Minissale A. Doveri M., Gola G., Trumpy E., Santilano A. and Manzella A. (2017)
201735 Geothermal resources within carbonate reservoirs in western Sicily (Italy): A review. *Earth Sci.*
201836 *Rev.* **169**, 180-201
201937 Noorollahi Y., Itoi R., Fujii H. and Tanaka T. (2007) GIS model for geothermal resource exploration
202038 in Akita and Iwate prefectures, northern Japan. *Computers & Geosci.* **33**, 1,008-1,021
202139 Noorollahi Y., Itoi R., Fujii H. and Tanaka T. (2008) GIS integration model for geothermal
202240 exploration and well siting. *Geothermics* **37**, 107-131
202341 Nuccio P.M., Caracausi A. and Costa M. (2014) Mantle-derived fluids discharged at the Bradanic
202442 foredeep/Apulian foreland boundary: the Maschito geothermal gas emissions (southern Italy).
202543 *Marine & Petrol. Geol.* **55**, 309-314
202644 Nuti S., Fancelli R., Dettori B., Passino A. and D’Amore F. (1977) Il termalismo della provincia di
202745 Sassari: possibile modello della circolazione idrotermale di Casteldoria. *Ital. Geol. Soc. Bull.* **96**,
202846 491-504
202947 Nuti S., Caprai A. and Noto P. (1985) Hypothesis on the origin of steam and on the deep
203048 temperatures of the fluid of Pozzuoli Solfatarata (Campania, Italy). *Geothermal Resources*
203149 *Council, Transaction* **9**, 26-3
203250 O’Nions R.K. and Oxburgh E.R. (1988) Helium, volatile fluxes and the development of continental
203351 crust. *Earth Planet. Sci. Lett.* **90**, 331-347
203452 Ortolani F., De Gennaro M., Ferreri M., Ghiara M.R., Stanzione D. and Zenone F. (1981)
203553 Prospettive geotermiche dell’Irpinia centrale: studio geologico-strutturale e geochimico. *Ital.*
203654 *Geol. Soc. Bull.* **100**, 139-159
203755 Panichi C. and Tongiorgi E. (1976) Carbon isotopic composition of CO₂ from springs, fumaroles,
2038 mofettes, and travertine of central and southern Italy: a preliminary prospection method of
2039
2040

2041
2042
2043
2044
2045
2046
2047
2048
2049
2050
2051
2052
2053
2054
2055
2056
2057
2058
2059
2060
2061
2062
2063
2064
2065
2066
2067
2068
2069
2070
2071
2072
2073
2074
2075
2076
2077
2078
2079
2080
2081
2082
2083
2084
2085
2086
2087
2088
2089
2090
2091
2092
2093
2094
2095
2096
2097
2098
2099
2100

- geothermal areas. *Proc. 2nd U.N. Symp. on the Develop. and Use of Geothermal Energy*, 20-29 May 1975, San Francisco, USA, 815-825
- Panichi C., Bolognesi L., Ghiara M.R., Noto P. and Stanzione D. (1992) Geothermal assessment of the Island of Ischia (south Italy) from isotopic and chemical composition of the delivered fluids. *J. Volcanol. Geothermal Res.* **49**, 329-348
- Panza G.F. and Calcagnile G. (1979) The upper mantle structure in Balearic and Tyrrhenian bathyal plains and the Messinian salinity crisis. *PalaeoPalaeoPalaeo* **29**, 3-14
- Paonita A., Caracausi A., Iacono-Marziano G., Martelli M. and Rizzo A. (2012) Geochemical evidence for mixing between fluids exolved at different depths in the magmatic system of Mt Etna (Italy). *Geochim. Cosmochim. Acta* **84**, 380-394
- Paonita A., Federico C., Bonfanti G., Capasso G., Inguaggiato S., Italiano F., Madonia P., Pecoraino G. and Sortino F. (2013) The episodic and abrupt geochemical changes at La Fossa fumaroles (Vulcano Is., Italy) and related constraints on the dynamics, structure and composition of the magmatic system. *Geochim. Cosmochim. Acta* **120**, 158-178
- Parello F., Allard P., D'Alessandro W., Federico C., Jean-Baptiste P. and Catani O. (2000) Isotope geochemistry of Pantelleria volcanic fluids, Sicily Channel rift: a mantle volatile end member for volcanism in southern Europe. *Earth Planet. Sci. Lett.* **180**, 325-339
- Parkhurst D. and Appelo D.L. (1999) User's guide to PHREEQC (version 2): a computer program for speciation batch-reaction, one-dimensional transport and inverse geochemical calculations. *USGS Water-Resources Investigations, Report 99-4259*, Denver, CO (USA), 309pp
- Patacca E., Scandone P., Di Luzio E., Cavinato G.P. and Parotto M. (2008) Structural architecture of the central Apennines: Interpretation of the CROP 11 seismic profile from the Adriatic coast to the orographic divide. *Tectonics* **27**, doi:10.1029/2005TC001917
- Peccerillo A. (2003) Plio-Quaternary magmatism in Italy. *Episodes* **26**, 222-226
- Peccerillo A. (2005) Plio-Quaternary volcanism in Italy. *Springer-Verlag*, Berlin, West Germany, 364pp
- Penta F. and Conforto B. (1951) Risultati di sondaggi e di ricerche geotermiche nell'isola d'Ischia dal 1939 al 1943. *Annali di Geofisica* **4**, 43-93
- Pescatore T. and Ortolani F. (1979) Schema tettonico dell'Appennino Campano-Lucano. *Ital. Geol. Soc. Bull.* **92**, 453-472
- Phuong N.K., Harijono A., Itoi R. and Unoki Y. (2012) Water geochemistry and soil gas survey at Ungaran geothermal field, central Java, Indonesia. *J. Volcanol. Geothermal Res.* **229-230**, 23-33
- Piscopo V., Allocca V., Brusa G., Cesario M., Monetti V. and Pianese L. (2000) Il fronte sorgivo di Castellammare di Stabia (NA): variazione del grado di mineralizzazione delle acque per l'eterogeneità dell'acquifero carbonatico costiero. *Ital. Geol. Soc. Bull.* **119**, 567-580
- Piscopo V., Barbieri M., Monetti V., Pagano G., Pistoni S., Ruggi E. and Stanzione D. (2006) Hydrogeology of thermal waters in Viterbo area, central Italy. *Hydrogeol. J.* **14**, 1,508-1,521
- Pizzi A. and Galadini F. (2009) Pre-existing cross-structures and active fault segmentation in the northern-central Apennines (Italy). *Tectonophysics*. **476**, 304-319
- Pizzino L., Cinti D., Barbieri M., Galli G., Voltattorni N. and Quattrocchi F. (2003) The October 31 (MI 5.4) and November 1 (MI 5.0) 2002 Molise earthquakes (southern Italy): first results from fluid geochemistry. *EGS-AGU-EUG Joint Assembly, Nice, France, 6-11 April. Geophys. Res. Abstr.*, (5), NH 10, p.345
- Polyak B.G., Prasolov E.M., Buachidza G.I., Kononov V.I., Mamirin B.A., Surovtseva L.I., Khabarin L. V. and Yudenich V.S. (1979) Isotopic distribution of helium and argon isotopes of fluids in the Alpine-Apennine region and its relationship to volcanism. *Russ. Acad. Sci. Rep.* **247**, 1220-1225 (in Russian); 1981: *Doklady Earth Sci. Section* **247**, 77-81
- Poreda R. and Craig H. (1989) Helium isotope ratios in circum-Pacific volcanic arcs. *Nature* **338**, 473-478
- Procesi M., Buttinelli M. and Pignone M. (2015) Geothermal favourability mapping by advanced geospatial overlay analysis: Tuscany case study (Italy). *Energy* **90**, 1377-1387
- Radicati di Brozolo F., Di Girolamo P., Turi B. and Oddone M. (1988) ⁴⁰Ar-³⁹Ar and K-Ar dating of K-rich rocks from the Roccamonfina Volcano, Roman comagmatic Region, Italy. *Geochim. Cosmochim. Acta* **52**(6), 1,435-1,441

2101
2102
2103 1 Regione Autonoma Sarda (2013) L'energia geotermica. In: "*Piano energetico ambientale della*
2104 2 *Sardegna*", Assessorato dell'Industria Publ., Sardinia Administration, Cagliari, Italy, 227pp
2105 3 Rizzo A., Grassa F., Inguaggiato S., Liotta M., Longo M., Madonia P., Brusca I., Capasso G.,
2106 4 Morici S, Rouwet D. and Vita F. (2009) Geochemical evaluation of observed changes in
2107 5 volcanic activity during the 2007 eruption at Stromboli (Italy). *J. Volcanol. Geothermal Res.* **182**,
2108 6 246-254
2109 7 Rogie J., Kerrick D., Chiodini G. and Frondini F. (2000) Flux measurements of non-volcanic CO₂
2110 8 emission from some vents in central Italy. *J. Geophys. Res.* **105**, 8,435-8,445
2111 9 Rollinson H. (1993) Using Geochemical Data. *Longman Publish.*, London, UK,352pp
211210 Sacchi E., Zuppi G.M., Pizzino L., Quattrocchi F. and Lombardi S. (2008) Fluid geochemistry as
211311 indicator of tectonically-related, deep water circulations in the Sardinian Rift-Campidano Graben
211412 (Italy): New insights from environmental isotopes. *Aquatic Geochem.* **14**, 301-319
211513 Sano Y., Wakita H., Italiano F. and Nuccio M. (1989) Helium isotopes and tectonics in southern
211614 Italy. *Geophys. Res. Lett.* **16**, 511-514
211715 Santaloia F., Zuffianò L., Palladino G., Limoni P., Liotta D., Minissale A., Brogi A. and Polemio M.
211816 (2016) Coastal thermal springs in a foreland setting: the Santa Cesarea Terme system (Italy)
211917 *Geothermics* **64**, 344-361
212018 Sborgi U. and Giovannini F. (1944) Analisi di gas naturali di Ischia, dei Campi Flegrei, della Mofeta
212119 dei Palici, di Pietramala. *Ann. Chim. Appl. Ital.* **34**, 86-91
212220 Shoell M. (1988) Multiple origins of methane in the Earth. *Chem. Geol.* **71**, 1-10
212321 Sinclair A.J. (1991) A fundamental approach to threshold estimation in exploration geochemistry:
212422 probability plots revisited. *J. Geochem. Explor.* **41**, 1-22
212523 Skord J. (2013) Implications of shallow temperature and soil gas surveys at Lee-Allen geothermal
212624 system, Churchill County, Nevada. *Geothermal Resources Council, Transactions* **37**, 37-40
212725 Sommaruga C. (1984) Le ricerche geotermiche svolte a Vulcano negli anni 50. *Ital. Soc. Mineral.*
212826 *Petrol. Rend.* **39**, 355-366
212927 Tassi F., Capaccioni B., Caramanna G., Cinti D., Montegrossi G., Pizzino L., Quattrocchi F. and
213028 Vaselli O. (2009) Low-pH waters discharging from submarine vents at Panarea Island (Aeolian
213129 Is., south Italy) after the 2002 gas blast: origin of hydrothermal fluids and implications for
213230 volcanic surveillance. *Appl. Geochem.* **24**, 246-254
213331 Tassi F., Fiebig J., Vaselli O. and Nocentini M. (2012) Origins of methane discharging from
213432 volcanic hydrothermal, geothermal and cold emissions in Italy. *Chem. Geol.* **310-311**, 36-48
213533 Tedesco D. (1996) Chemical and isotopic investigations of fumarolic gases from Ischia island
213634 (southern Italy): evidences of magmatic and crustal contribution. *J. Volcanol. Geothermal Res.*
213735 **74**, 233-242
213836 Tedesco D. (1997) Systematic variations in the ³He/⁴He ratio and carbon of fumarolic fluids from
213937 active volcanic areas in Italy: evidence for radiogenic ⁴He and crustal carbon addition by the
214038 subducting African plate ? *Earth Planet. Sci. Lett.* **151**, 255-269
214139 Tedesco D. and Scarsi P. (1999) Reply to "Helium isotopes in historical lavas from Mount
214240 Vesuvius", a comment on "Noble gas isotopic ratios from historical lavas and fumaroles at
214341 Mount Vesuvius". *Earth Planet. Sci. Lett.* **174**, 245-246
214442 Tedesco D., Nagao K. and Scarsi P. (1998) Noble gas isotopic ratios from historical lavas and
214543 fumaroles at Mount Vesuvius (southern Italy): constraints for current and future volcanic activity.
214644 *Earth Planet. Sci. Lett.* **164**, 61-78
214745 Tedesco D., Allard P., Sano Y., Wakita H. and Pece R. (1990) Helium-3 in subaerial and
214846 submarine fumaroles of Campi Flegrei caldera, Italy. *Geochim. Cosmochim. Acta* **54**, 1105-
214947 1116
214948 Totaro C., Koulakov I., Orecchio B. and Presti D. (2014) Detailed crustal structure in the area of
215049 the southern Apennines-Calabrian Arc border from local earthquake tomography. *J.*
215150 *Geodynamics* **82**, 87-97
215251 Trumphy E., Donato A., Gianelli G., Gola G., Minissale A., Montanari D., Santilano A. and Manzella
215352 A. (2015) Data integration and favourability maps for exploring geothermal systems in Sicily,
215453 southern Italy. *Geothermics* **56**, 1-16
215554 Trumphy E. and Manzella A. (2017) Geothopica and the interactive analysis and visualization of the
215655 updated Italian National Geothermal Database. *Intern. J. Appl. Earth Observation and*
215756 *Geoinformation* **54**, 28-37

2158
2159
2160

2161
2162
2163 1 Valentino G.M., Cortecchi G., Franco E. and Stanzione D. (1999) Chemical and isotopic
2164 2 composition of minerals and waters from the Campi Flegrei volcanic system, Naples, Italy. *J.*
2165 3 *Volcanol. Geothermal Res.* **91**, 329-344
2166 4 Vaselli O., Tassi F., Tedesco D., Poreda R.J. and Caprai A. (2011) Submarine and inland gas
2167 5 discharges from the Campi Flegrei (southern Italy) and the Pozzuoli Bay: geochemical clues for
2168 6 a common hydrothermal-magmatic source. *Procedia Earth Planet. Sci.* **4**, 57-73
2169 7 Vespasiano G., Apollaro C., Muto F., Dotsika E., De Rosa R. and Marini L. (2014) Chemical and
2170 8 isotopic characteristics of the warm and cold waters of the Luigiane Spa near Guardia
2171 9 Piemontese (Calabria, Italy) in a complex faulted geological framework. *Appl. Geochem.* **41**, 73-
217210 88
217311 Voltattorni N., Lombardi S. and Rizzo S. (2010) ²²²Rn and CO₂-soil gas geochemical
217412 characterization of thermally altered clays at Orciatico (Tuscany, Central Italy). *Appl. Geochem.*
217513 **25**, 1,248-1,256
217614 Washington H.S. (1906) The Roman Comagmatic Region. *Carnegie Institution of Washington* 36,
217715 Washington, USA, 220pp
217816 Watts M.D. (1987) Geothermal exploration of Roccamonfina volcano, Italy. *Geothermics* **16**, 517-
217917 528
218018 Yousefi H., Noorollahi Y., Ehara S., Itoi R., Yousefi A., Fujimitsua Y, et al. (2010) Developing the
218119 geothermal resources map of Iran. *Geothermics* **39**, 140-151
218220 Zuppi G.M., Fontes J.C. and Letolle R. (1974) Isotopes du milieu et circulations d'eaux sulfurees
218321 dans le Latium. In *"Isotope Techniques in Groundwater Hydrology"*, IAEA Wien (Austria), 341-
218422 361
2185
2186
2187
2188
2189
2190
2191
2192
2193
2194
2195
2196
2197
2198
2199
2200
2201
2202
2203
2204
2205
2206
2207
2208
2209
2210
2211
2212
2213
2214
2215
2216
2217
2218
2219
2220

2221
2222
2223
2224
2225
2226
2227
2228
2229
2230
2231
2232
2233
2234
2235
2236
2237
2238
2239
2240
2241
2242
2243
2244
2245
2246
2247
2248
2249
2250
2251
2252
2253
2254
2255
2256
2257
2258
2259
2260
2261
2262
2263
2264
2265
2266
2267
2268
2269
2270
2271
2272
2273
2274
2275
2276
2277
2278
2279
2280

16. Figure captions

Fig. 1 - Schematic illustration of a geothermal exploration program with proceeding phases.

Credits for pictures and images: Map of geothermal resource of the United States (from [Billy, 2009](#)). Photo of the geological outcrop (New York State Museum). 3D geological model (<http://www.pdgm.com/products/skua-gocad/>) Geothermal field development (http://www.thinkgeoenergy.com/nevada-geothermal-power-reports-on-progress-for-blue-mountain-plant/nevadageothermal_bluemountain_may19/).

Fig. 2 - Illustrative geological cross section through a conventional geothermal system located along the Central Italy -Tyrrenian margin, compared with P_{CO_2} (pCO_2) values (expressed both in bar and log bar) in shallow groundwater. Following [Doveri et al. \(2010\)](#), three P_{CO_2} classes are taken as reference: *i*) highly anomalous, $P_{CO_2} > 0.18$ bar; *ii*) weakly anomalous, $0.078 < P_{CO_2} < 0.18$; *iii*) non-anomalous, $P_{CO_2} < 0.078$ bar.

Fig. 3 - Schematic geological map of Southern Italy showing main tectonic units and approximate location of thermal water and gas emissions.

Fig. 4 - Map of Latium region (east side), Abruzzi and Molise regions (west side) with location of thermal springs, some cold springs and gas emissions. The figure shows, with different colours, the type of main gas phase associated to the water, namely: CO_2 -dominated in purple, N_2 -dominated in blue, orange if CH_4 -dominated. The map also shows outcrops of the regional Mesozoic carbonate reservoir and outcrops of Quaternary volcanics. In italics is the number referring to the gas phase data base.

Fig. 5 - Map of Campania, Puglia and Lucania regions, with location of natural thermal emissions. For the legend see figure 4.

Fig. 6 - Map of Calabria, Sicily and Sardinia regions, with location of natural thermal emissions. For the legend see figure 4.

Fig. 7 - [Langelier-Ludwig \(1942\)](#) diagram for the water samples investigated (mostly springs). Numbers refer to the file of water samples in additional material.

Fig. 8 - HCO_3 - SO_4 -Cl (left) and (Na+K)-Ca-Mg (right) ternary diagram for the water samples investigated. Numbers refer to the file of water samples in additional material.

Fig. 9 - δD - $\delta^{18}O$ (left) and δD -Cl (right) binary diagrams for the water samples investigated. Numbers refer to the file of water samples in additional material.

Fig. 10 - N_2 - CO_2 diagram for the gas samples investigated. Numbers refer to the file of water samples in additional material.

Fig. 11 - Diagrams of CO_2 vs. $\delta^{13}C$ of carbon in CO_2 (top) and $\delta^{13}C$ of carbon in CO_2 gas phase vs. the $\delta^{13}C$ of carbon in dissolved inorganic carbon (D.I.C.) of the associated water phase (bottom), for the gas samples investigated. Numbers refer to the file of water samples in additional material.

2281
2282
2283
2284
2285
2286
2287
2288
2289
2290
2291
2292
2293
2294
2295
2296
2297
2298
2299
2300
2301
2302
2303
2304
2305
2306
2307
2308
2309
2310
2311
2312
2313
2314
2315
2316
2317
2318
2319
2320
2321
2322
2323
2324
2325
2326
2327
2328
2329
2330
2331
2332
2333
2334
2335
2336
2337
2338
2339
2340

1 **Fig. 12** - Plot of $\delta^{13}\text{C}$ of carbon in CO_2 gas phase vs. the $\delta^{13}\text{C}$ of carbon CH_4 (Giggenbach, 1982).

2 Numbers refer to the file of water samples in additional material.

3 **Fig. 13** - Plot of ^3He vs ^4He (left) and ^3He vs. R/Ra (right) for the gas samples investigated.

4 Numbers refer to the file of water samples in additional material.

5 **Fig. 14** - K-Mg-Na ternary diagram (Giggenbach, 1988) for the water samples investigated.

6 Numbers refer to the file of water samples in additional material.

7 **Fig. 15** - Plot of $\log(x\text{H}_2/x\text{Ar})$ vs. $\log(x\text{CH}_4/x\text{CO}_2)$ (Giggenbach, 1993) for the gas samples
8 investigated. See text.

9 **Fig. 16** - Isodistribution maps of: *i*) CO_2 concentration in the gas phase (top); *ii*) $\delta^{13}\text{C}$ of carbon in
10 CO_2 in the gas phase (middle); *iii*) calculated (Parkhurst D. and Appelo, 1999) $p\text{CO}_2$ [as -
11 $\log(p\text{CO}_2/P_{\text{CO}_2})$] in the water samples. Uncoloured areas of eastern and south-eastern Italy and
12 Sardinia island are due to insufficient concentration of CO_2 or low number of samples.

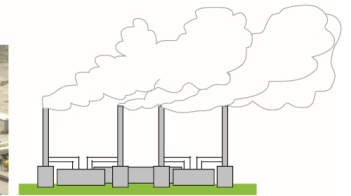
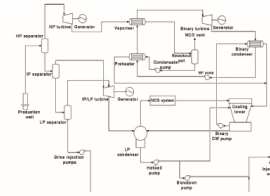
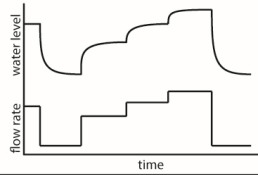
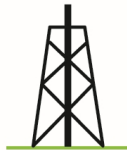
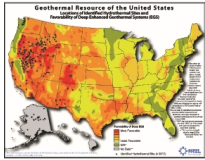
13 **Fig. 17** - Isodistribution maps of: *i*) concentration of total helium in the gas phase (top); *ii*) $^3\text{He}/^4\text{He}$
14 (as R/Ra) ratio (bottom), prevalently measured in the free gas phase.

2341
2342
2343
2344
2345
2346
2347
2348
2349
2350
2351
2352
2353
2354
2355
2356
2357
2358
2359
2360
2361
2362
2363
2364
2365
2366
2367
2368
2369
2370
2371
2372
2373
2374
2375
2376
2377
2378
2379
2380
2381
2382
2383
2384
2385
2386
2387
2388
2389
2390
2391
2392
2393
2394
2395
2396
2397
2398
2399
2400

1 **17. Table captions (additional material)**

2
3
4 **Table 1** - Chemical and isotopic analyses of thermal emissions in liquid phase of Southern Italy;
5 ts= thermal spring; tsg=thermal spring with gas; sg=spring with gas; twg=thermal well with gas;
6 wg=well with gas; mv=mud volcano; mo=mofette; fu=fumarole).

7 **Table 2** - Chemical and isotopic analyses of gas emissions in gas phase of Southern Italy; ts=
8 thermal spring; tsg=thermal spring with gas; sg=spring with gas; twg=thermal well with gas;
9 wg=well with gas; mv=mud volcano; mo=mofette; fu=fumarole).



GEOHERMAL FAVOURABILITY MAPPING

PRELIMINARY SURVEY

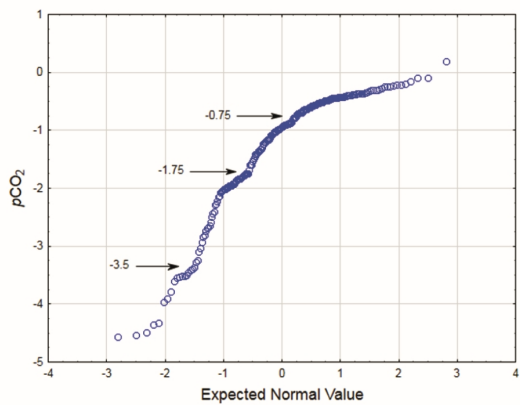
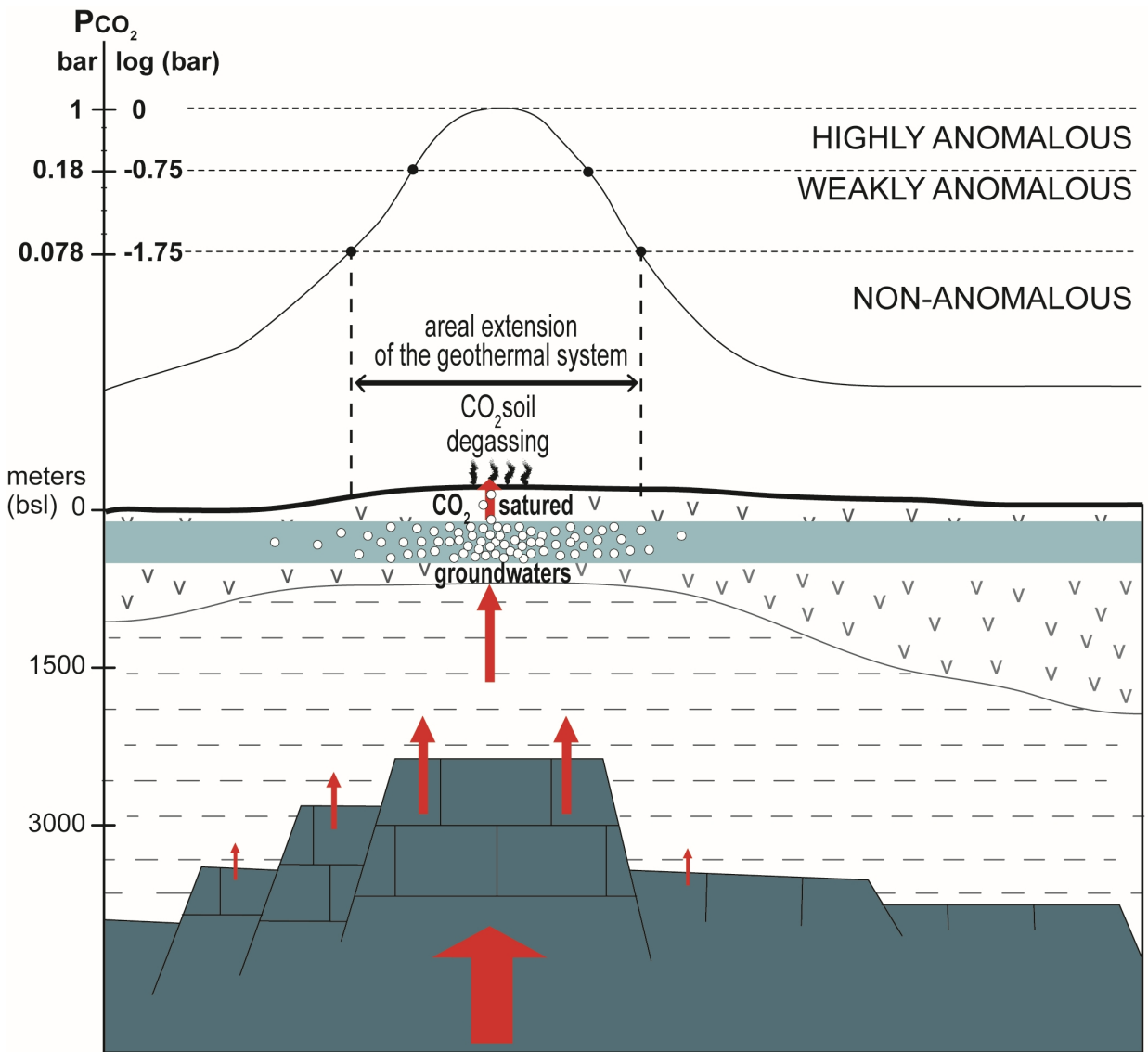
EXPLORATION & DRILLING








TEST DRILLING

PROJECT REVIEW & PLANNING

FIELD DEVELOPMENT

**POWER PLANT CONSTRUCTION
COMMISSIONING & OPERATION**



-  volcanic cover
 -  clayish cover
 -  carbonatic geothermal RESERVOIR
 -  shallow aquifer
 -  dissolved CO₂
-  CAP-ROCK
-  CO₂-rich geothermal fluid (the arrow size is proportional to the degassing rate)

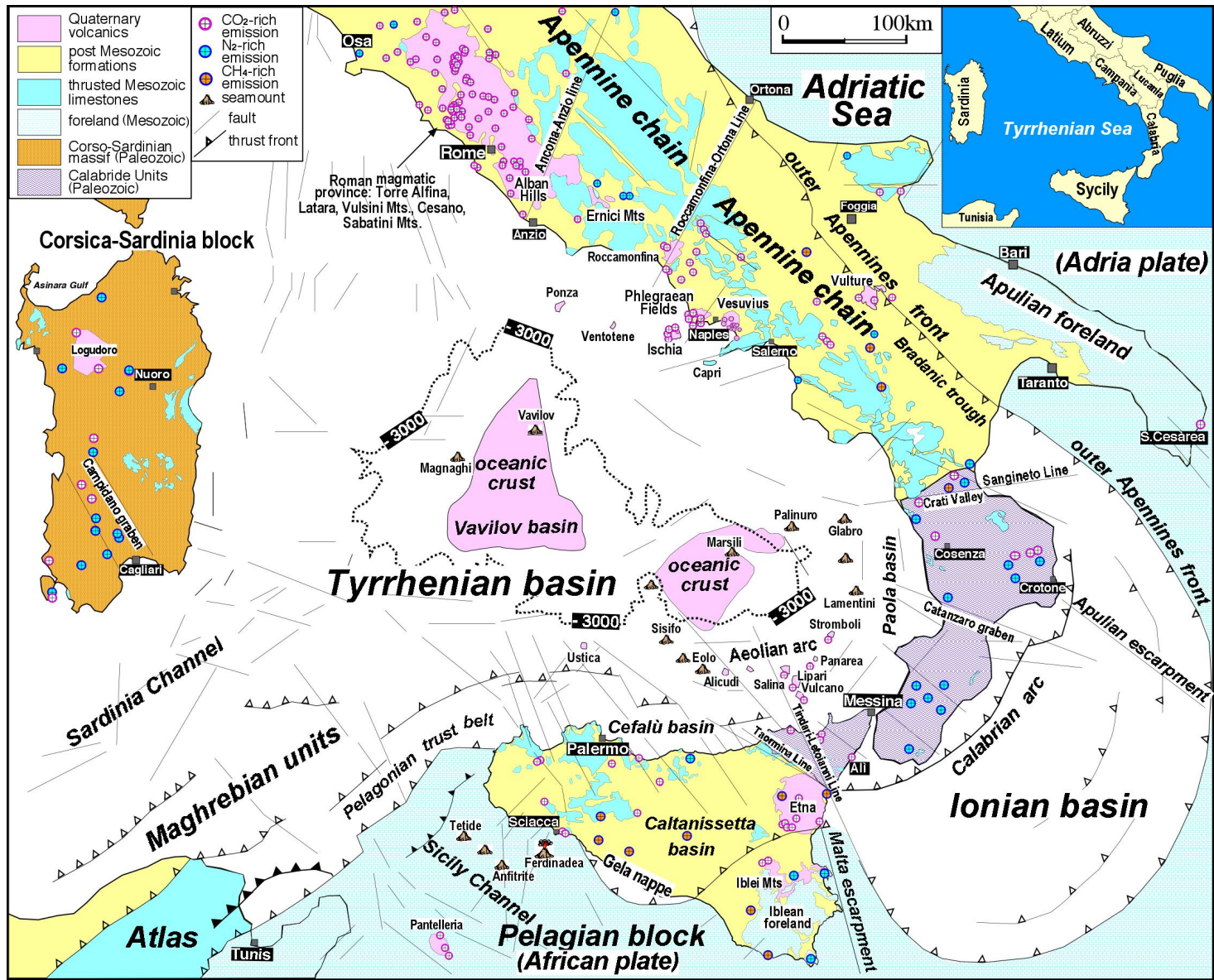


Fig. 3 - Schematic geological map of Southern Italy showing main tectonic units and approximate location of thermal water and gas emissions.

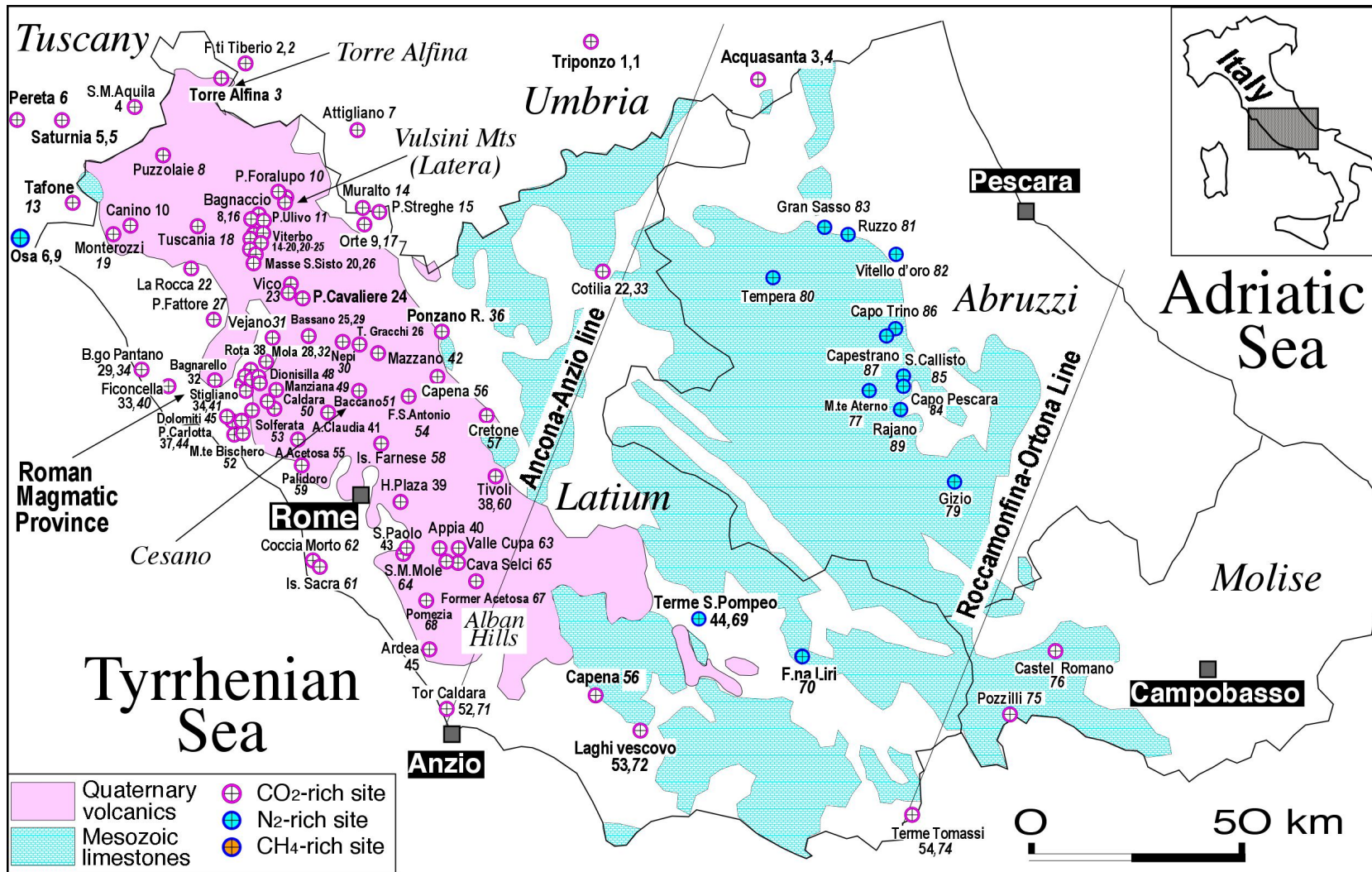


Fig. 4 - Map of Latium region (east side), Abruzzi and Molise regions (west side) with location of thermal springs, some cold springs and gas emissions. The figure shows, with different colours, the type of main gas phase associated to the water, namely: CO₂-dominated in purple, N₂-dominated in blue, orange if CH₄-dominated. The map also shows outcrops of the regional Mesozoic carbonate reservoir and outcrops of Quaternary volcanics. In italics is the number referring to the gas phase data base.

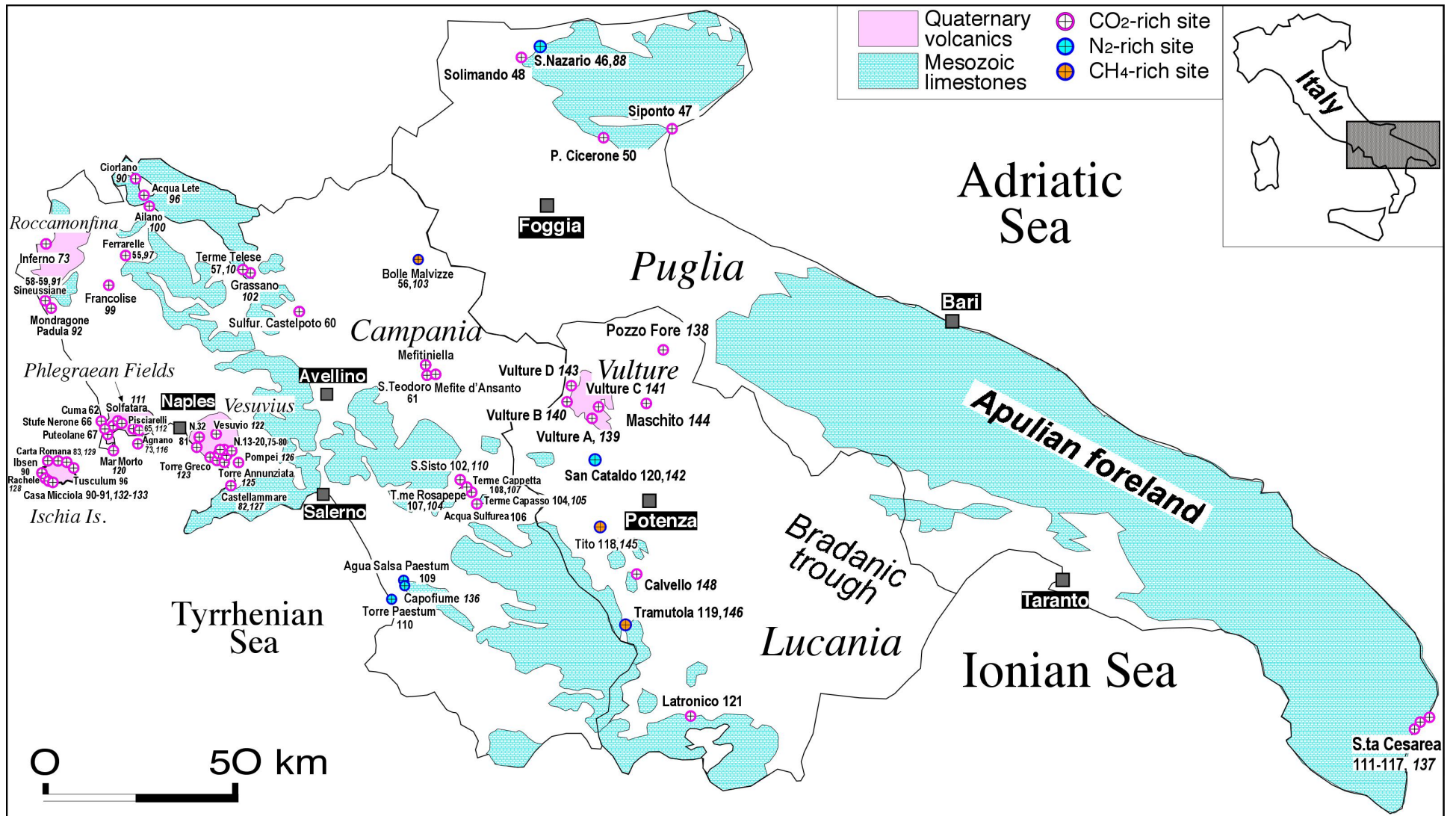


Fig. 5 - Map of Campania, Puglia and Lucania regions, with location of natural thermal emissions. For the legend see figure 4.

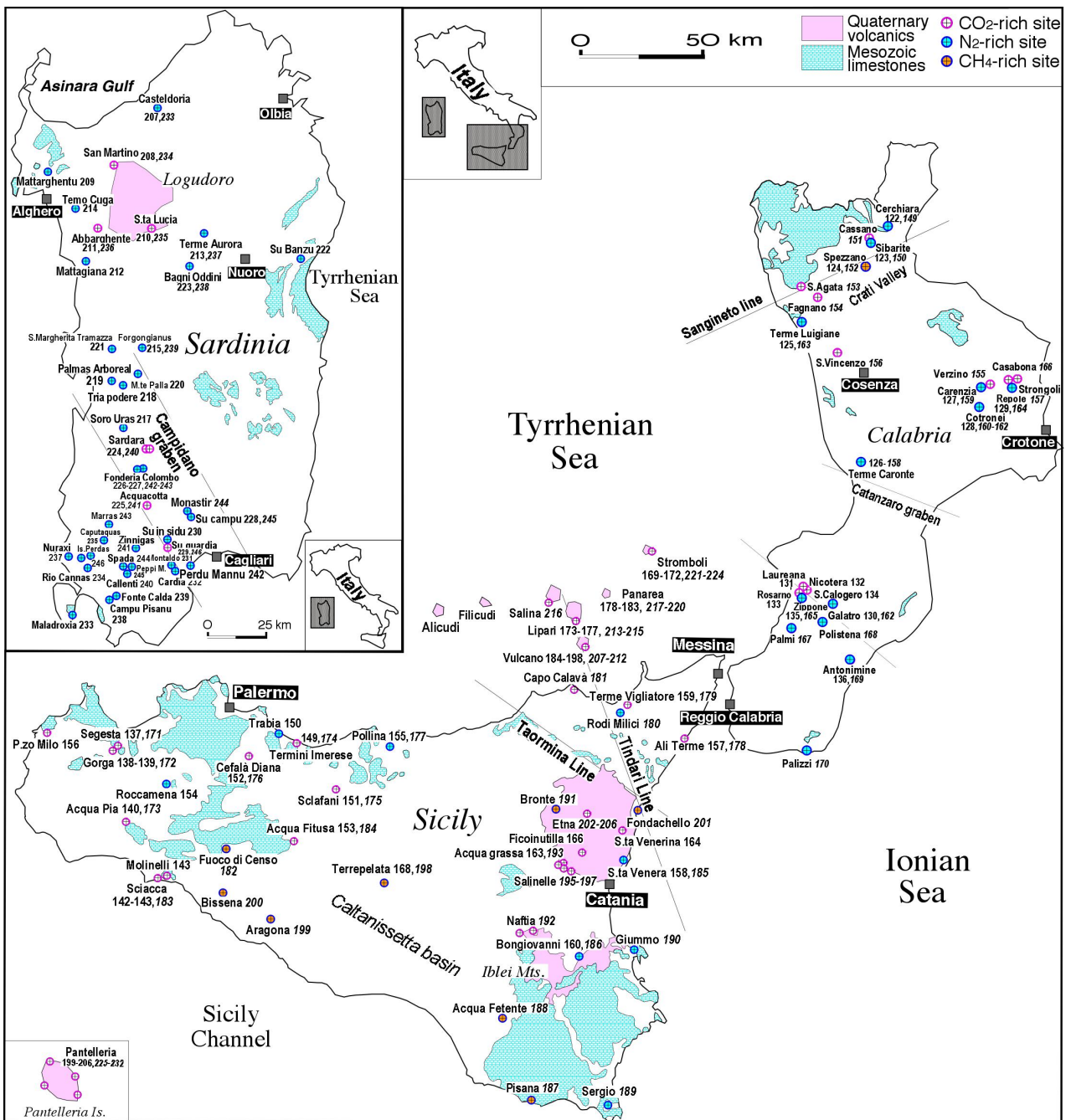


Fig. 6 - Map of Calabria, Sicily and Sardinia regions, with location of natural thermal emissions. For the legend see figure 4.

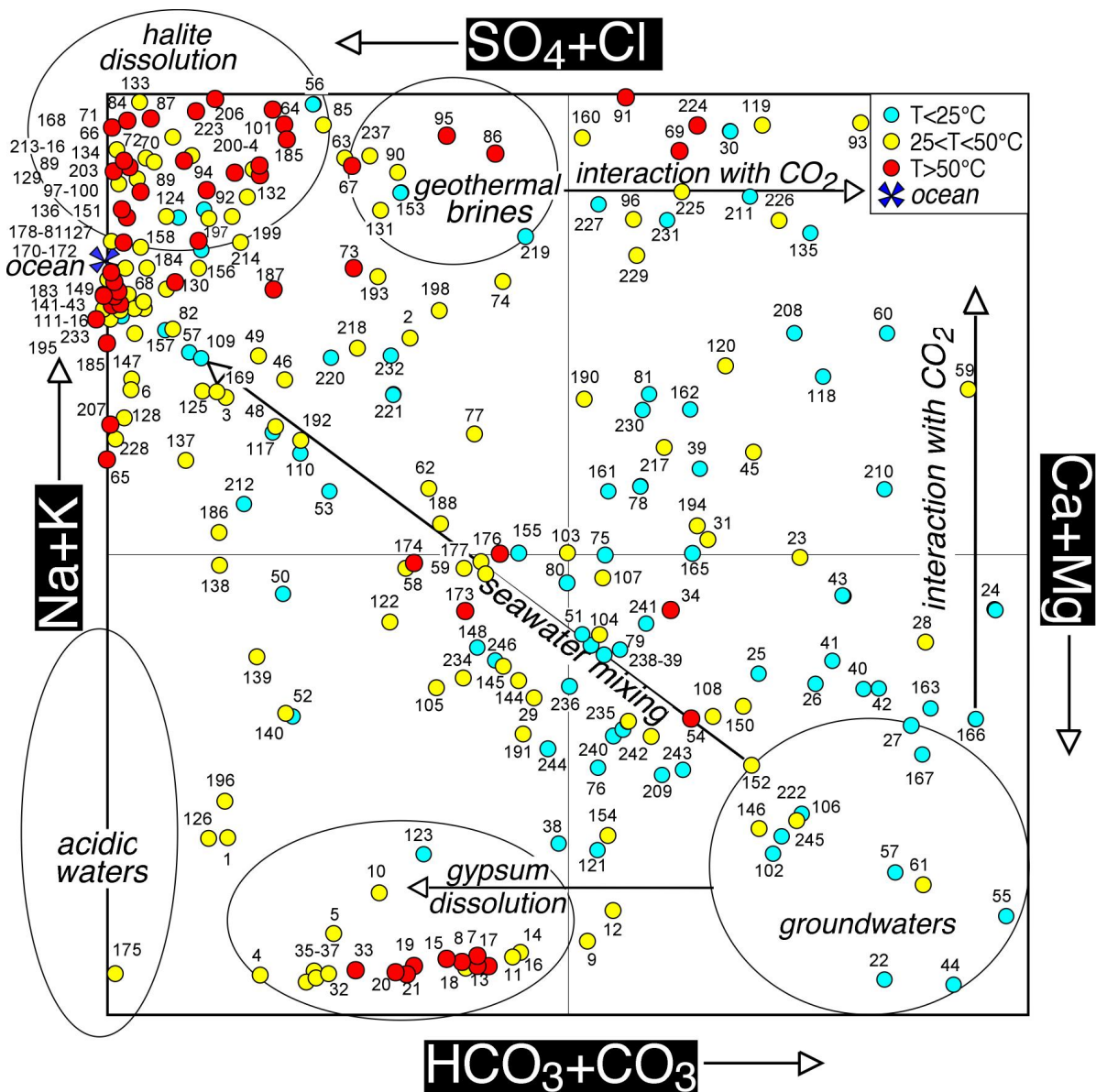


Fig. 7 - Langelier-Ludwig (1942) diagram for the water samples investigated (mostly springs). Numbers refer to the file of water samples in additional material.

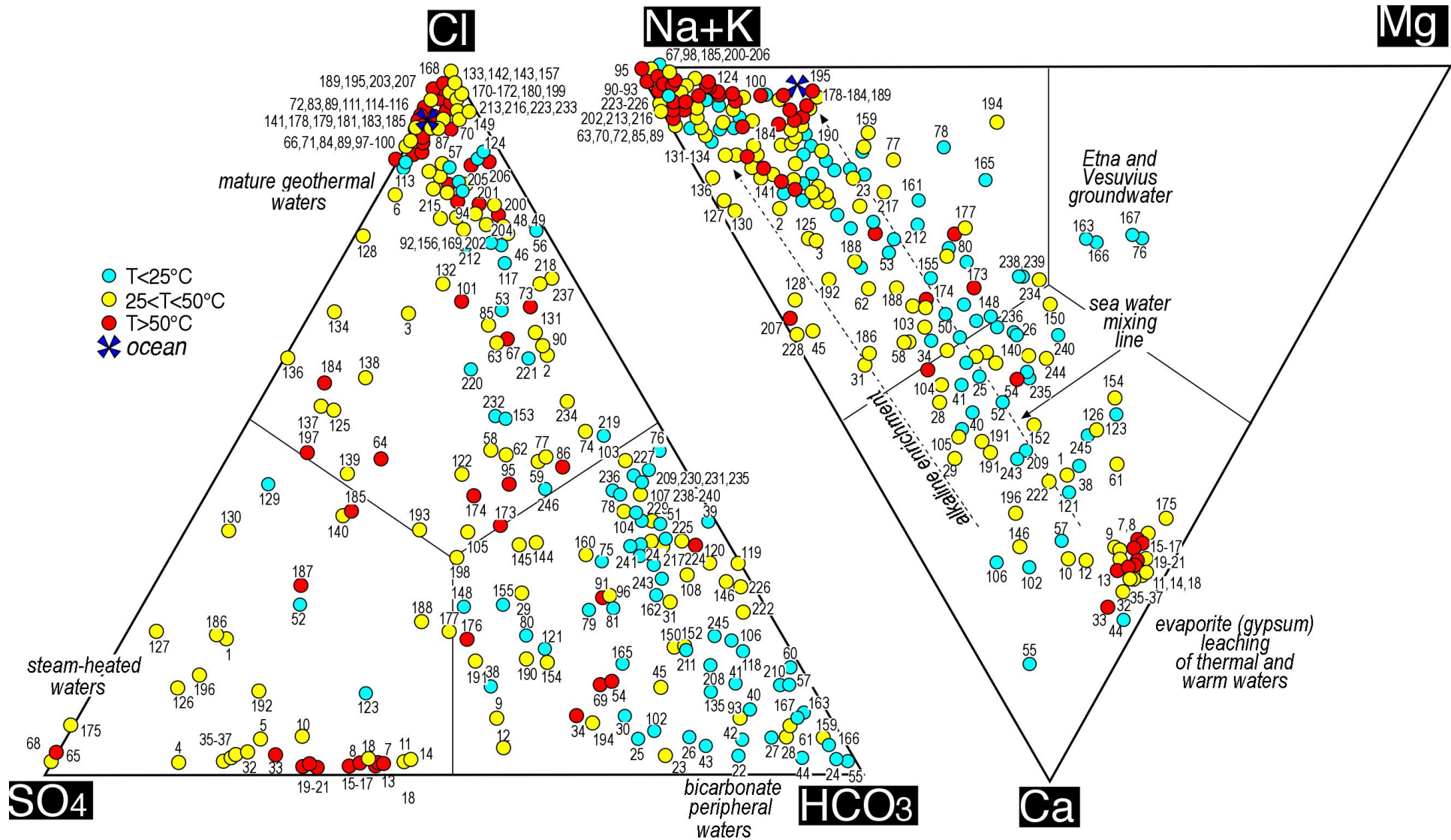


Fig. 8 - HCO₃-SO₄-Cl (left) and (Na+K)-Ca-Mg (right) ternary diagram for the water samples investigated. Numbers refer to the file of water samples in additional material

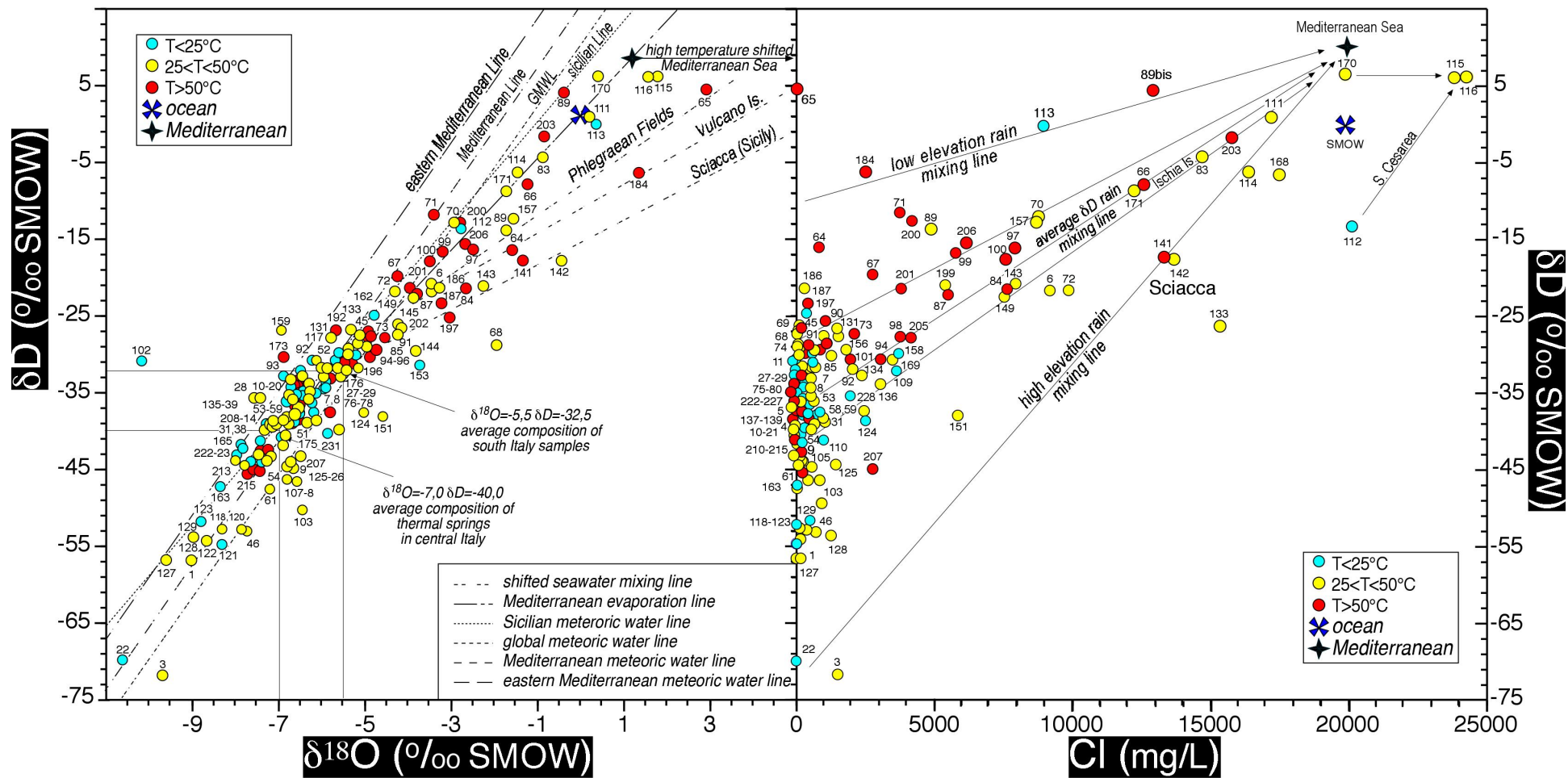


Fig. 9 - δD - $\delta^{18}O$ (left) and δD -Cl (right) binary diagrams for the water samples investigated. Numbers refer to the file of water samples in additional material.

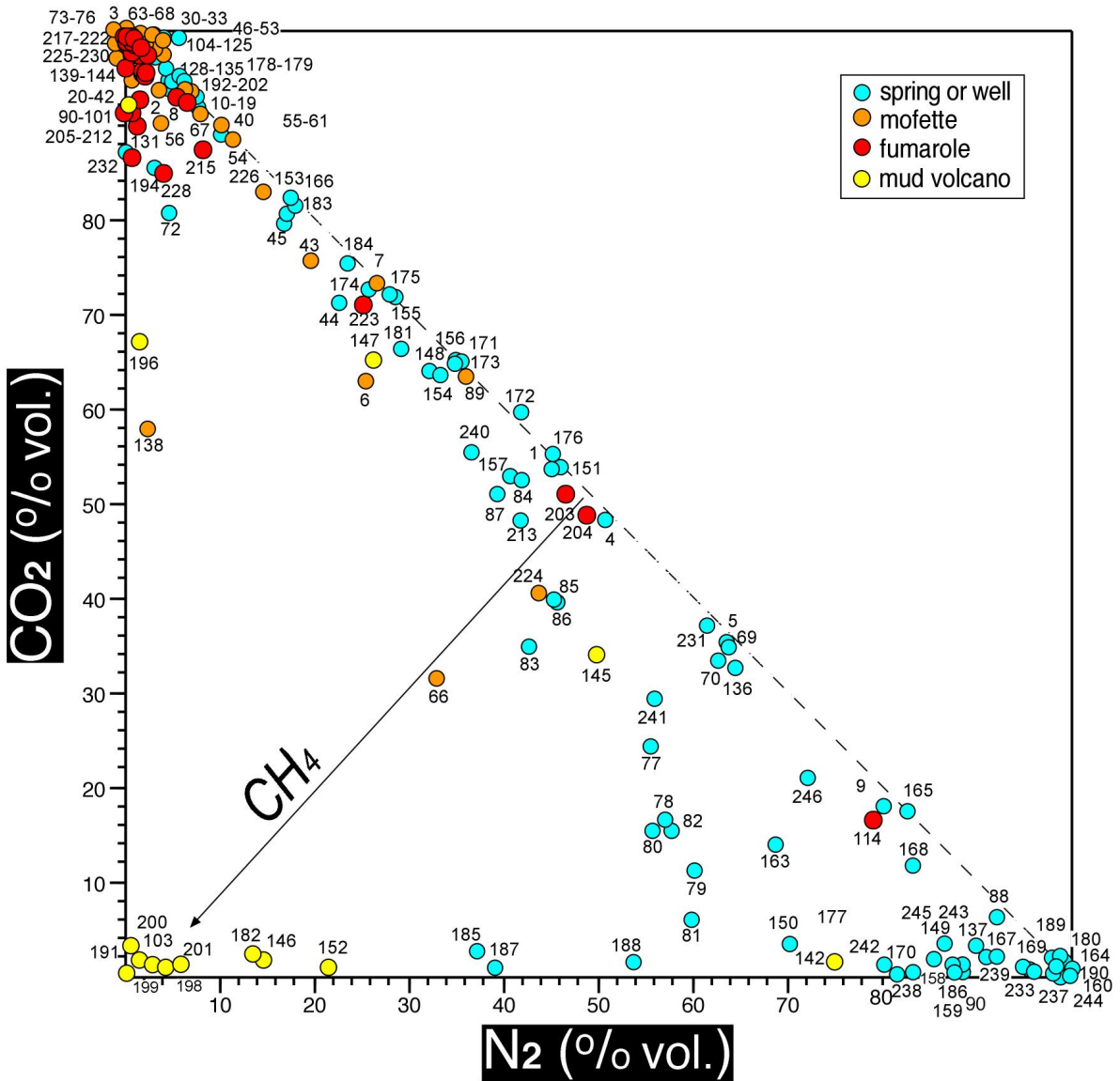


Fig. 10 - N₂-CO₂ diagram for the gas samples investigated. Numbers refer to the file of water samples in additional material.

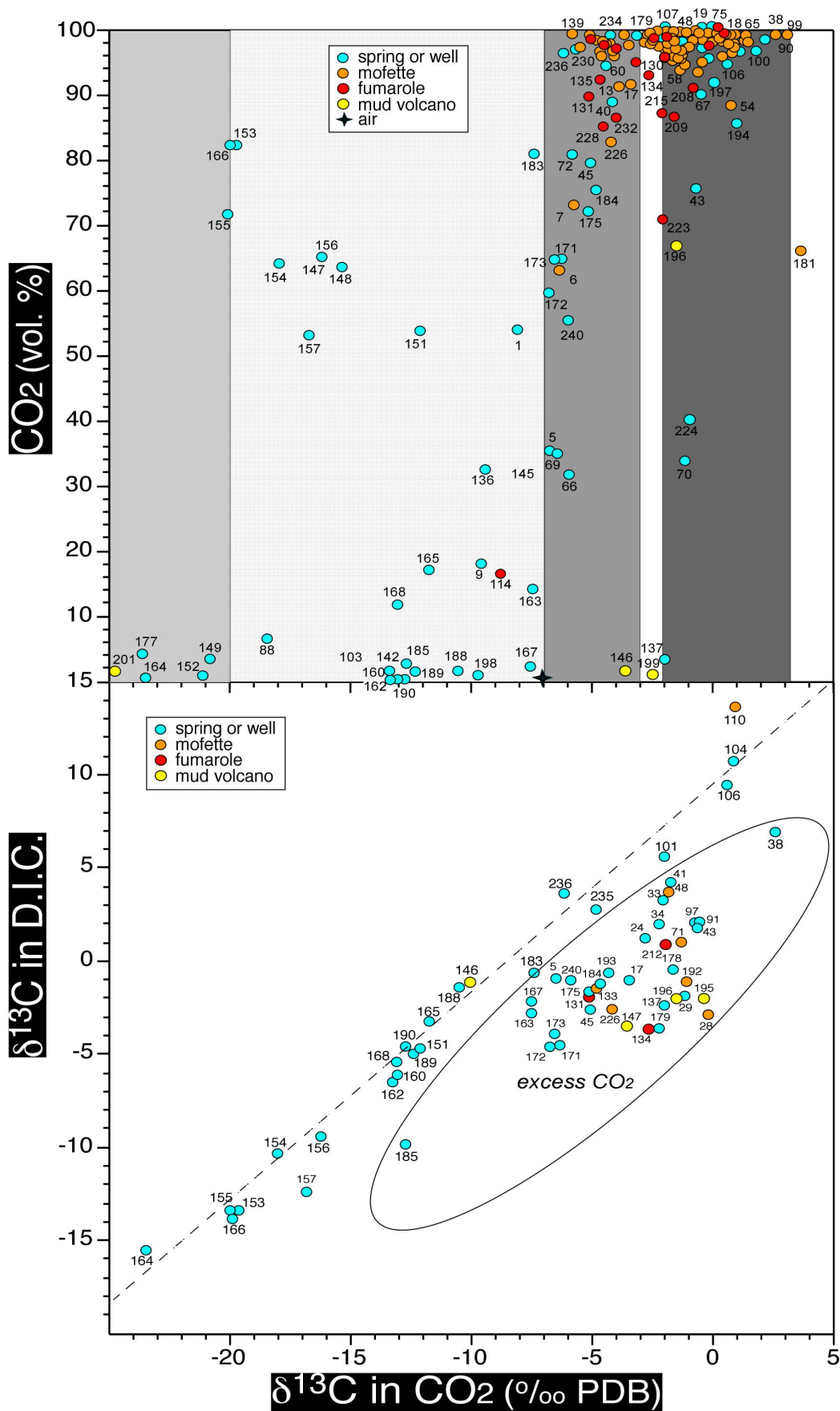


Fig. 11 - Diagrams of CO₂ vs. δ¹³C of carbon in CO₂ (top) and δ¹³C of carbon in CO₂ gas phase vs. the δ¹³C of carbon in dissolved inorganic carbon (D.I.C.) of the associated water phase (bottom), for the gas samples investigated. Numbers refer to the file of water samples in additional material.

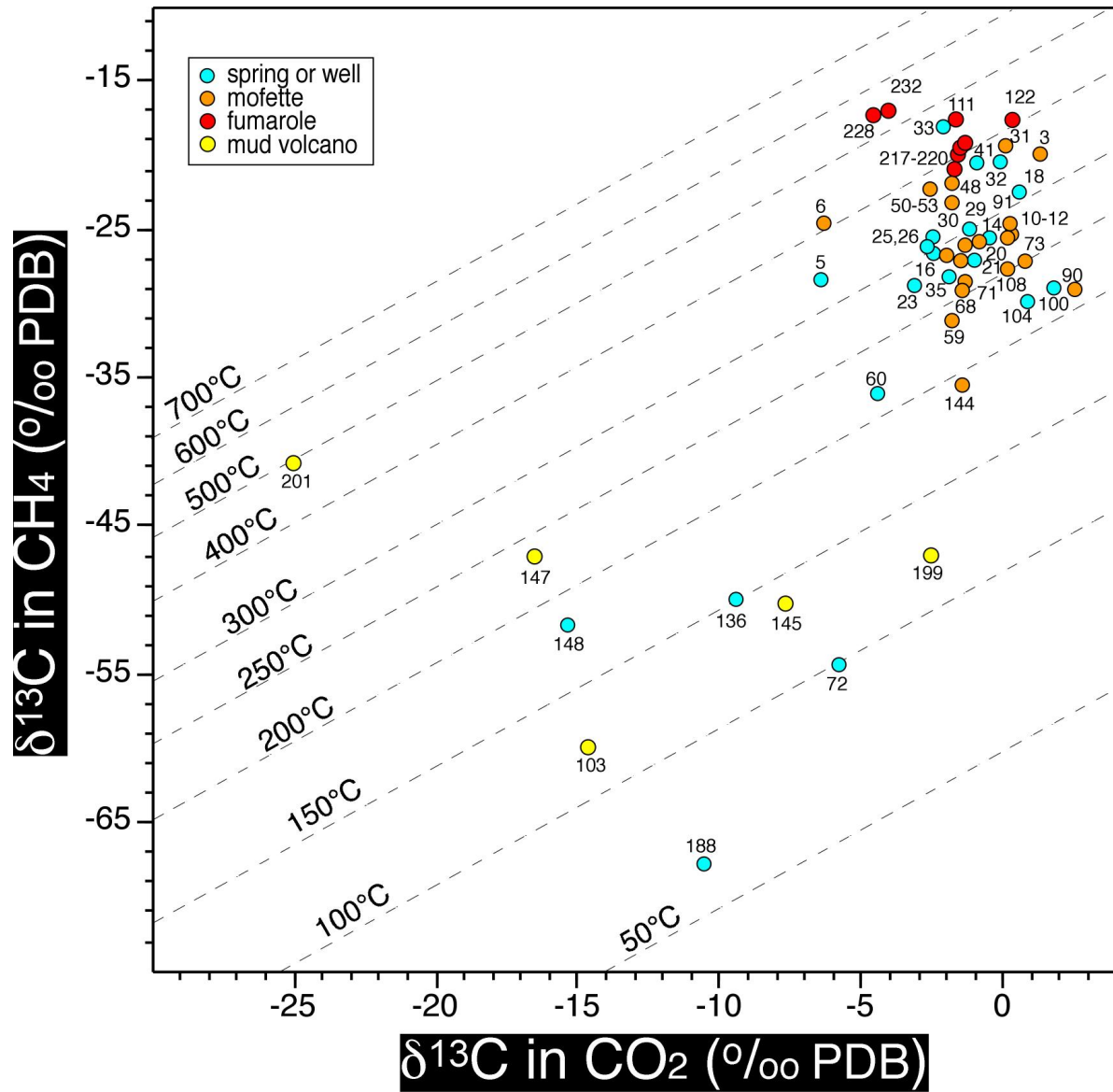


Fig. 12 - Plot of $\delta^{13}\text{C}$ of carbon in CO_2 gas phase vs. the $\delta^{13}\text{C}$ of carbon CH_4 (Giggenbach, 1982). Numbers refer to the file of water samples in additional material.

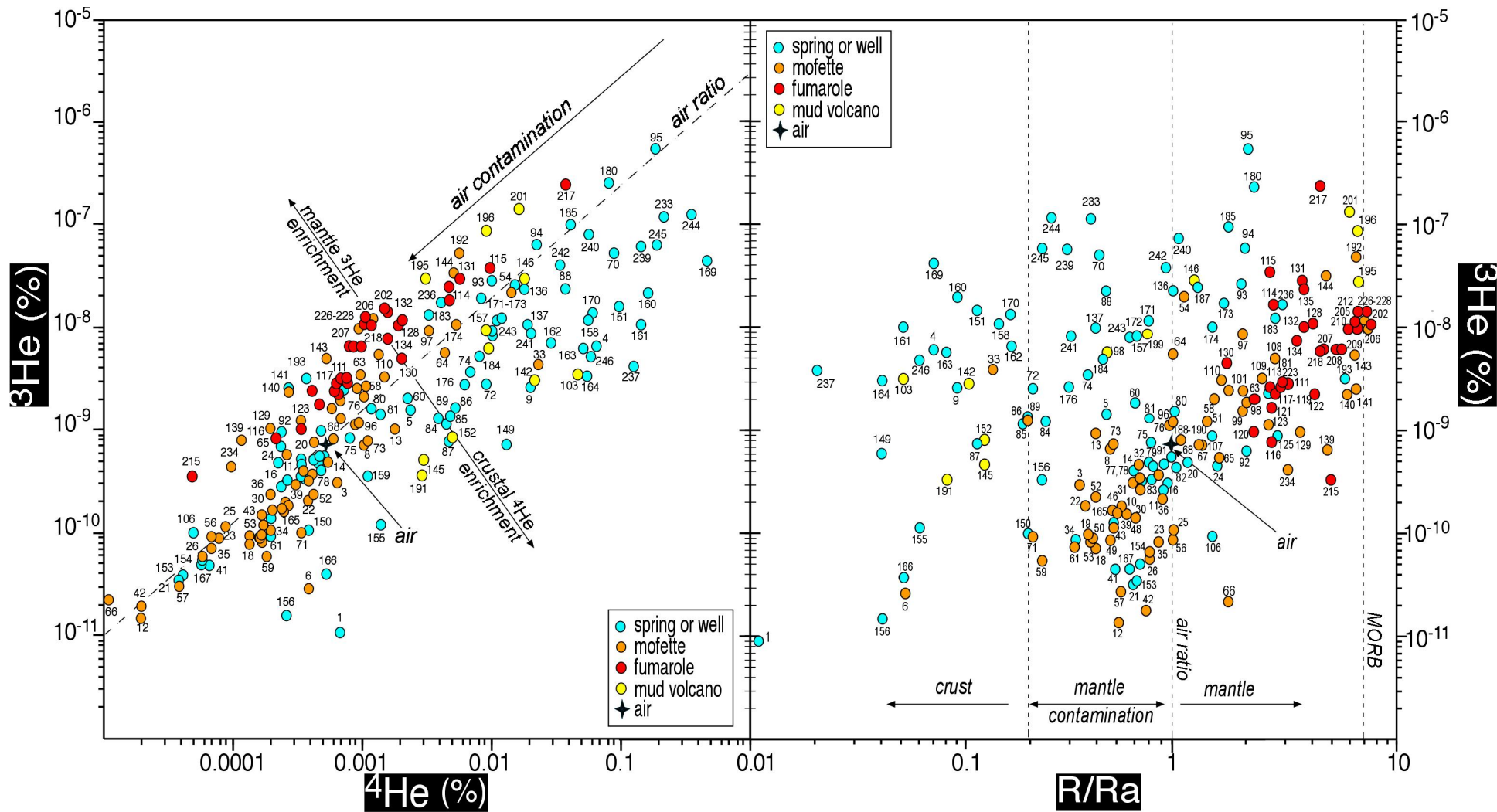


Fig. 13 - Plot of ^3He vs ^4He (left) and ^3He vs. R/Ra (right) for the gas samples investigated. Numbers refer to the file of water samples in additional material.

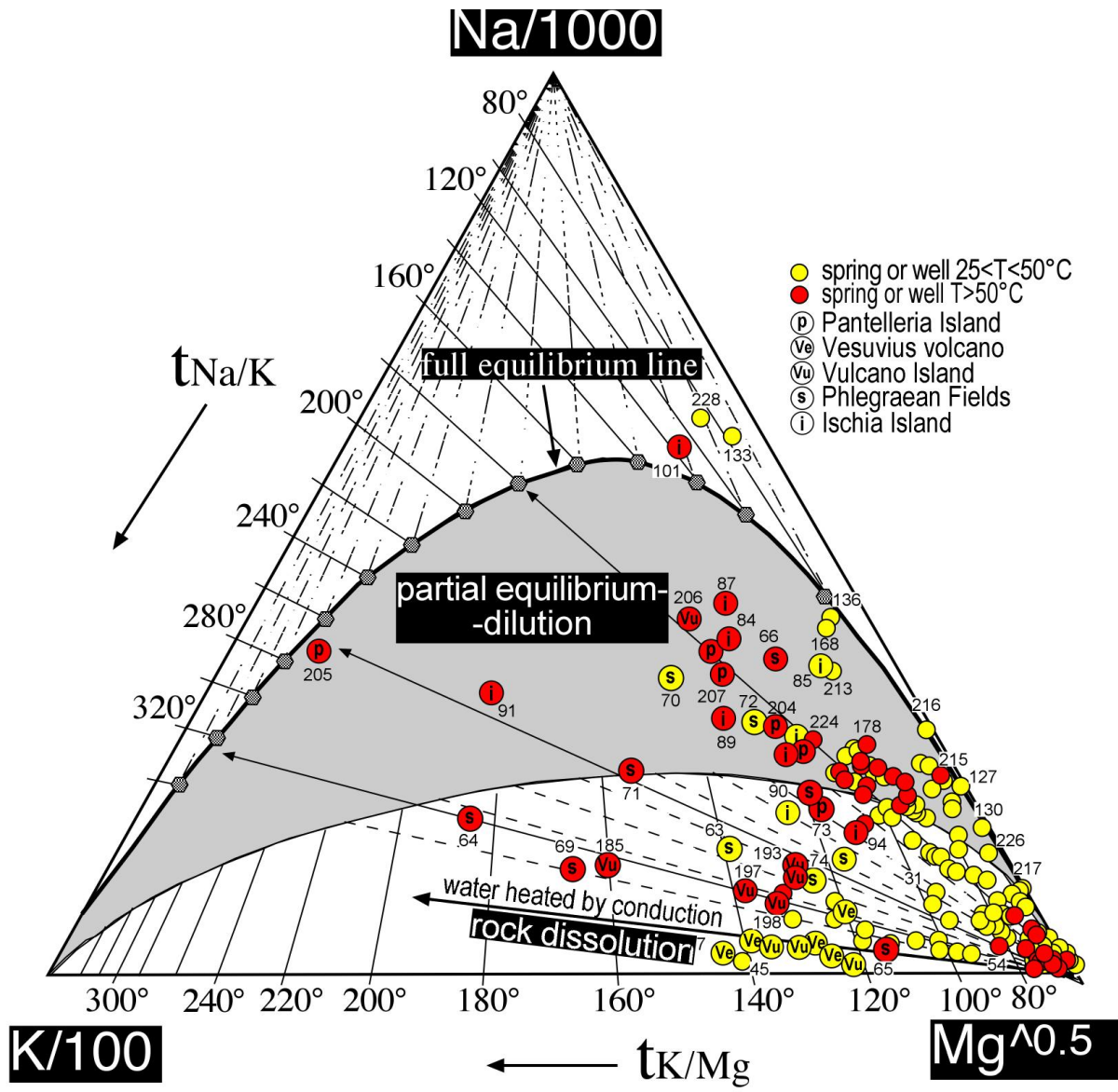


Fig. 14 - K-Mg-Na ternary diagram (Giggenbach, 1988) for the water samples investigated. Numbers refer to the file of water samples in additional material.

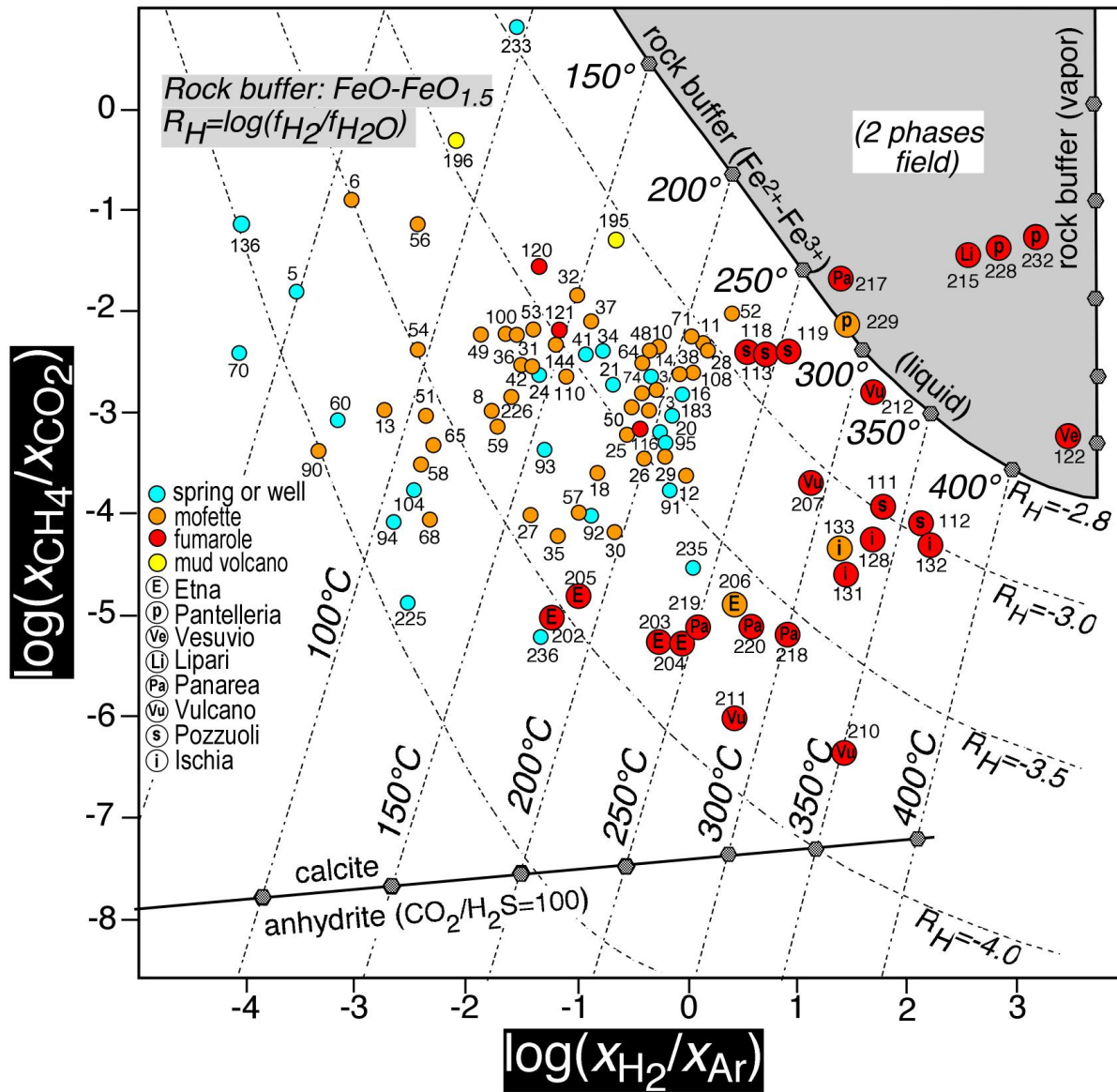


Fig. 15 - Plot of $\log(x_{\text{H}_2}/x_{\text{Ar}})$ vs. $\log(x_{\text{CH}_4}/x_{\text{CO}_2})$ (Giggenbach, 1993) for the gas samples investigated. See text.

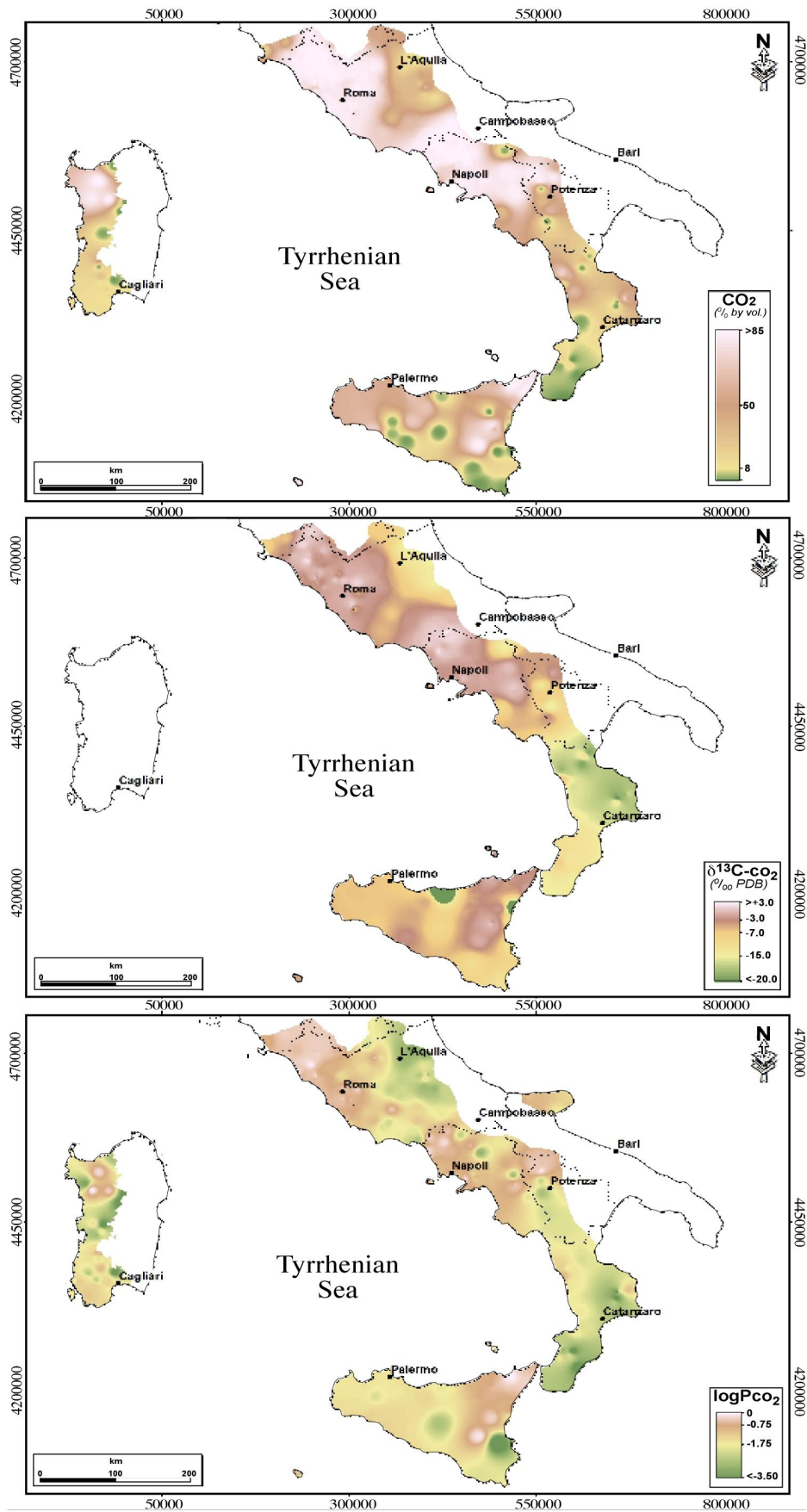


Fig. 16 - Isodistribution maps of: *i*) CO₂ concentration in the gas phase (top); *ii*) δ¹³C of carbon in CO₂ in the gas phase (middle); *iii*) calculated (Parkhurst D. and Appelo, 1999) pCO₂ [as -log(pCO₂Pco₂)] in the water samples. Uncoloured areas of eastern and south-eastern Italy and Sardinia island are due to insufficient concentration of CO₂ or low number of samples.

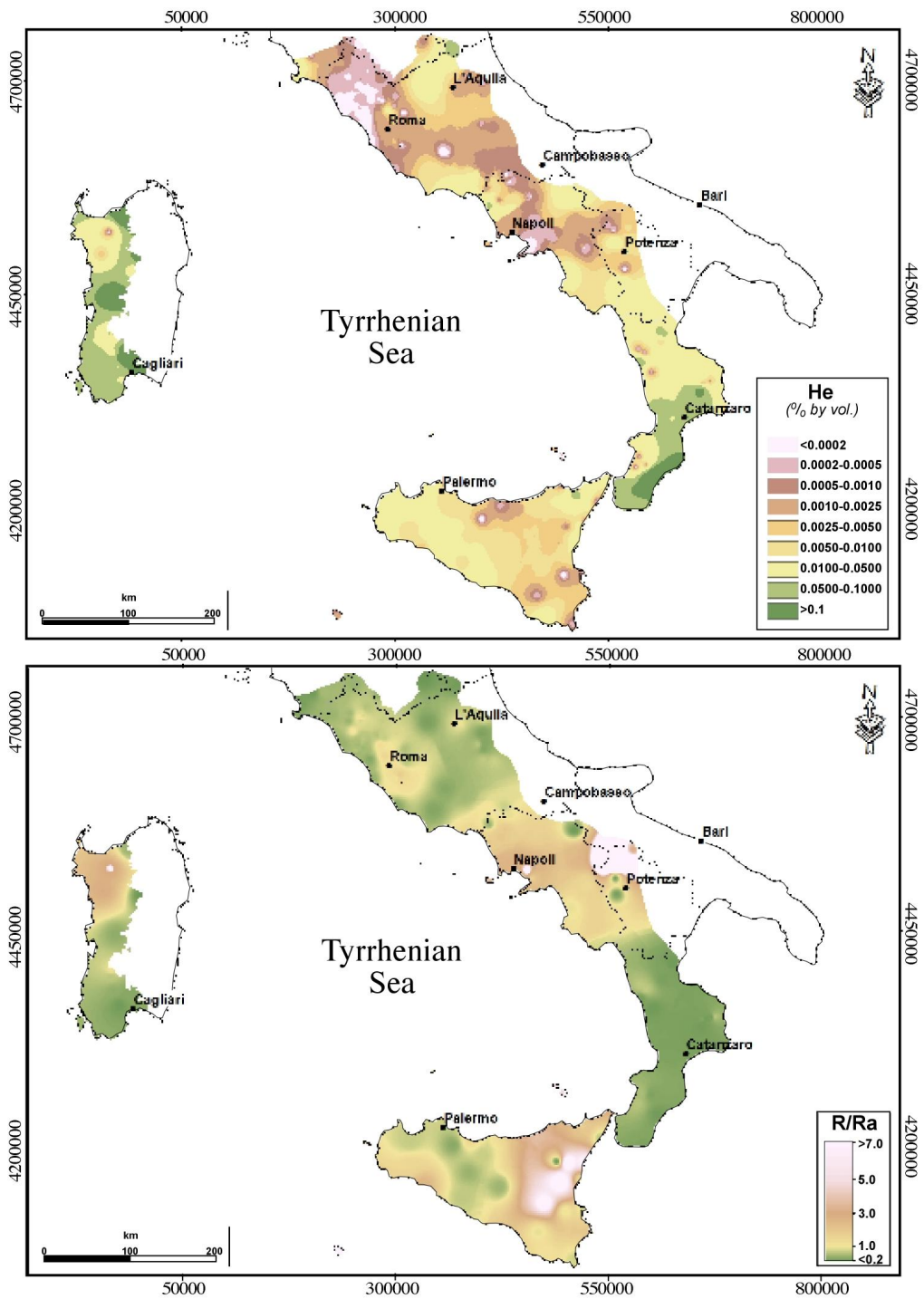


Fig. 17 - Isodistribution maps of: *i*) concentration of total helium in the gas phase (top); *ii*) $^3\text{He}/^4\text{He}$ (as R/Ra) ratio (bottom), prevalently measured in the free gas phase.